ÉCOLE DE TECHNOLOGIE SUPÉRIEURE
UNIVERSITÉ DU QUÉBEC

THESIS PRESENTED TO
ÉCOLE DE TECHNOLOGIE SUPÉRIEURE

IN PARTIAL FULFILLMENT OF THE REQUIREMENTS FOR
THE DEGREE OF DOCTOR OF PHILOSOPHY
Ph.D.

BY
Mohammadreza MOTAMEDI

THE USE OF MULTI-MODAL HAPTIC FEEDBACK TO CONVEY VARIOUS ASPECTS OF TOUCH SENSITIVITY

MONTREAL, "SEPTEMBER 04TH, 2015"

BOARD OF EXAMINERS

THIS THESIS HAS BEEN EVALUATED

BY THE FOLLOWING BOARD OF EXAMINERS:

Prof. Vincent Duchaine, Thesis Supervisor
Department of Automated Production Engineering at École de technologie supérieure

Prof. Pascal Bigras, Thesis Co-supervisor
Department of Automated Production Engineering at École de technologie supérieure

Prof. Handy Fortin Blanchette, President of the Board of Examiners
Department of Electrical Engineering at École de technologie supérieure

Prof. Ilian Bonev, Member of the Jury
Department of Automated Production Engineering at École de technologie supérieure

Prof. Clément Gosselin, External Evaluator
Department of Mechanical Engineering at Laval University

THIS THESIS WAS PRESENTED AND DEFENDED

IN THE PRESENCE OF A BOARD OF EXAMINERS AND THE PUBLIC

ON "AUGUST 31TH, 2015"

AT ÉCOLE DE TECHNOLOGIE SUPÉRIEURE

This thesis is dedicated to:

my beloved wife, Ameneh,

and

my parents, Simin & Mashaallah,

for all their support and encouragement.

ACKNOWLEDGEMENTS

"The price of success is hard work, dedication to the job at hand, and the determination that whether we win or lose, we have applied the best of ourselves to the task at hand."

Vince Lombardi

First I must thank my supervisor, Prof. Vincent Duchaine, whose sincerity and encouragement has guided me through my studies. I express my heartfelt gratefulness for his support and I believe that from him I have learned from the best. I would also like to thank the rest of my thesis committee for evaluating my research: Prof. Pascal Bigras, Prof. Handy Fortin Blanchette, Prof. Ilian Bonev, and Prof. Clément Gosselin. I greatly appreciate your work on my behalf.

I am grateful to my friends and colleagues, who have always shared their experiences with me and made my work environment friendly and productive.

My deepest gratitude goes to my loving wife. Her patience and positive attitude towards life have always given me confidence and the courage to step toward my goals with hope. My success is hers and her happiness is mine. I would also like to thank my parents and my sisters. I have been blessed with a very supportive family. My main goal in life is to deserve the pride they have always had in me.

L'UTILISATION D'UN RETOUR HAPTIQUE MULTIMODAL AFIN DE TRANSMETTRE DIVERS ASPECTS DE LA SENSIBILITÉ TACTILE

Mohammadreza MOTAMEDI

RÉSUMÉ

Malgré les grands progrès survenus dans le développement des prothèses, le manque de sensibilité tactile reste un problème important: les prothèses ne fournissent toujours pas de rétroaction tactile aux utilisateurs, nécessitant donc leur attention visuelle continue lors de l'accomplissement d'une tâche. Cette thèse étudie la façon dont la technologie haptique, en fonction du retour extéroceptif généré grâce au mouvement de la prothèse, peut être utilisée pour remédier à cette situation. Nous émettons l'hypothèse qu'un dispositif haptique portable peut compléter la boucle communicationnelle entre la prothèse et l'utilisateur, en stimulant les mécanorécepteurs de la peau d'une partie intacte du corps de usager.

Nous avons commencé notre recherche en enquêtant sur l'efficacité relative de trois types de retour haptique - le stress normal, la force tangentielle ainsi que la stimulation vibrotactile - afin de déterminer quel type de rétroaction haptique fonctionne le mieux dans des conditions statiques. Les résultats ont indiqué que la stimulation de la contrainte normale est le type le plus efficace dans des conditions statiques; il constitue donc la meilleure des trois options pour transmettre une sensation de pression à l'utilisateur, telle que la force de préhension appliquée par la prothèse lors de la manipulation d'un objet. Sur la base de ce résultat, nous avons développé un nouveau dispositif haptique portable qui fournit à l'utilisateur la reconnaissance d'une force verticale, par application d'une pression à trois endroits différents sur son corps. Nous avons ensuite investigué l'impact de l'application simultanée de deux types de rétroaction haptique différents sur la perception sensorielle humaine, la façon dont la stimulation vibrotactile peut être utilisée pour transmettre une sensation de texture et les répercussions de la quantité d'entraînement reçue par des sujets humains sur leur capacité à utiliser avec succès le système haptique. Enfin, notre dispositif haptique a été intégré au sein d'un système robotique et nous avons vérifié son efficacité dans le cadre de tâches d'application de pression et de reconnaissance de la texture.

Notre travail contribue donc à établir de nouvelles connaissances sur l'efficacité relative des différents types de rétroaction haptique dans des conditions statiques et dynamiques, de sorte que les systèmes haptiques puissent être optimisés pour des conditions telles que celles exigées par les applications industrielles et biomédicales.

Mots clés: Haptique, rétroaction tactile, sens du toucher, actuateur par câble, modalités statique et dynamique, proprioception, extéroception

THE USE OF MULTI-MODAL HAPTIC FEEDBACK TO CONVEY VARIOUS ASPECTS OF TOUCH SENSITIVITY

Mohammadreza MOTAMEDI

ABSTRACT

Despite much progress in the development of prosthetic limbs, the lack of touch sensitivity remains a significant problem: prosthetic limbs still do not provide any tactile feedback to users, requiring continuous visual attention from the user during task accomplishment. This thesis examines how haptic technology, based on exteroceptive feedback from the motion of the prosthesis, can be used to remedy this situation. We hypothesize that a portable haptic device can complete the communicational loop between the prosthetic limb and the user, by stimulating the mechanoreceptors in the skin of an unimpaired part of the user's body.

We began our research by investigating the relative effectiveness of three types of haptic feedback - normal stress, tangential force, and vibrotactile stimulation - in order to determine which type of haptic feedback performs best under static conditions. Results indicated that normal stress stimulation is the most effective under static conditions; it is therefore the best of the three options at conveying a sense of pressure to the user, such as the grasping force applied by the prosthetic limb during object manipulation. Based on this result, we developed a novel wearable haptic device that provides the user with knowledge of a normal force, by applying pressure at three different locations on the user's body. We then investigated how the simultaneous application of two different types of haptic feedback impacts human sensory perception, how vibrotactile stimulation can be used to convey a sense of texture, and how the amount of training that the human subjects receive affects their ability to successfully use the haptic system. Finally, our haptic device was integrated within a robotic system and we verified its effectiveness for use during pressure and texture recognition tasks.

Ultimately, our work contributes new knowledge about the relative effectiveness of different types of haptic feedback under static and dynamic modalities, so that haptic systems may be optimized for use under the conditions demanded by industrial and biomedical applications.

Keywords: Haptics, tactile feedback, touch sensitivity, wire actuator, static and dynamic modalities, proprioception, exteroception

CONTENTS

LIST OF TABLES

LIST OF FIGURES

LIST OF ABREVIATIONS

3D	Three-dimensional space
CoRo	Control and Robotics Laboratory
CÉR	Comité d'éthique de la recherche
ETS	École de Technologie Supérieure
Ee	End Effector
FA	Fast-Adaptive
F_m	Motor force
GPA	Dèpartement de gènie de la production automatisèe
GUI	Graphic User Interface
MDEIE	Ministère du Développement économique, de l'Innovation et de l'Exportation du Québec
MN	Manhattan Norm
NIB	Neodymium Magnet
NSERC	Natural Sciences and Engineering Research Council of Canada
PV1	Pressure and vibration applied simultaneously at the same location
PV2	Pressure and vibration applied simultaneously at different locations
P_{min}	Minimum torque
QA	Quick-Adaptive
RA	Rapid-Adaptive
SA	Slow-Adaptive

SD	Standard Deviation
SE	Standard Error
VP1	Vibration and pressure applied simultaneously at the same location
VP2	Vibration and pressure applied simultaneously at different locations

LISTE OF SYMBOLS AND UNITS OF MEASUREMENTS

θ	Angle
A	Area
D	Diameter
f	Frequency
gr	Gram
G	Gravity
k	Stiffness factor
kg	Kilogram
L	Length
ϕ_{min}	Minimum twisting angles
N	Newton
Nm	Newton meter
Nm/rad	Newton meter per radian
R	Radius
τ_s	Rotational stiffness
rad	Radian
T_m	Rise time
sec	Second
ϕ	Twisting angle

λ	Time constant
τ	Torque

INTRODUCTION

Tactile receptors in human skin are a crucial link between ourselves and the outside world, allowing us to feel our way around even when we cannot see. The sense of touch thus allows most people to complete simple tasks without constantly needing to look at what they are doing. Unfortunately, due to the lack of touch sensitivity in current prostheses, upper-limb amputees do not have this ability. To provide tactile receptors to amputees, is, therefore, to provide freedom from the need for constant visual attention.

Despite the progress that medical science has made over recent decades, there has been relatively little change in the daily lives of people who suffer from upper-limb amputation. Considering the current number of amputees, this problem affects many people: studies claim that in North America alone, more than 0.3% of people are living with minor or major upper-limb loss or deficiency, and approximately $200,000$ amputations occur annually (Biddiss and Chau, 2007; Blank *et al.*, 2010). As a result, a significant portion of the population is dependent on the use of prosthetic limbs.

Although modern prosthetic hands look more like real human hands than their predecessors, most prosthetics still use the conventional hook at the end that does not provide any sensory feedback (Yoshikawa *et al.*, 2013). This forces amputees to rely primarily on their vision to gather information about any types of environmental modalities or the surface properties of objects they encounter. A study of $2,477$ upper-limb amputees highlights the qualities that researchers should prioritize Atkins *et al.* (1996). According to the study's participants, the ideal prosthetic hand will: 1) allow ordinary tasks to be completed without requiring as much visual attention; 2) allow small and large objects to be grasped more firmly; and 3) be more like a real human hand in overall look and function. Indeed, beyond the simple mechanical structure and limited functionality of current prosthetic hands, the inability to transmit exteroceptive and proprioceptive information through the nerves makes them extremely difficult to control (Klinge, 1972; Prior *et al.*, 1976; Davis *et al.*, 2000). Overcoming these problems requires a more mechanically-sophisticated prosthesis, such as an under-actuated hand (Baril

et al., 2010). We hope that further developments in this area will provide the enhanced versatility, gripping capability, and touch sensitivity that are so highly in demand.

Aside from mechanical functionality, prosthetic limbs that function at the same level as the human sensory apparatus must be able to sense both static and dynamic events. For unimpaired people, tactile events are detected by an extensive network of tactile receptors that are spread throughout the skin, and that enable the conscious perception of touch (Lederman and Klatzky, 2009; Hager-Ross *et al.*, 1996). Any task that involves the skin coming into contact with an object will activate either the fast-acting (FA) or slow-acting (SA) group of mechanoreceptors, which immediately transmit information through the nerves to the brain so that the person may react properly to the given stimuli (Dargahi and Najarian, 2004; Ferrington *et al.*, 1977).

Several researchers have proposed haptic feedback as a way to compensate touch sensitivity to upper-limb amputees (Kim and Colgate, 2012; Bark *et al.*, 2009; Gillespie *et al.*, 2010). A haptic feedback system restores the sense of touch to amputees by completing the communicational loop between an external stimulus and an amputee's brain (Kim *et al.*, 2013). It does this by taking an external stimulus that cannot be perceived by the user, like an object's texture or motion, and turning it into a different type of stimulus that the user can easily recognize. Sensation of tactile events can thus be restored using a haptic interface that applies normal stress, shear, and vibration to the amputee's skin (Lee *et al.*, 2004; Caldwell *et al.*, 1999; Okamura *et al.*, 1998). However, the haptic system must meet several conditions in order to play the part of the missing tactile receptors: it must be able to sense the surface properties of an object, convert this information into the appropriate type of stimulation, and then apply this stimulation to the user (Kaczmarek *et al.*, 1991; Caldwell *et al.*, 1999), in a way that the user can quickly understand.

Amputees who lack touch sensitivity due to the loss of upper limbs may be able to compensate the sense of touch through the use of a haptic feedback system involving prosthetic fingertips equipped with tactile sensors (Tanaka *et al.*, 2007; Beebe *et al.*, 1998). As can be seen from Figure 0.1, the prosthetic fingers will recognize an object's properties or grasp quality (i.e.,

how well an object is being grasped by the robotic hand), and transfer this information to the haptic device, which then applies the desired type of stimuli to a healthy part of the user's skin.

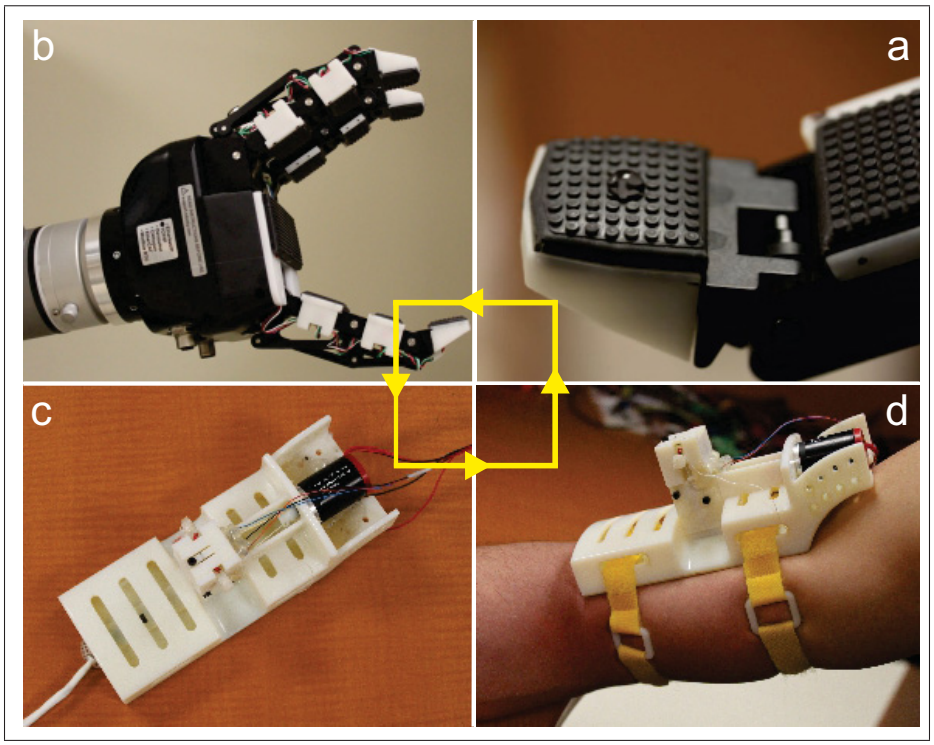

Figure 0.1 The loop of human interaction through the sensory robotic hand-gripper and a haptic interface. The tactile sensor (a) mounted on robotic fingers (b) detects an external event. Tactile information is then transferred to the haptic interface (c) and the device applies the desired stimuli onto the human forearm (d)

Researchers face many challenges in achieving this goal. They must design modern prosthetic limbs that are capable of the same functions as the human hand, and that are optimized to satisfy the amputees who use them.

Objectives and Scope of Study

The main objective of our research is to compensate touch sensitivity to upper-limb amputees through the use of haptic feedback. In the pursuit of this goal, we have several more specific objectives that we must accomplish:

a. To design a wearable haptic device for restoring touch sensitivity under static and dynamic modalities:

   - By comparing the effectiveness of normal stress, skin stretch and vibrotactile stimulation to convey information about static events; and
   - By prototyping and validating a novel twisting wire actuator-based haptic device, for providing feedback of tactile pressure information.

b. To examine the effectiveness of haptic feedback during task-oriented experiments:

   - By investigating the impact of simultaneously applying two or more types of stimuli to different areas of the human body; and
   - By studying the use of normal stress to convey steady pressure information, and vibrotactile stimulation to restore texture recognition capabilities.

The mechanoreceptors in human skin are responsible for detecting a tactile event and transmitting it to the nerves. The lack of a sensory system in current prosthetics causes amputees to require continuous visual attention for the accomplishment of any task.

We hope that by means of various tactile sensors mounted on the prosthetic fingers, the needed information will be passed through the haptic interface that is placed on the healthy parts of the amputee's body. This research is mainly focused on information that has been obtained from tactile sensors, and how this information can be transmitted to amputees via a haptic interface.

In this research project, we followed a long goal-oriented approach to provide a functional study that can be used in the next generation of prosthetic applications. We began our research by finding the proper way to stimulate the tactile receptors, according to the conditions of different events (i.e., static or dynamic). We then designed and prototyped a haptic device, and investigated the impact that different types of modalities have on each other. Finally, we carried out several task-oriented experiments in order to prove the functionality of our mechanism.

Impact on Industry and Society

Considering the current state of prosthetics that we have described above, this project has the potential to have a significant social impact by restoring the partial sense of touch to amputees. It may also prove fruitful to investigate the use of haptic devices for industrial robotic applications. For instance, it could be possible for robots to be used in dangerous environments, while haptic feedback allows a human to control the robot from a safe distance away. For this reason, our research has been funded by the Natural Sciences and Engineering Research Council of Canada (NSERC) and the Ministère du Développement économique, de l'Innovation et de l'Exportation du Québec (MDEIE).

Organization of the Thesis

Chapter 1 - To carry out the research project, we will need to examine the anatomy of the human body, and the design and assembly of different mechanical components. This section provides a comprehensive review of current touch sensitivity systems, the different mechanisms that can be used for prosthetic applications, and recent approaches that have been used in haptic technology.

Chapter 2 - The first phase of the project is to explore the different methods that can be used to convey static event information. In this section, we conduct an experiment to compare the exteroceptive feedback of normal stress, tangential force, and vibrotactile stimulation, in which each device provides feedback while pressure is applied to the finger pads of human subjects. The subjects then attempt to press on a force sensor with the same amount of pressure that the devices had conveyed to them through the haptic feedback. Results show that normal stress (normal pressure) is a functional way to convey static pressure information.

Chapter 3 - We present our design of a wearable haptic device, that can apply pressure based on the information that it receives from a tactile sensor, and that is based on a twisted wire actuator. The third chapter of this thesis will describe the whole procedure: the background of

the twisted wire mechanism, kinematic and static analysis, the design process, and the tests for validation under different conditions.

Chapter 4 - Here, we investigate how the simultaneous application of two different types of haptic feedback impacts human sensory perception. Now that we have designed a haptic device for the purpose of applying pressure, by means of a vibrator motor implemented with the mechanism, we can apply both vibrotactile stimulation and normal stress at the same time. Our experiments test whether subjects experience more or less accurate sensory perception when vibration is applied in different combinations: at the same time as the normal stress, at a different time, at the same location, and at a different location (6 cm away).

Chapter 5 - In this section we develop a robotic system that is used to study the restoration of touch sensitivity. The robotic system is composed of a combination of tactile sensors, robotic fingers, and a haptic interface. We conduct two separate tests on eight human subjects in order to assess the effectiveness of the static and dynamic modalities in different detectable ranges of skin sensitivity.

Chapter 6 - We present a vibrotactile haptic feedback system for use under dynamic conditions, verify its functionality, and show how results may be affected by the amount of training that subjects receive. We hope that by using vibrotactile feedback to distinguish between different textures, upper-limb amputees may be able to partially compensate the sense of touch.

Chapter 7 - We test a robotic sensory system (that includes the use of haptic feedback) by having subjects attempt to use it to carry out simple tasks that humans may encounter in their everyday lives. These tasks require grasping, pushing, and pressure-application skills, in order to determine the functionality of the proposed mechanism under various conditions.

Chapter 8 - In the last section of this thesis, we conclude our research and discuss the work that remains to be done in future studies.

CHAPTER 1

BACKGROUND AND REVIEW OF LITERATURE

1.1 Introduction

To carry out the research project, we will need to examine the anatomy of the human body, and the design and assembly of different mechanical components. The present section provides a comprehensive review of current touch sensitivity systems, the different mechanisms that can be used for prosthetic applications, and recent approaches that have been used in haptic technology.

We begin the section by briefly defining some critical terms in the field of touch sensitivity. Our discussion will include an overview of human tactile receptors, their capabilities, and the correct method of stimulating them. We will then consider the different mechanisms that have been used in haptic technology, to provide the context for our innovations in this area. Finally, we will discuss the scientific originality of our research.

1.2 General Definitions

1.2.1 Somatosensory Systems

Human skin involves a vast network of nerve endings and tactile receptors called the somatosensory system. Johansson and Vallbo (1979) estimate that more than $17,000$ tactile receptors exist in the glabrous skin area of the hand alone. The somatosensory system allows us to recognize the tactile properties of an object, and react to any external events that occur during physical contact with the object. Patrick Dougherty (2013) has shown that the system also provides proprioceptive information, allowing us to know how our body parts are spatially positioned. This system also informs us of pain, itching, environmental temperature, and in general anything related to our surroundings.

As shown in Table 1.1, the sensation of pain, temperature, touch, and proprioception are the fundamental modalities that are processed by the somatosensory system. Each of these modalities, depending on its type and intensity, can also be divided into several sub- and sub-sub-modalities. For example, discriminative touch can divided into four different sensation sub-modalities, namely vibration, flutter, pressure, and simple touch.

The next two sections of the table involve the different anatomical pathways along which the sensory information travels. As one can see by looking at the list of somatosensory pathways, this information is carried by certain neurons, based on the type of tactile information that the neurons are conveying. For instance, based on the literature provided by Patrick Dougherty (2013), the spinothalamic pathways carry information regarding the pain and temperature of the body, whereas the spinal trigeminal pathway carries the same information from the face. For discriminative touch and proprioception, this process is limited to the medial lemniscal (body) and main sensory trigeminal (face) pathways.

Table 1.1 The sensory modalities represented by the somatosensory system (Patrick Dougherty, 2013)

Modality	**Sub Modality**	**Sub-Sub Modality**	**Somatosensory Pathway (Body)**	**Somatosensory Pathway (Face)**
Pain	sharp cutting pain	-	Neospinothalamic	Spinal Trigeminal
	deep aching pain	-	Archispinothalamic	
Temperature	warm / hot	-	Paleospinothalamic	
	cool / cold	-	Neospinothalamic	
Touch	itch, tickle & crude touch	-	Paleospinothalamic	
	discriminative touch	touch	Medial Lemniscal	Main Sensory Trigeminal
		pressure		
		vibration		
Proprioception	Position: Static Forces	muscle length		
		muscle tension		
		joint pressure		
	Movement: Dynamic Forces	muscle length		
		muscle tension		
		joint pressure		
		joint angle		

1.2.2 Somatic Stimuli

Mechanical forces such as vibration, pressure, temperature changes, and even chemical reactions are the somatosensory stimuli to which the neurons are most sensitive. Among them, discriminative touch, and the proprioceptive systems (as shown in Table 1.1) are the ones that are most sensitive to a variety of mechanical forces. These forces include normal and tangential forces which result in skin displacement and shear (skin stretch), and the linear and rotational vibrations that characterize dynamic sensitivity capabilities.

1.2.2.1 Tactile Stimuli

Tactile stimuli are the external forces that are applied to the skin during physical contact. These forces enable us to perceive discriminative touch. Each of the sub-sub sensory modalities provides a certain type of touch sensitivity depending on how the object is being manipulated (Davis *et al.*, 2000). For instance, a minimal force resulting from the brief touch of an object results in very little distortion of the skin (Patrick Dougherty, 2013). This nominal force can become a greater force and can cause so much skin displacement in the given direction that it is finally categorized as the pressure in discriminative touch. Also, the movement of skin across a rough surface can provide motion sensitivity to the skin.

1.2.3 Exteroception and Proprioception

Exteroception and proprioception, which are also known as supplementary sensory feedback, are the fundamental parameters that enable us to interact with our surroundings (Davis *et al.*, 2000; Prior *et al.*, 1976). Exteroception is the feedback of cutaneous receptors reacting to various stimuli originating from outside the body (Childress, 1980). These outer stimuli can involve touch, pain, taste, or whatever is imposed by the environment. Proprioception is defined as the intuitive sense, with no visual attention required, of the relative positioning of one's body parts in space (Blank *et al.*, 2010).

1.2.4 Sensory Receptors (Mechanoreceptors)

In the somatosensory system, mechanoreceptors are among the skin receptors that enable humans to recognize a variety of environmental modalities. These modalities include pressure, skin stretch, skin motion, the temperature of a contact surface, and high frequency vibrations (such as the vibrations that occur when an object is slipping out of one's grasp, or when one's hand is sliding across a surface). These modalities are the main parameters of skin sensations (Gonzalez-Crussi, 1989; Caldwell *et al.*, 1997; Provancher *et al.*, 2005). As shown in Figure 1.1, in the glabrous skin area there are four types of tactile units, which are classified according to the presence of two features: i) the structure of their receptive fields and ii) their rate of adaptation to sustained indentation (Vallbo *et al.*, 1984). These features enable researchers to place each type of mechanoreceptors into one of two categories, according to the speed of their adaptability: Fast-Adaptive (FA) and Slow-Adaptive (SA).

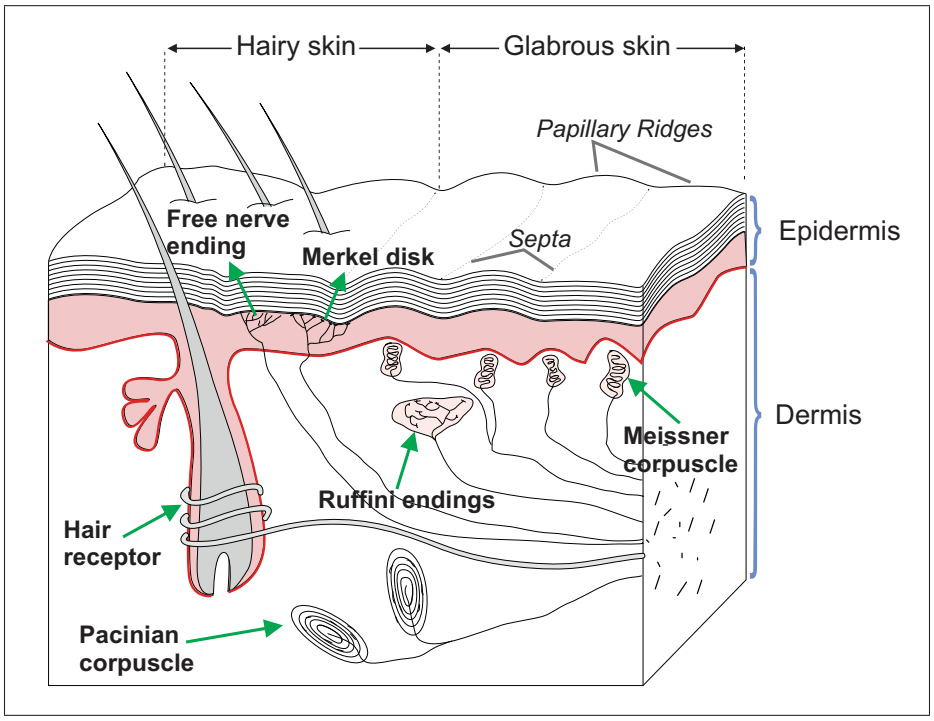

Figure 1.1 The locations of cutaneous receptors in the skin (Boundless, 2014)

Table 1.2 Summary of the location and function of skin mechanoreceptors (Dargahi and Najarian, 2004; Patrick Dougherty, 2013)

Receptor	Location	Activation Stimuli
Hair Follicle Ending	Hairy skin areas	Hair displacement
Ruffini Endings	Dermis of hairy and glabrous skin	Pressure and skin stretch
Pacinian Corpuscle	Deep layers of dermis	Motion and vibration
Meissner's Corpuscle	Dermis of glabrous skin	Flutter and vibration
Free Nerve Endings	Throughout the skin	Tissue damage and changes in temperature
Merkel Disk	Epidermis of glabrous skin	Pressure and texture

Table 1.3 Characteristics of skin mechanoreceptors (Caldwell *et al.*, 1997)

Receptor	Class	Receptive Field (mm2)	Frequency Range (Hz)	Receptors (cm2)
Pacinian Corpuscle	FC	10–1000	0–800	21
Meissner's Corpuscle	FA	1–100	10–200	140
Ruffini Endings	SA II	10–500	7	49
Merkel Disk	SA I	2–100	0.4–100	70

FA receptors are also known as Rapid Adapting (RA) or Quick Adapting (QA) mechanoreceptors. Researchers have estimated that more than 56% of the total number of tactile units consist of FA units. There are two sub-categories of FA mechanoreceptors, known as FA I and FA II (Figure 1.2). The first type, FA I, consists of Meissner corpuscles, and makes up 43% of the total number of tactile units. These occupy a small receptive field. The second type, FA II,

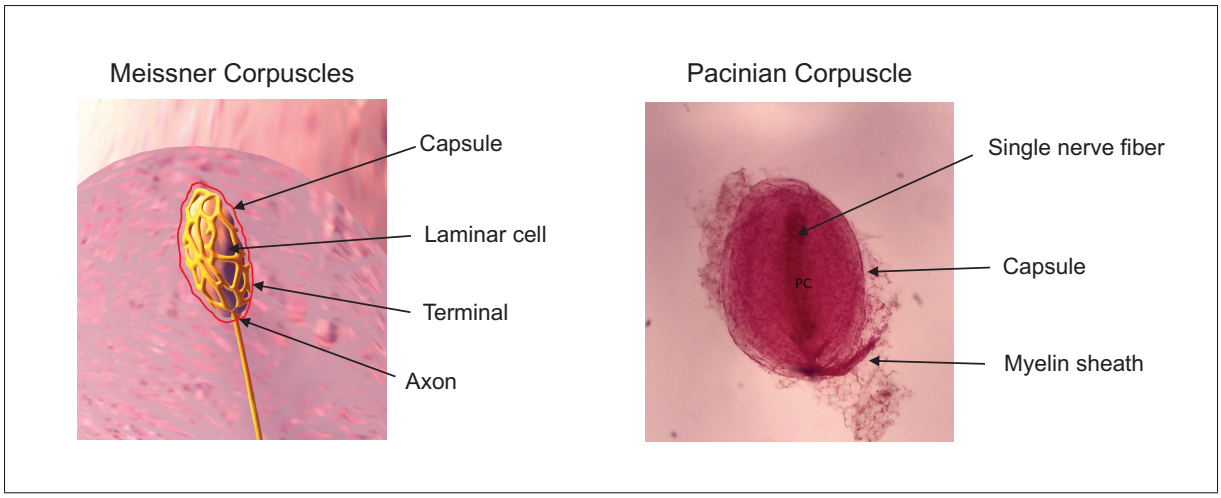

Figure 1.2 Fast adapting (FA) tactile receptors (Gallery, 2014)

consists of Pacinian corpuscles, and occupies a large receptive field. FA II receptors make up 13% of the total number of tactile units.

According to a terminology introduced by Iggo and Muir (1969), the Meissner corpuscles, located in the deep layers of the dermis, generally respond to pressure on the skin and to texture. The Pacinian corpuscles, meanwhile, are located in the epidermis of the glabrous skin area and respond directly to motion and vibration (Dargahi and Najarian, 2004; Provancher *et al.*, 2005).

SA tactile receptors are also sub-divided into SA I and SA II types. By comparison with the FA units, the SA tactile units constitute a smaller number of tactile units of the glabrous skin of the hand. Out of the 17,000 total tactile units, SA receptors make up approximately 44% (25% SA I and 19% SA II). In this group, Merkel nerve endings (Merkel Disk) in SA I and Ruffini Endings in SA II are considered the main tactile receptors (Figure 1.3). In accordance with Dargahi and Najarian (2004), the majority of Merkel Disks receptors are scattered throughout the epidermis of the glabrous skin area with the aim of responding to pressure applied to the skin and to texture. By contrast, the Ruffini Endings are typically distributed in the dermis of hairy and glabrous skin areas and respond to pressure and skin stretch.

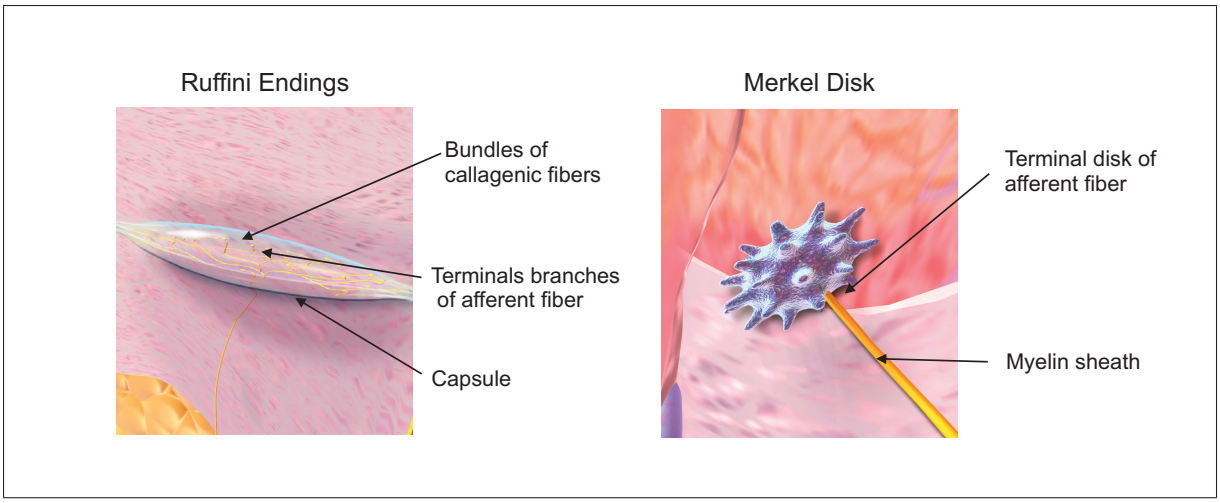

Figure 1.3 The slow-adaptive (SA) tactile receptors (Gallery, 2014)

1.2.5 Sensory Transduction

The membranes of both FA and SA mechanoreceptors contain bunches of ion channels that respond to various mechanical distortions by changing the amount of sodium and potassium. In this regard, the magnitude and duration of the applied forces have a direct relationship with the impulses. Whenever the magnitude of the applied forces is greater, there will be greater depolarization of the ion channels. By contrast, forces that are applied for a greater length of time will take longer to depolarize.

As shown in Figure 1.4, mechanoreceptors encode the tactile information as a series of pulses, similar to those used in digital serial communications. These serial communications may vary depending on the magnitude of the force that is applied to certain types of tactile receptors. However, the behavioral responses of these receptors, whether regular or irregular, follow a unique pathway for each type. A summary of the mechanoreceptors' locations, functions, characteristics, and physical parameters is presented in Table 1.2 and Table 1.3.

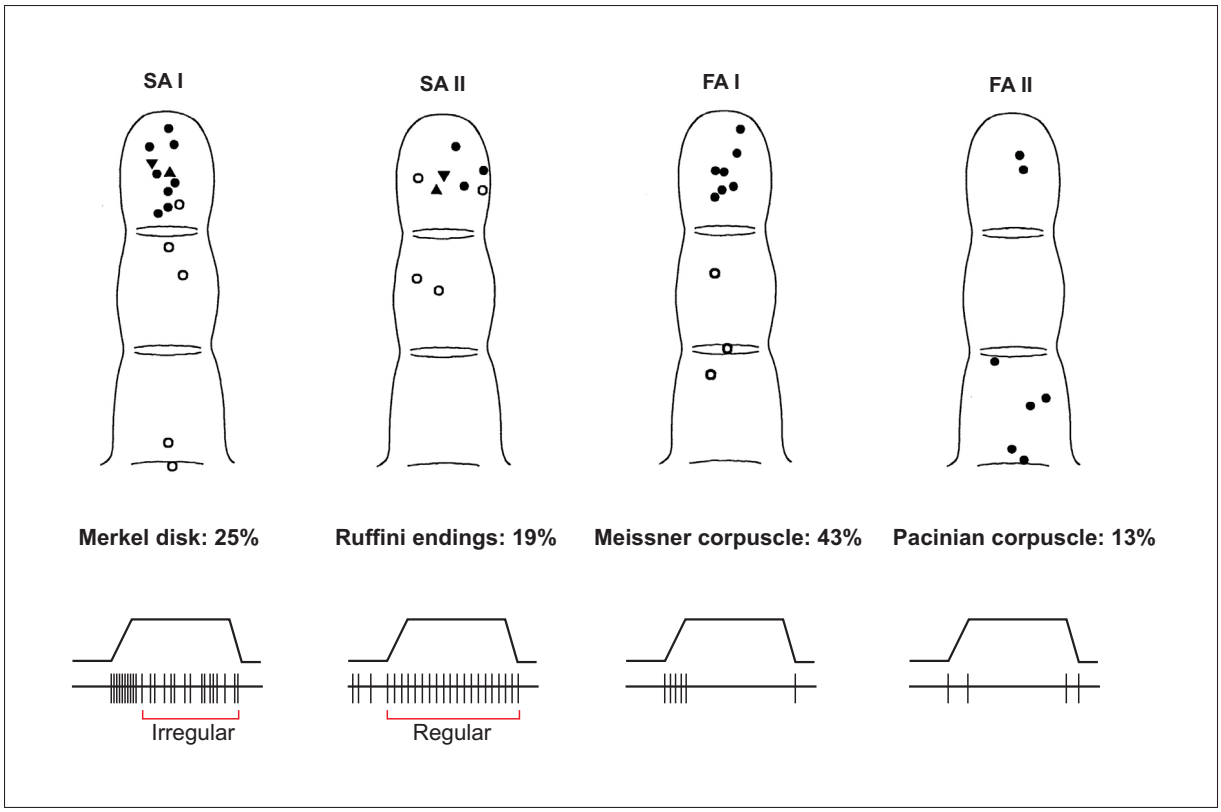

Figure 1.4 Responses of the four types of mechanoreceptors to normal indentation of the skin. The percentages listed indicate the relative number of each type of receptor that is found in the skin of a human fingertip
(Goodwin *et al.*, 1997)

1.2.6 Touch Sensitivity Thresholds of Various Areas of the Human Body

Lederman and Klatzky (2009) have presented an overview of human body perception (Figure 1.5). They provide information about "what" and "where" a system deals with perceptual functions. Figure 1.5 depicts the sensitivity thresholds of various parts of the human body, as measured by Weinstein (1968). The measurements are presented according to the results of two different methods: the point-localization method and the two-point threshold method.

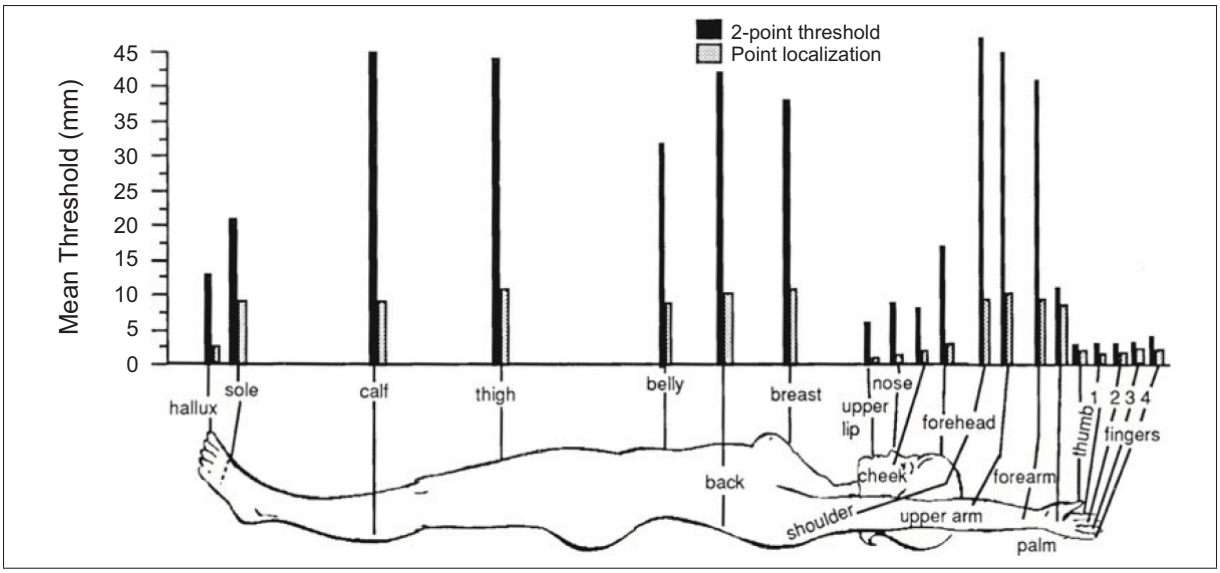

Figure 1.5 Two-point threshold and point localization measurements are shown for various areas
(Lederman and Klatzky, 2009)

1.2.7 Mechanoreceptor Stimulation Methods

There are a number of ways to stimulate tactile receptors. With regards to the objective of the present research, here we describe the most fundamental types of stimuli: normal stress (normal force), vibrotactile stimulation, and skin stretch (tangential force, shear force).

1.2.7.1 Normal stress

As shown in Figure 1.6, any compressing strain on the skin activates Merkel Disk and Ruffini Endings receptors. These are categorized as SA mechanoreceptors (Dargahi and Najarian, 2004), and are located in the epidermis of the glabrous skin area. They typically respond to steady pressure on the skin and to surface textures, and they provide the sense of contact with an external stimulus when it is applied slowly.

Within a haptic feedback system, applying pressure to the skin is considered the best way of informing us of any static modalities occurring in our surroundings. Normal stress can be used

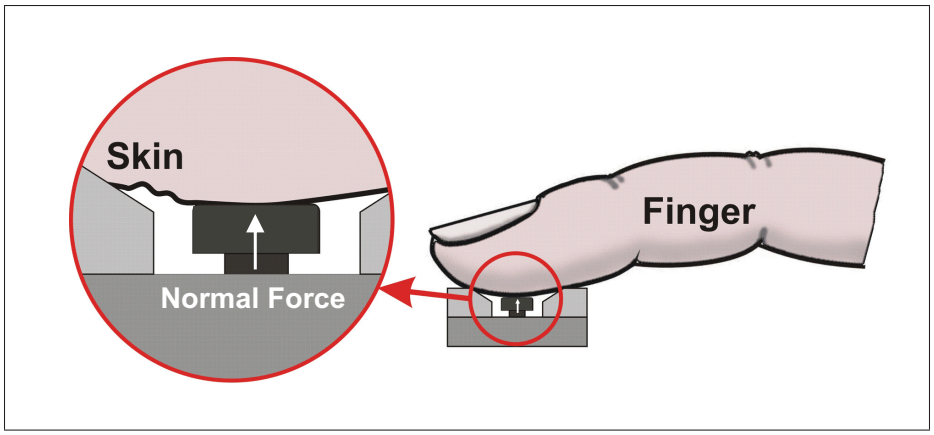

Figure 1.6 Normal force applied to the fingertip

at different magnitude levels, based on the amount of force that the object is applying to the skin (and vice-versa).

1.2.7.2 Vibrotactile Stimulation

The FA mechanoreceptors (Meissner and Pacinian Corpuscles) are not activated by pressure, but by vibration. This stimulus can be used for the feedback of dynamic modalities in a variety of receptive fields (Silverthorn, 2003). The FA receptors are very sensitive to even the slightest of variations, and react immediately to the given stimulation (Russell, 1990). Previous studies of vibrotactile stimuli have identified a functional range of $100 - 300\ Hz$ to ensure the proper stimulation of FA mechanoreceptors (Biggs and Srinivasan, 2002; Caldwell *et al.*, 1999).

Vibration is particularly useful in prosthetic applications due to its fast and convenient ability to restore a sense of motion (Damian *et al.*, 2011; Fortin *et al.*, 2014). It can be applied directly to the skin, and patients can quickly recognize its effect. Furthermore, when multiple vibrator motors are placed on the skin, vibrotactile stimulation can be used to provide a sense of motion and direction (Tan *et al.*, 2003). Among the various types of vibration motors available on the market, pancake and cylindrical motors are most frequently used in haptic interfaces (Biggs and Srinivasan, 2002; Yao and Hayward, 2010). Schätzle *et al.* (2006) have stated that pancake motors cause the skin to feel something like shear forces whereas cylindrical motors

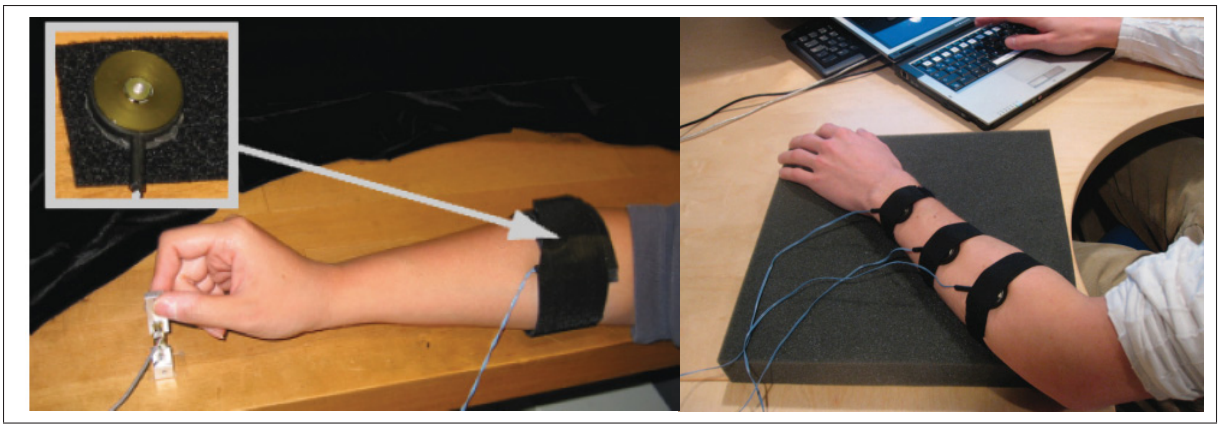

Figure 1.7 Vibrator motor attached to a person's forearm in order to provide haptic feedback
(Bark *et al.*, 2008)

cause normal forces. Both types of motors are compact in size and feature a wide range of vibrational amplitude and intensity; and both motors can stimulate vibration by using unbalanced inertia at various frequencies and amplitudes, based on the input voltage level.

1.2.7.3 Tangential Force and Skin Stretch

Unlike vibration, tangential forces result in skin stretch, which can activate both SA and FA cutaneous mechanoceptors. This stimulus is considered as a well-defined solution for use in wireless devices due to its low level of required power supply. Tangential forces are widely considered to be ideal for use in wireless devices due to the fact that they require a relatively small power supply. Previous approaches have thoroughly described the quick and accurate responses of mechanoreceptors to skin strain change (Edin, 2004; Paré *et al.*, 2002). Researchers have also developed innovations in the mechanisms behind the skin stretch (LaMotte *et al.*, 1998; Edin, 2001; Bark *et al.*, 2009). However, the impacts of skin stretch on the non-glabrous skin area in comparison with the hairy area have been largely unexplored.

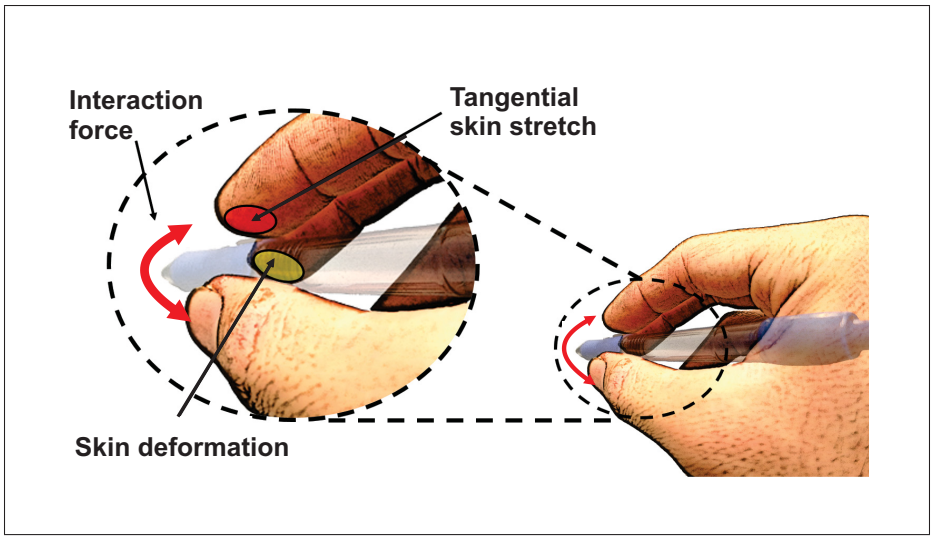

Figure 1.8 Tangential skin stretch evoked while holding a pen (Kirk *et al.*, 2015)

1.2.8 Haptics

According to Robles-De-La-Torre (2006), "haptics refers to the ability to experience the environment through active exploration, typically with our hands, as when palpating an object to gauge its shape and material properties."

In general, the word haptics refers to all touch-related exteroceptive and proprioceptive sensory capabilities. In this regard, haptic devices play a critical role in transmitting the sense of contact between the skin and objects. These devices are classified into either grounded or portable classes, as described below.

In the grounded class, the device is in a fixed location, limiting the freedom of motion of the user. This group of devices is capable of performing fixed-object simulation (Figure 1.9). Typically, tapping on both surfaces in a virtual environment and a soft foam, provides same feelings with this kind of haptic devices. Academic environments and industrial research laboratories are the primary users of this type of haptic device. The main advantages of these devices are the possibilities they offer for use within a virtual environment, and for simulating virtual touch sensitivities.

Figure 1.9 Left: High-definition haptic device. Right: PHANTOM Omni (Sensable, 2012; Quanser, 2013)

Portable haptic devices are capable of interacting with their surroundings without major restrictions (Figure 1.10). These types of haptic devices can be used in modern prosthetic limbs, and in industrial robotic applications, due to the freedom of the user's movement. For this reason, portable haptic devices will be the main focus of the present work.

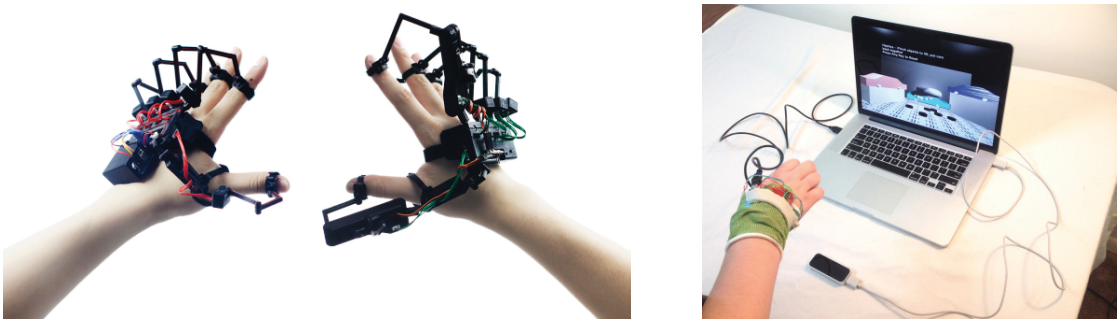

Figure 1.10 Haptic devices for the restoration of touch sensitivity (Dexta, 2014)

1.3 Related Works

Researchers have integrated haptic feedback with robotics in the hope of adding touch sensitivity to prosthetic limbs. In this section, we examine the different approaches that employ haptic feedback, and discuss the human touch sensitivity in different body organs. Finally, we describe the novel haptic interfaces that can be used in prosthetic applications.

1.3.1 Comparing the Advantages of the Different Types of Haptic Feedback

This subsection will begin with a description of pressure, and explain the types of static stimuli that can be used to convey pressure. The feedback can be applied vertically or tangentially, according to the desired effect. After going over these functionalities, we will proceed with a comparison of several other types of haptic feedback.

Applying pressure to one or two sides of the skin, or grasping a part of the body (e.g., an arm), can provide some information about vertical skin displacement (Figure 1.6). In this regard, Biggs and Srinivasan (2002) have investigated the relative effectiveness of tangential and normal skin displacement for producing tactile sensations. The authors state that "At both forearm and finger pad, subjects chose tangential displacements only 0.3 to 0.6 times as large as the reference normal displacement, indicating a significantly higher sensitivity to tangential displacement." The second key finding of this experiment is the greater sensitivity of the forearm to tangential force rather than normal force. By contrast, "the sensitivity of the finger pad to tangential force is lower than the normal force due to the approximately five-fold greater stiffness of the finger pad to tangential traction."

Narrowing over tangential forces, Paré *et al.* (2002) have provided the estimated magnitude of the tangential force that is applied to the distal pad of the index finger. They tried to determine the human tactile sensitivity in different levels of the tangential forces ranging from 0.15 to $0.70N$. As shown in Figure 1.12, they realized that the majority of the human subjects participating in the experimental test could scale magnitude levels of the normal forces

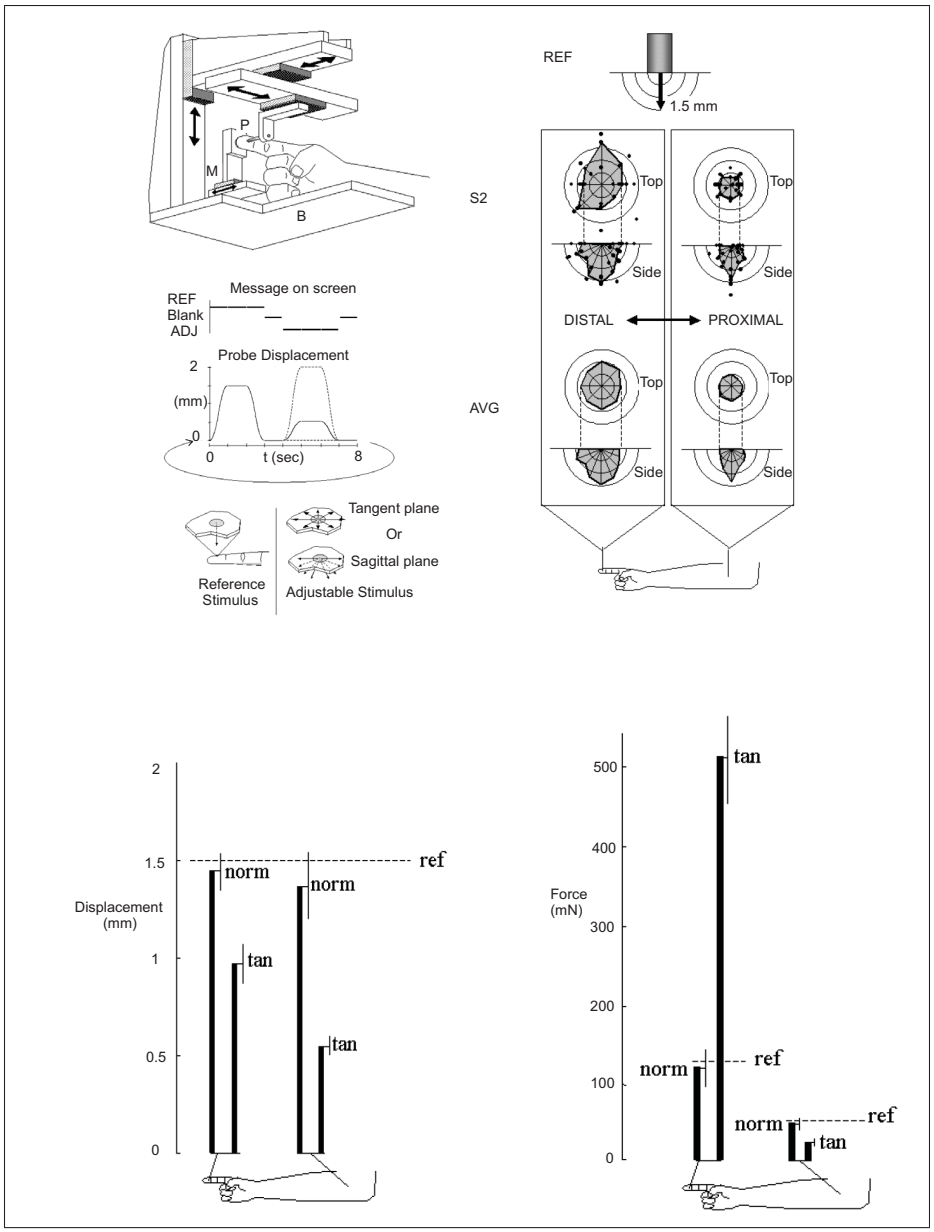

Figure 1.11 Points of subjective equality are shown for skin displacements in various directions on the finger pad (left column) and hairy skin of the forearm (right column). Plots at bottom, averaged over five subjects (AVG) showed no statistically significant difference in subjects' responses to displacements in different tangential directions
(Biggs and Srinivasan, 2002)

and the tangential forces. This led us to consider the potential of the skin stretch for further investigation.

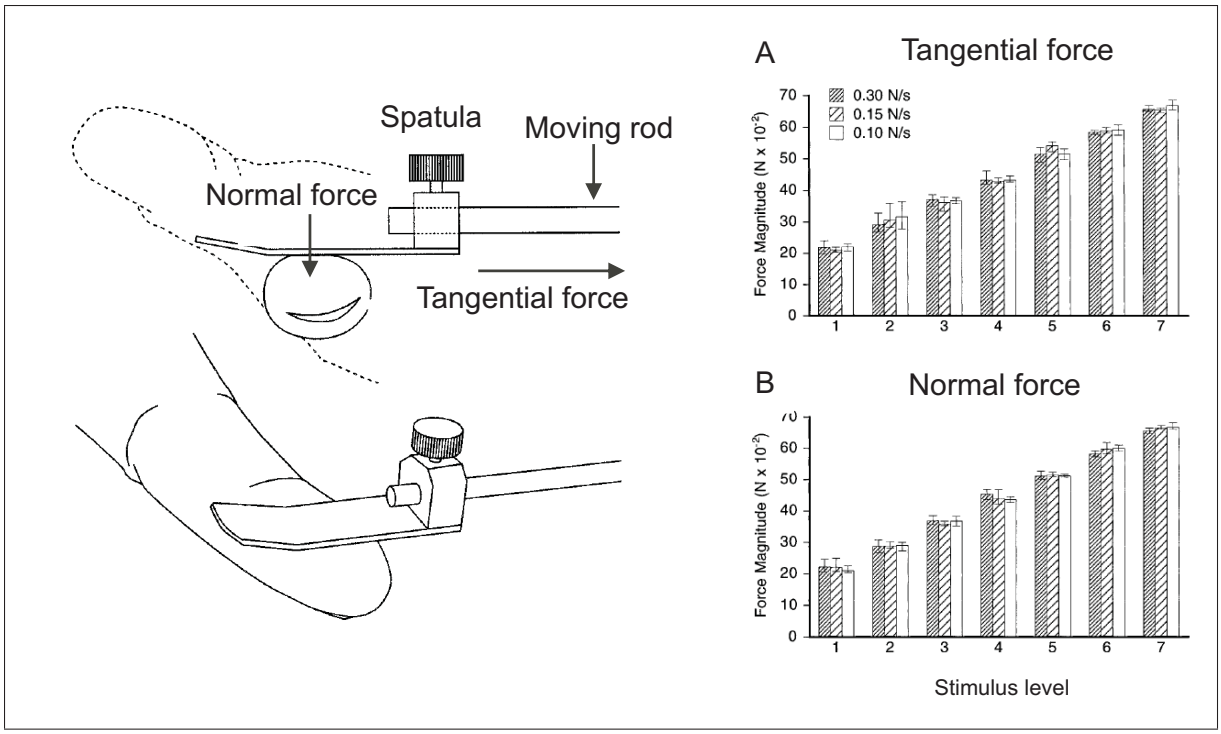

Figure 1.12 Histogram of mean applied force (five trials) for the seven force magnitudes and three rates of force application for both tangential (A) and normal (B) forces of one subject, along with the minimum and maximum values (error bars) (Paré *et al.*, 2002)

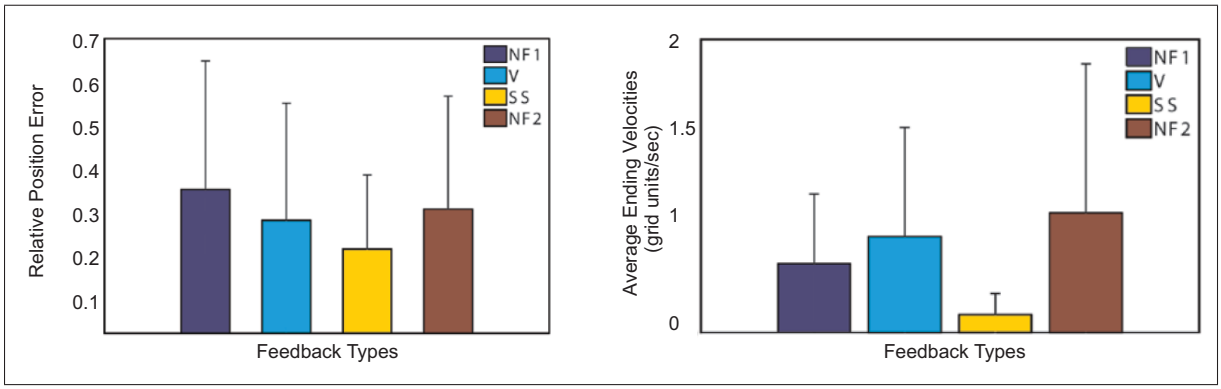

Figure 1.13 No feedback (NF1), vibration (V), skin stretch (SS), and the final no feedback case (NF2) (Bark *et al.*, 2008)

Biggs and Srinivasan (2002) believed that the tactile receptors on hairy skin are more sensitive to tangential force, whereas the receptors on glabrous skin and the finger pads are more sensitive to normal force.

Bark *et al.* (2008) compared the proprioceptive information of the skin stretch and the vibrotactile feedback (Figure 1.13). Their results showed that skin stretch (shear force) provides more reliable feedback, especially when the haptic device operates at low velocity and under low inertia. The authors suggest that the use of compact devices for applying shear force could be a good choice when worn on the human body. These devices can be used in different experiments that involve virtual environments, such as motion training during rehabilitation processes, and athletes' training.

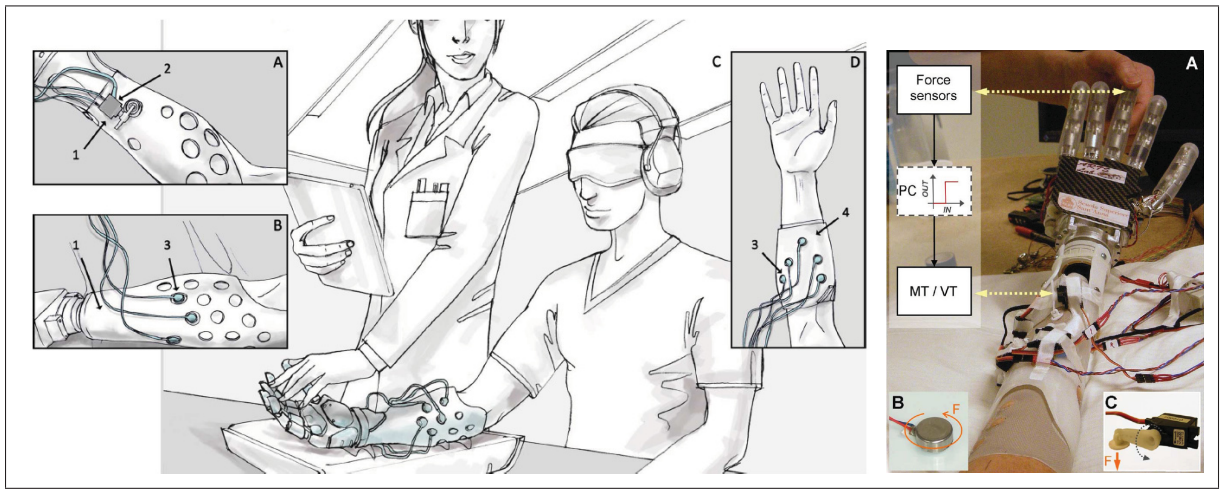

Figure 1.14 A) Placement of one of the mechanotactile stimulators on amputee's residual limb. B) Representative placement of a vibrotactile stimulator. C) Setup of experiment. D) Representative placement of vibrotactile stimulators on forearm of healthy subject
(Antfolk *et al.*, 2013)

Another interesting application is mapping (phantom hand mapping). Antfolk *et al.* (2013) set up an experiment on eight transradial amputees to assess their ability to distinguish between multi-site tactile stimuli in sensory discrimination tasks (Figure 1.14). They had two separate groups of participants (A and B) that were divided according to the integrity of their phan-

tom map. The A group contained participants with an intact phantom map on their residual limbs, whereas the group B contained participants with an incomplete or non-existent map. Results indicated that pressure provides more reliable feedback than vibration in multi-site sensory feedback tests. The researchers also showed that the participants of group A had better discrimination performances than those of group B.

1.3.2 Haptic Devices for Prosthetic Applications

A vast number of haptic devices have been developed for prosthetic applications with the goal of providing amputees with touch sensitivity. In this section, we explain the different types of haptic devices that are more specifically related to our applications.

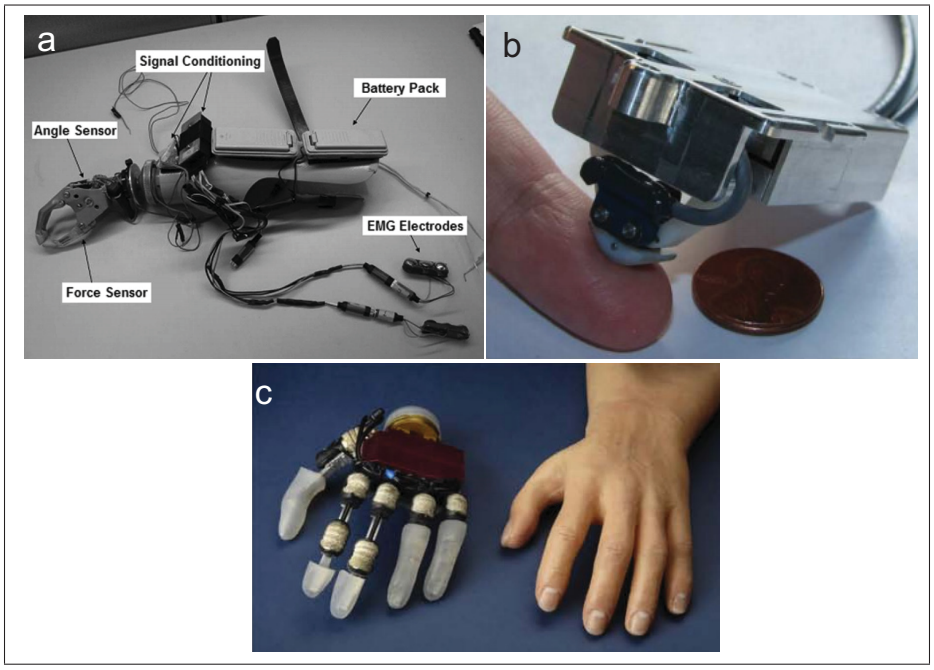

Figure 1.15 Prosthetic limbs used haptic devices
(Chatterjee *et al.*, 2008; Kim *et al.*, 2010; Kargov *et al.*, 2007)

Srinivasan and Basdogan (1997) states that the human hand consists of 19 bones, which are connected by joints and covered by soft tissues and skin. In order to develop a haptic interface designed for optimal interaction with the amputee, it is necessary to fully realize the role of

the sensory, mechanical, and cognitive subsystems of the haptic device. To this end, a haptic feedback stimulator has been designed by Chatterjee *et al.* (2008) to assess the control of the grasp force at three different target force levels. A series of tests, done on eight subjects, proved that the control of the grasping force in prosthetic users can be improved by using a haptic feedback system (Figure 1.15 a). Clearly, it will be important to integrate haptic feedback systems with prosthetics in order to improve the user's experience.

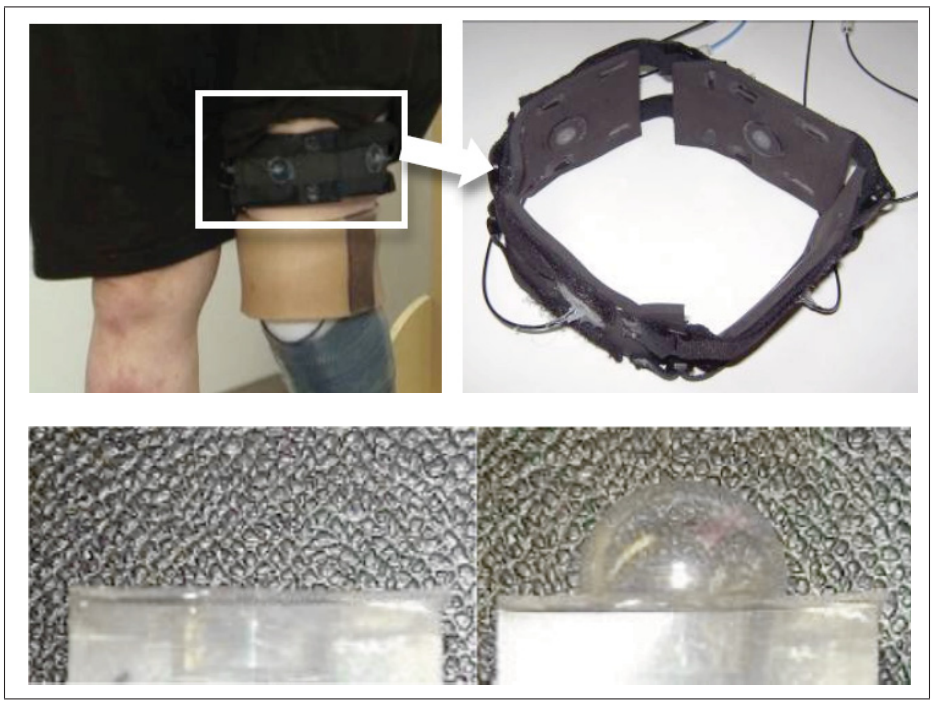

Figure 1.16 The ergonomic cuff worn on the residual limb of a lowerlimb-balloon based haptic feedback actuator. Left: no inflation. Right: Full hemispherical inflation (Fan *et al.*, 2009)

While our study is focused on prosthetic applications, it is interesting to note how haptics are used in the surgical field as well. Kim *et al.* (2010) presents a design of a miniature haptic device for upper-limb prostheses. Interestingly, this device is capable of conveying numerous aspects of touch to the skin of an upper-limb amputee, including normal and shear force (static), vibration (dynamic), and temperature (thermal). It is especially effective for females who have had tubal reserval surgery (TR) (Figure 1.15 b).

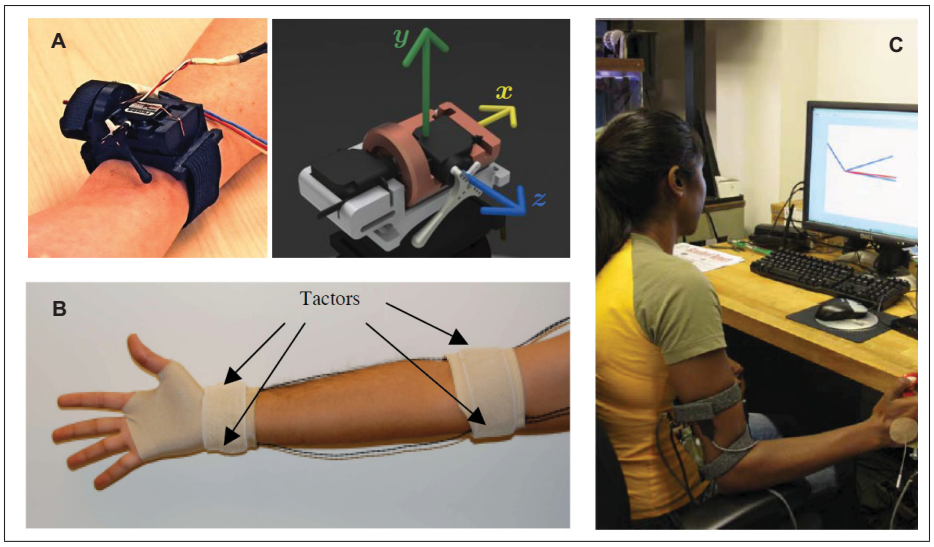

Figure 1.17 A) The master device for real-time control of the dragger. B) Vibrotactile rehabilitation system. C) Skin stretch haptic interface attached to subject's arm (Stanley and Kuchenbecker, 2011; Kapur *et al.*, 2009; Wheeler *et al.*, 2010)

Kargov *et al.* (2007) describe the development of a multifunctional device capable of restoring sensory and motor ability to the amputees. The paper discusses the high-power actuating method that the researchers used to maximize the potential benefit of using upper-limb prosthetics. It also describes how mechanical vibration can be used to obtain the optimal sensory feedback (Figure 1.15 c).

After presenting technology that uses haptic devices to compensate touch sensitivity, it is time to focus more precisely on haptic interfaces that have been mainly developed as independent devices to restitute one or multiple modalities in the human subject. For instance, Fan *et al.* (2009) have developed a haptic feedback rehabilitation system that can be used for lower-limb amputees. Their haptic device is actually a balloon-based actuator that can restore the tactile feedback of static events (Figure 1.16).

As can be seen from Figure 1.17, there are a number of devices that can compensate touch sensitivity to upper-limb amputees through the use of different types of haptic feedback (normal forces, vibrotactile, and skin stretch). Stanley and Kuchenbecker (2011) have designed a

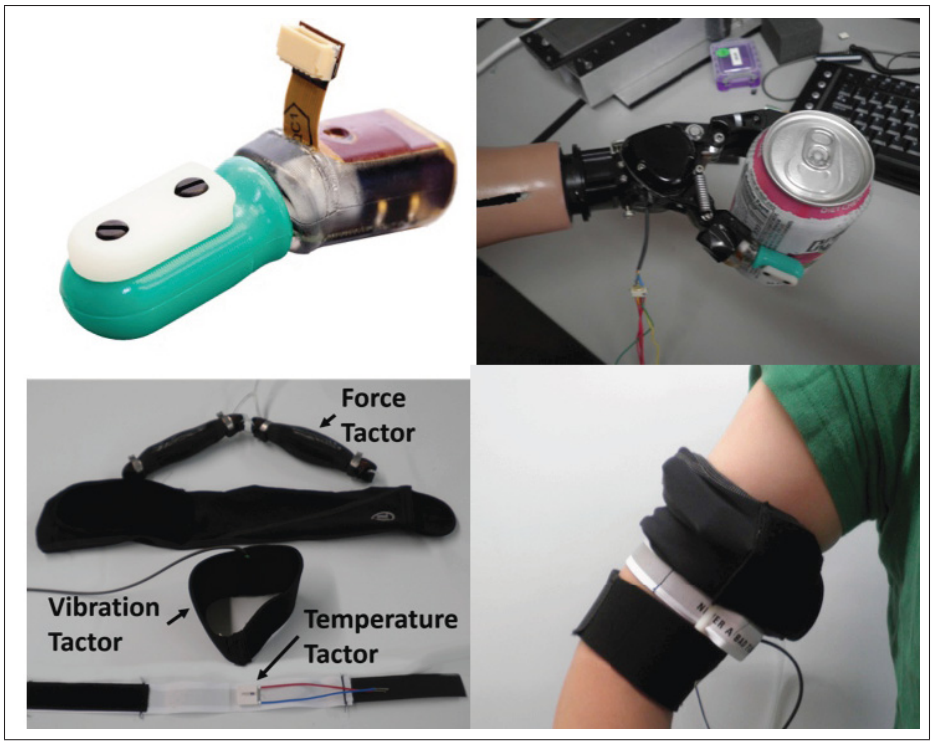

Figure 1.18 Top-Left: Multimodal BioTac tactile sensor. Top-Right: Prosthetic hand equipped with multimodal tactile sensors Bottom-Left: Various tactors. Bottom-Right: Tactors worn by subject
(Jimenez and Fishel, 2014)

wearable body-grounded tactile actuator for feedback of human physical contact (Figure 1.17 A). Kapur *et al.* (2009) have created a vibrotactile feedback system made by different tactors for intuitive upper-limb rehabilitation (Figure 1.17 B). Finally, Wheeler *et al.* (2010) have investigated the rotational skin stretch with a myoelectric haptic application (Figure 1.17 C).

The work that is most similar to what we are doing, in designing a haptic device, is by Jimenez and Fishel (2014) and Matulevich *et al.* (2013). As can be seen in Figure 1.18, they have designed a wearable haptic device to evaluate the force, vibration, and thermal tactile feedback in prosthetic limbs. As they describe, the proposed system can transmit tactile information to the amputee in order to identify the weight, temperature, and thermal properties of the objects or surfaces in contact.

1.4 Scientific Originality of the Research

For years it was believed that prosthetic devices could never convey an artificial sense of touch to users, because of the complex structure and external power supply and control systems that they would require. However, over the past two decades continuous progress in haptic technology has restored hope in the prospect of providing amputees with the sense of touch.

While much work has been done towards this goal, our review of the literature showed that the majority of research in haptics and prosthetics has focused on a single area. In prosthetics research, the main focus was on conveying proprioceptive, rather than exteroceptive feedback. In haptics research, many haptic devices have been designed to convey just one type of feedback, generally either pressure, skin stretch, or vibration, so they are suitable for use under either static or dynamic conditions, but not both. Few researchers, meanwhile, have attempted to convey multi-modal exteroceptive feedback by means of portable haptic devices, for use in prosthetic and industrial applications. As concluded by Chatterjee *et al.* (2008), neither the current commercially-available prosthetic devices, nor the latest versions that have come out of research laboratories, are very portable and easy-to-use.

At present there is a need for more multi-responsive actuated devices. We aim to design a portable haptic device that will apply both pressure and vibrotactile feedback to the user, so that the device can be used for conveying information under both static and dynamic conditions. The simultaneous application of multiple types of feedback might help amputees to minimize, and possible even eliminate, the visual attention they must pay during everyday life. Furthermore, our research will attempt to answer several questions. These include: what is the optimal type of exteroceptive feedback for conveying information through the human sensory system? Which area of the body is most effective at recognizing such haptic feedback?

From a design perspective, we intend our device to be portable, light-weight, and durable, as well as effective enough to have a significant impact on the market for prosthetic devices. Finally, we hope our research will inspire further investigation in this field.

CHAPTER 2

COMPARING DIFFERENT TYPES OF STIMULATION METHODS FOR RESTITUTION OF STATIC EVENTS UNDER EXTEROCEPTIVE CONDITIONS

2.1 Introduction

In this chapter, we seek to determine the most effective type of haptic feedback, whether normal stress, tangential force, or vibrotactile stimulation, for conveying a level of force that is applied to the subjects' finger pads. Our main goal is to use haptic feedback to alert amputees about how their prosthetic limb is interacting with the environment. The results could pave the way for further research in developing a prosthetic hand system that uses haptic feedback to compensate for the dearth of touch sensitivity.

To this end, we begin by describing the technological components of our experiment, specifically the actuator and vibrator motor that we used. We then discuss the procedure of the experiment, including the participants and the exact method that was used to produce the static and dynamic stimuli. Next we present our results and explore the functionality of each type under static conditions. We conclude with a discussion of the factors influencing our results, and explore how future work might improve upon our current study.

2.2 Materials and Methods

As can be seen from Figure 2.1, the experiment was performed using three types of feedback: normal force, tangential force, and vibrotactile stimulation. The protocol of our experiment was approved by the Ethics Committee of Research (Comité d'éthique de la recherche, or CÉR) at École de Technologie Supérieure (ÉTS), Montréal, Canada.

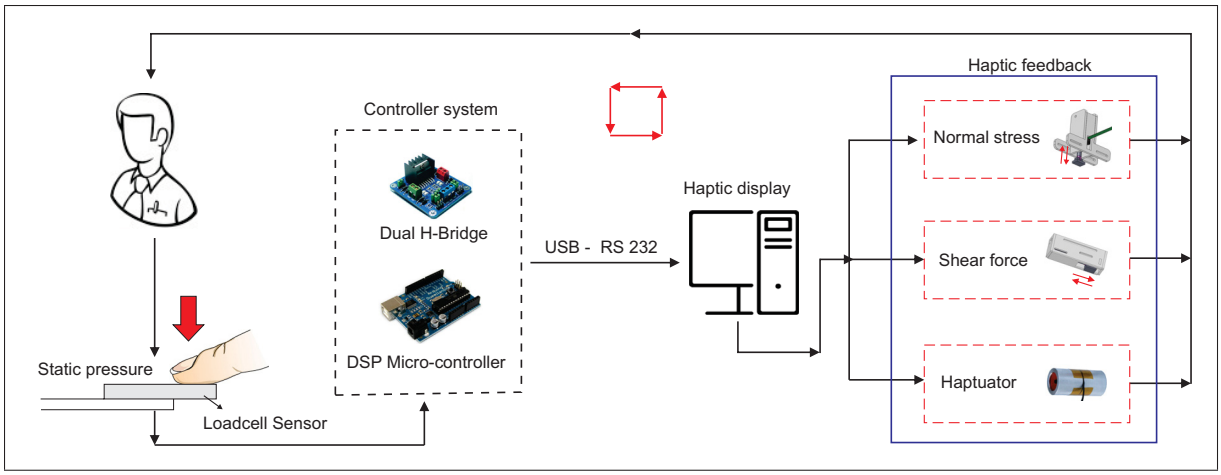

Figure 2.1 Architecture of the experiment

2.2.1 Subjects

The subject population consists of six men and six women, ranging in age from 22 to 34. The majority of the subjects were recruited from among the students of ÉTS. Subjects were informed of the procedures prior to starting the experiment, and all signed the participation form.

2.2.2 Vibrotactile Apparatus

The vibrotactile stimulator we used is an unbalanced linear vibrator called the Haptuator (Figure 2.2), made by Tactile Labs, Inc. Yao and Hayward (2010). The Haptuator is a vibrotactile transducer with a bandwidth of 50-500Hz, and it depends on frequency as well as voltage for the oscillation of mass in its formation. For better performance, a signal source was used to supply a sine/square wave with various frequencies and amplitudes. As this device has a low input impedance (8Ω), an Op-amp was used for impedance matching to avoid current loading and voltage fading. During the experiment, the signal was transmitted from a function generator to a signal conditioner, the LM675 IC op-amp, to provide vibration at the output. A serial communication cable (RS-232) was used to form a loop between the actuator, the micro-controller (DSP 56807), and the user interface.

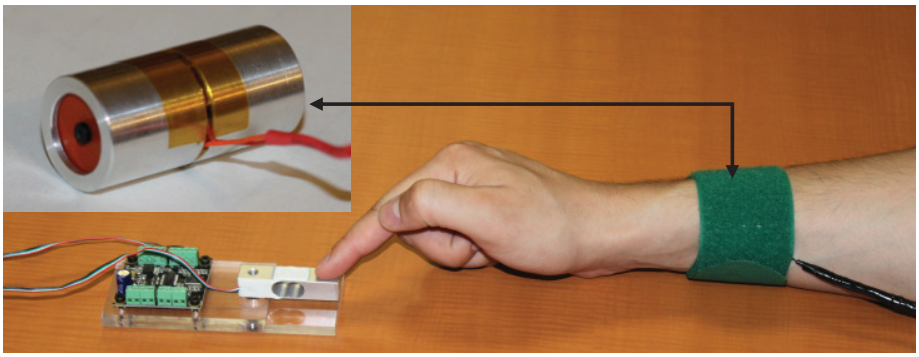

Figure 2.2 Linear unbalanced vibrator motor used to produce vibrotactile stimulation

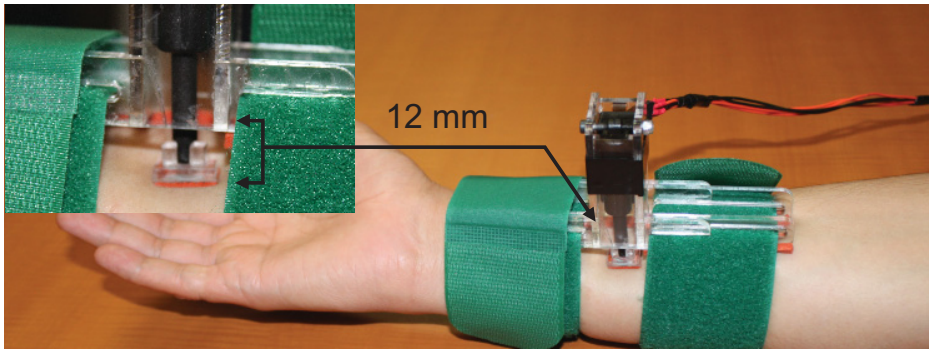

Figure 2.3 Application of normal stress (normal force) to the glabrous skin area

2.2.3 Normal and Tangential Force Apparatus

Two miniature linear-motion actuators (PQ12 from Firgelli Technologies, Inc.) were used for this stage of the experiment. We used one of the actuators for the normal force device, and the other for the tangential force-application device. The PQ12 features position feedback to provide more sophisticated position control, and is capable of pulling a load along its full stroke length. The input voltage of the actuator was 6 V DC, with maximum a load of 20 mm. This

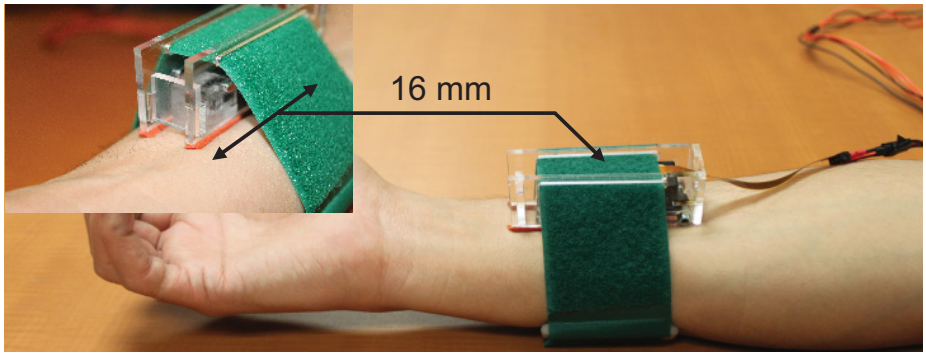

Figure 2.4 Application of tangential force (shear) to the glabrous skin area

enabled us to determine the speed of movement of the end effector. When power is cut off, the actuator will hold its position, unless the load is applied in the back-drive. The final prototypes of the two devices are shown in Figure 2.3 and Figure 2.4.

Figure 2.5 shows the specifications of the PQ12 actuator. The three gearing options (30:1, 63:1, 100:1) give us the possibility of having various force configuration ratios. Each force configuration ratio represents a trade-off between force and motion. The ratio of 30:1 is lower in force but faster in motion; 63:1 provides moderate levels of both speed and motion; and 100:1 is higher in force but slower in motion.

2.3 Experiment

2.3.1 Stimuli

Subjects were manually exposed to the three types of stimuli. In both normal force and tangential force tests, forces were delivered at five different levels ranging from 2 N to 10 N (increasing in increments of 2 N). A rectangular unit (14 mm $\times$ 10 mm) was placed at the head of the piston to act as an end effector. This was done for both the normal and the tangential devices in order to enlarge the area of contact between the piston and the subjects' skin.

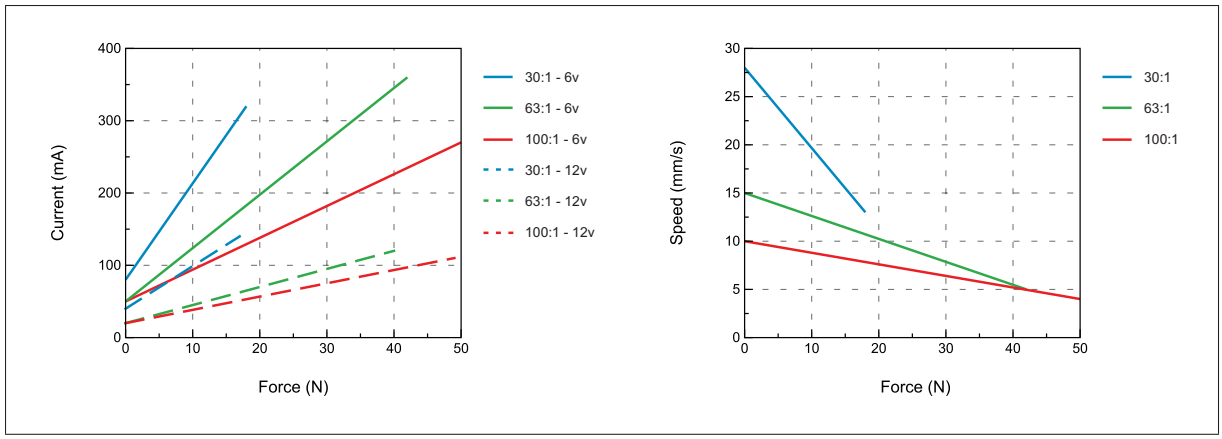

Figure 2.5 Specifications of the PQ12 actuator under different gearing forces. Gear reduction ratio (refers to load curves above): 30, 63, 100. Note that lower ratios are faster, but provide less force, and vice versa. 6, 12 refer to the DC volts

In the tangential force device, the initial position of the rectangular unit was set at 8 mm away from the actuator. This gap was left in order to avoid inducing pain by pinching the subjects' skin. The maximum distance travelled by the piston was 12 mm. Also, during the skin stretch tests, double-sided adhesive tape was used to attach the device to each subjects' skin.

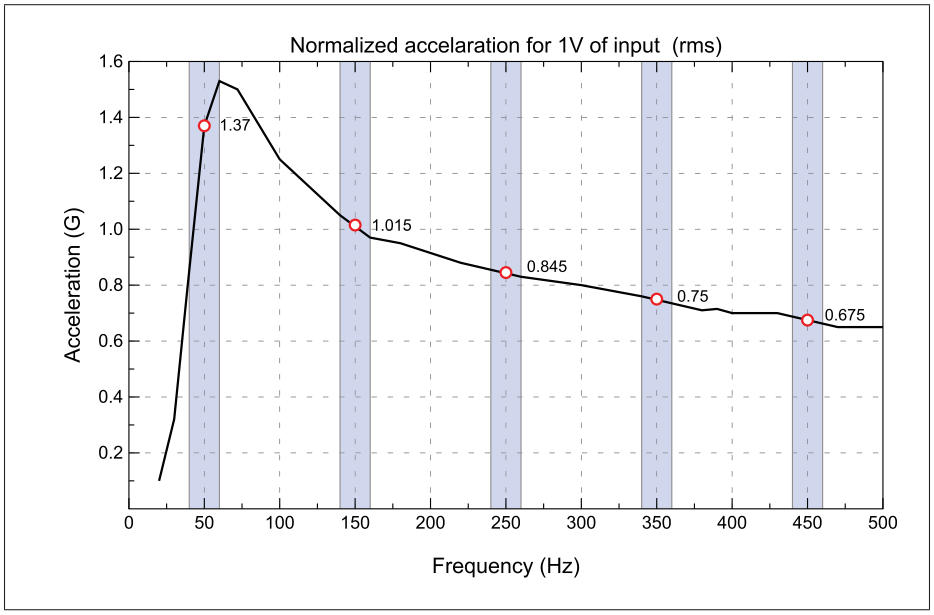

Figure 2.6 Normalized acceleration of the Haptuator for 1 V of input

The vibration frequency for the vibrotactile test was set at 250 Hz, which corresponds to the level of maximum human touch sensitivity Bark *et al.* (2008); Wheeler *et al.* (2010). Most cellphones today are built to operate at this vibration threshold, in order to maximize their chances of being noticed by the user while in vibration mode. As shown in Figure 2.6, in our vibrotactile experiment five different input voltages (2-10 V) were delivered to the Haptuator. This allowed us to study a wide range of input voltages while observing how the feedback was received by the subjects.

2.3.2 Procedure

At the start of the experiment, each subject was seated comfortably at a table. The subject's dominant hand was placed on an inflatable pillow, and the device was strapped to the subject's forearm (Figure 2.7). Subjects wore noise-cancelling headphones and had their eyes covered with blindfolds to allow them to concentrate on their tasks without the influence of environmental events. To assist with force scaling, subjects were familiarized with the various levels of the force stimuli during trial sessions.

During the experiments, the subjects were asked to replicate the amount of feedback that each device applied to their forearms by pressing on a force sensor with their finger pads. The subjects were not aware of the actual voltage levels that were input to each device, and the order in which the devices were tested, until all the experiments were complete.

We began the vibrotactile tests by running one of the input voltages (randomly selected from 2, 4, 6, 8, or 10 V) into the Haptuator for about fifteen seconds. The Haptuator then applied vibrotactile feedback, corresponding to this voltage level, to the subject's forearm. Immediately afterwards, the subject was asked to press on the load-cell force sensor with his or her finger pad. The amount of force that the subject applied to the load-cell force sensor was then transferred to the Haptuator, and the Haptuator again applied vibrotactile feedback, corresponding to this new voltage level, to the subject's forearm. The subject's task was to apply enough

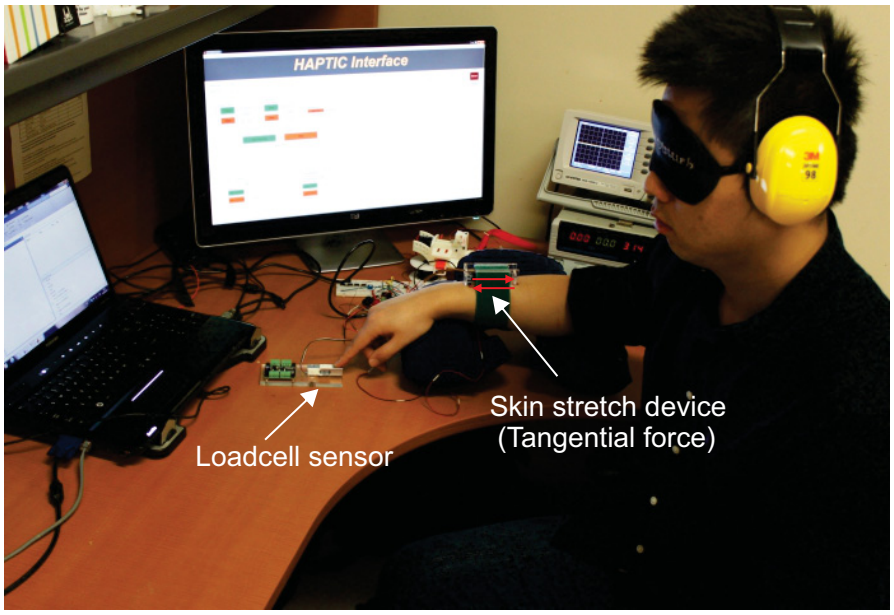

Figure 2.7 Subject applying pressure to the load-cell sensor

pressure to the force sensor so that the device would apply the same level of feedback as it did the first time.

The tests for the normal stress and tangential feedback devices proceeded in much the same way, except that the Haptuator was replaced by either a normal force actuator (for normal stress) or a tangential force actuator (for shear stress). As mentioned above, the order in which each device and voltage level was tested was randomly varied for each subject. Subjects were given 5 minutes to recover in between tests in order to prevent skin numbness. By the end of the experiments, each of the five magnitude levels was thus used as an input three times, providing fifteen numerical data per subject, and a total of 180 trials for all twelve subjects.

When the participants' tasks were over, they were asked simple questions about the effectiveness of the feedback they received from each device. Finally, all the subjects were presented with a graph showing the results of the experiment.

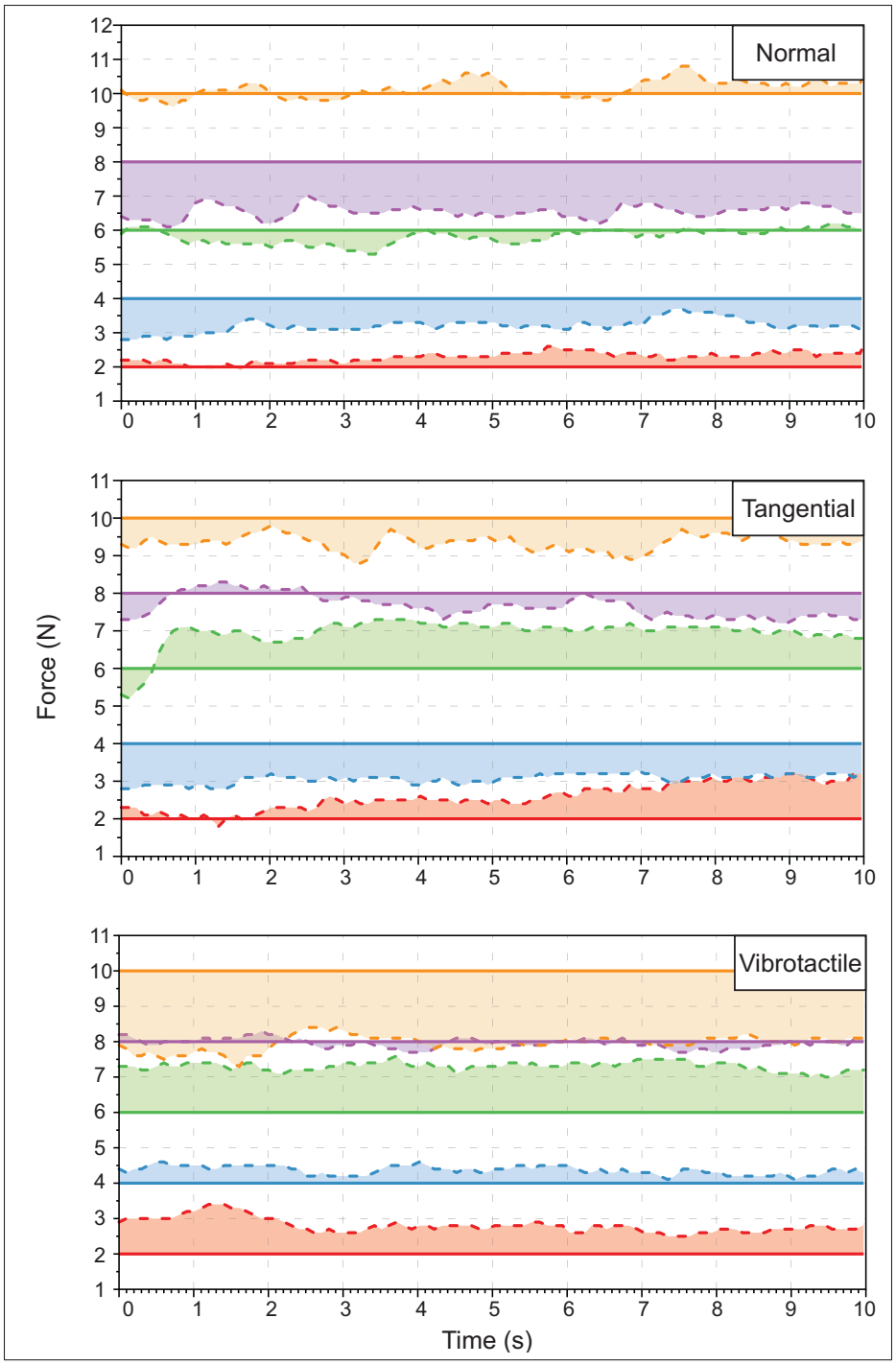

Figure 2.8 Sample subject feedback for normal force, tangential force (shear force), and vibrotactile stimulation

2.4 Results and Analysis

2.4.1 General Analysis

Figure 2.8 displays diagrams, which represent the normal stress, tangential force, and the vibrotactile stimulation feedback from a subject, as a sample for each input level. The straight lines represent the desired level of the forces (2,4,6,8, and 10N) that were applied from the devices, and the margins around the lines indicate the feedback from the subjects at that specific level. All collected data were statistically analyzed to determine the type of stimulation that best provides exteroceptive feedback under static conditions. Note that in order to avoid transient false data, only the last ten seconds of each experiment were used in our statistical analysis.

When we gathered all the feedback from the twelve subjects, it was clear that all the stimulation methods provide some level of feedback. However, when we examine the data based on the critical statistical parameters, normal stress leads to a better restitution of static conditions than the other two for all five force levels. This can be observed from both Table 2.1 and Figure 2.9.

Table 2.1 Statistical analysis of the collected data for the three types of stimulation

Types	Statistics	2	4	6	8	10
Normal Force (N)	mean	2.32	3.44	6.39	7.43	9.81
	s-deviation	0.54	0.41	0.65	0.42	0.68
	variance	0.08	0.29	0.52	0.26	0.14
Tangential Force (N)	mean	2.88	4.96	6.54	6.99	10.7
	s-deviation	0.39	0.65	0.63	0.44	0.13
	variance	0.26	1.8	0.65	0.29	0.41
Vibrotactile (V)	mean	2.62	4.68	7.14	7.18	9.17
	s-deviation	0.14	0.14	0.05	0.34	0.49
	variance	0.41	0.02	0.73	0.27	0.20

Out of the five input voltages, three (2, 4, and 8 V) have absolute means and variances that strongly show the superiority of normal stress. At these input levels, the second best type of feedback is vibrotactile, while tangential comes in last place. Although all input levels indicate

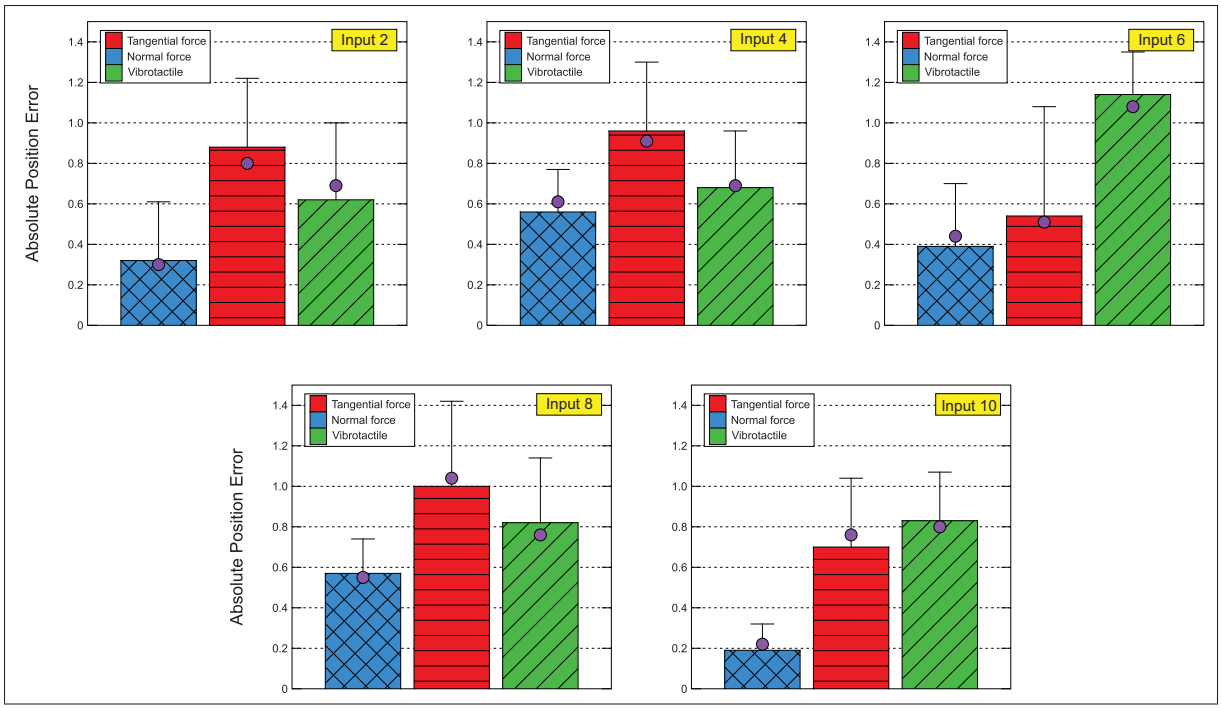

Figure 2.9 Subjects' feedback under the three types of stimulation. The bars show the absolute mean, the lines show the absolute error, and the purple circles indicate the median for all tests

the superiority of the normal stress feedback, tangential force is more effective than vibrotactile feedback at input levels of 6 and 10 V. In general it seems that the vibrotactile stimulation is harder to recognize at high input voltages; it was inferior to tangential force at 6 and 10 V, and only marginally better at 8 V.

2.4.2 Norm vs. Variance

A critical parameter that should be considered in our analysis is the amount of error that is based on the variances and the norms. As smaller variances and norms lead to less error in the feedback from the human subjects, here we seek to find the best type of feedback by comparing the Manhattan, Euclidean, and Infinite norms of each type. The results of this process are illustrated in Figure 2.10, in which each subject's individual feedback, along with the average feedback for each stimulus from all twelve participants, is distinguished by its variance versus the desired norms.

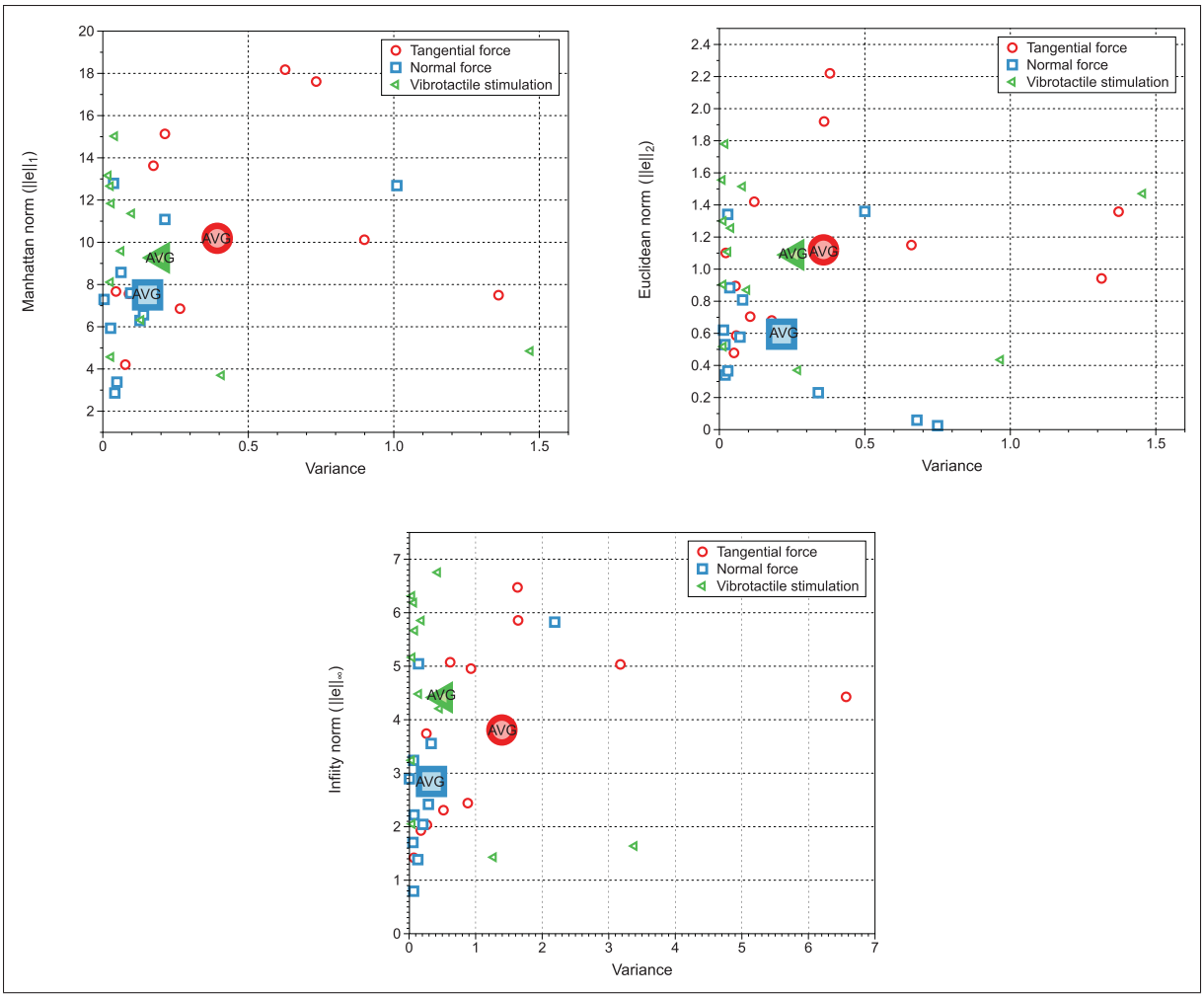

Figure 2.10 Manhattan norm analysis for the feedback provided by normal stress, skin stretch and vibrotactile stimulation

Again, the haptic device that applies normal stress appears to lead to the smallest error, based on the average of norms and variances among all three types. This superiority remains the same in all types of calculated norms. We also conducted an ANOVA test with a threshold of 95% to determine whether the mean of the position error was significantly different at all levels (Table. 2.2).

The test statistics for our hypothesis (i.e., that normal stress is superior to vibrotactile and tangential force stimulation) do indeed show that there is a significant difference between the norms of the collected data (F=9.68, $F_{.05;5,66}$= 2.35, α= 0.05 and P=5.7E-07).

Table 2.2 ANOVA Table showing the significance of the differences between the subjects' feedback

Types	SS	df	MS	F	$P-value$	$F_{critical}$
Between Groups	12.63	5	2.52	9.68	5.7E-07	2.35
Within Groups	17.21	66	0.26			

2.4.3 Relative Effectiveness of the Stimuli

We also evaluated the best type of stimulation by comparing the performances of each subject during the tests. These results are gathered in Figure 2.11. As we anticipated, normal stress seems to be the most functional, with six subjects displaying their best performances, five in the middle, and only one performing worst. Vibrotactile stimulation is in second place, with four subjects performing best, three in the middle, and five performing worst. Finally, tangential force feedback was evidently the least effective of the three, as only two subjects performed best while using it, four were in the middle, and six performed worst.

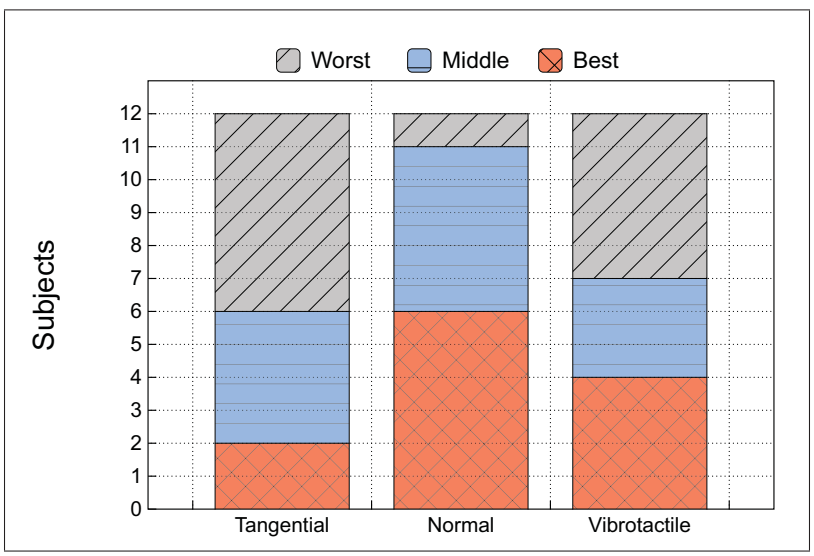

Figure 2.11 Subjects' performances under normal stress, skin stretch and vibrotactile stimulation

2.4.4 Subjects' Success Rates

As mentioned earlier, at the end of the participants' tasks we questioned them about how they felt during the experiments. We asked them to rate each device's overall effectiveness on a scale of 0 to 10. As shown in Figure 2.12, the subjects' ratings are linked to their performances. Eight of them believed normal stress was the most suitable for restitution of steady pressure under static conditions. Only three of the subjects were not completely satisfied with normal stress, and just one subject did not like the feeling of normal stress at all. Clearly, subjects preferred the type of feedback that was easiest for them to use.

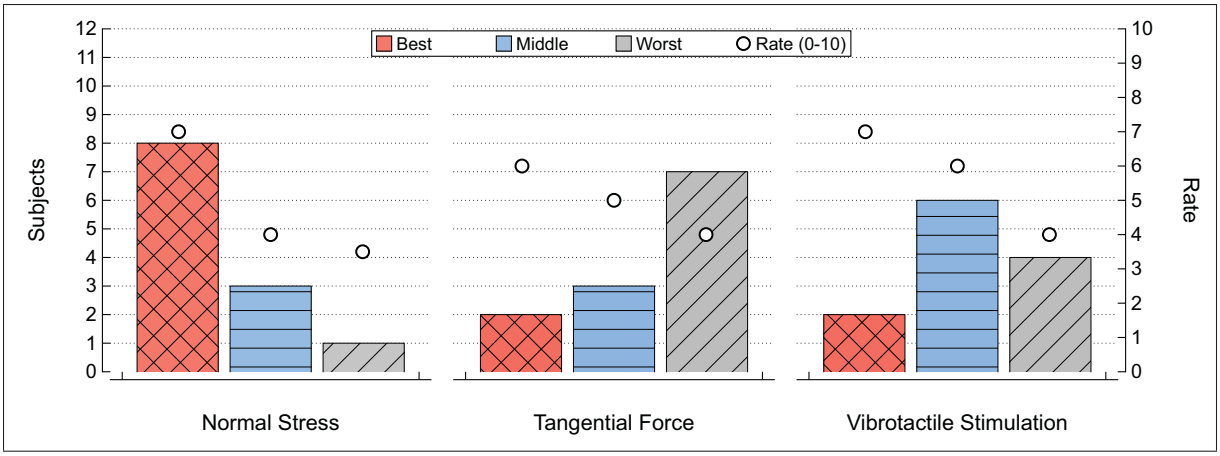

Figure 2.12 Preference rating in different feedback conditions from the twelve participants

During the rating process, several complaints cropped up that were repeated by many of the subjects. Although they found the vibrotactile stimulation to be effective, they recommended that it not be applied for more than five seconds. Subjects agreed that vibrotactile stimulation is better for use in short-term conditions, such as conveying the sense of brief contact with an object, because the sensation quickly becomes annoying. The participants were even less comfortable during the tangential force tests. Although we made sure that the tangential force device would not hurt the subjects during testing, they reported feeling uneasy about the device because they feared it would stretch their skin too far. For this reason, we believe tangential force is the least suitable feedback method. The normal stress stimulation, aside from being

more effective overall, prompted few complaints from subjects. Participants liked that the device moved softly over their skin, and that it conveyed the sense of pressure in a way that was easy to understand.

2.5 Conclusion

Three of the most widely used types of haptic feedback were involved in our experiment. Although the normal stress stimulation gives the best and most reliable feedback, based on the particular implementation of our experiment, in order to restitute the static pressure applied to the finger pads, the other two, tangential force and vibrotactile stimulation, also provided an acceptable result. When we look at the overall results and the subjects' rate of success, we see that many parameters affected the subjects' performances.

In vibrotactile stimulation, as mentioned earlier, the operation time plays a critical role. People are more interested in dynamic feedback for the purpose of being quickly alerted to some external event, and they prefer when the vibration motor is not in direct contact with their skin. We believe the subjects were not as accurate when using vibrotactile feedback because they are not used to having a vibrator motor placed directly on their skin. For instance, when a cellphone vibrates, it is generally in a pocket or bag.

We found that it was relatively difficult to stimulate the tactile receptors via tangential force. The device requires more precision, as a high level of pressure can be easily become annoying for the users. This became clear when we asked subjects about how they found the devices, as many of them complained that the tangential device applied an uncomfortably high amount of pressure. Aside from this, our experiment used tangential force applied to glabrous areas of the body; past researchers have found that it is much more effective when applied to hairy (Biggs and Srinivasan, 2002).

Finally, normal stress, due to its similarity to the pressing tasks, specially in a application that we used in our experiment, seems highly functional and easy to recognize. Although it comes with many advantages, we should take into consideration that applying too much pressure, such

as more than 10 mm of skin displacement, can be as painful to the subjects as skin stretch. In general, based on the subjects' feedback, normal stress is highly recommended for conveying travelled force of less than 10 mm. Within this limit, we can easily convey each increment of force (of 1 N) by matching it to each millimetre of the distance traveled by the piston.

Taking everything into consideration, in order to design a haptic interface that can work under both dynamic and static conditions, the use of both normal stress and vibrotactile stimulation seems mandatory. Following their successful integration, the system can then be made yet more functional by adding tangential force and temperature sensors, in order to deal with dynamic as well as static modalities.

CHAPTER 3

A WEARABLE HAPTIC DEVICE BASED ON TWISTING WIRE ACTUATORS FOR FEEDBACK OF TACTILE PRESSURE INFORMATION

3.1 Introduction

In previous chapter, we demonstrated that normal stress (normal pressure), applied to healthy skin, is an optimal way to convey the sense of exteroceptive pressure to amputees. Building a device that can provide this type of feedback requires the use of a linear reciprocating actuator. In this regard, this chapter presents a novel wearable haptic device that provides the user with knowledge of a normal force, measured at the fingertips, by applying pressure at three different locations on the user's body. In our proposed mechanism, an orthogonal force is applied to the surface of the skin in order to activate the Merkel disk (Dargahi and Najarian, 2004) receptors that respond to pressure on the skin.

This chapter is organized as follows. Section 3.2 provides the context for our research, and discusses past developments in wire actuators. Section 3.3 then presents the kinematic and dynamic modelling of the actuator that was used in our device, followed by the overall mechanical design in Section 3.4. Our design is validated by our experiments, as shown in Section 3.5. The chapter concludes with an evaluation of the system's performance, and a discussion of how it might be improved in further research.

3.2 Background

Different types of actuators, including electro-active polymer actuators (Gels, 2004), hydraulic or pneumatic actuators (Fan *et al.*, 2009), and magnetic actuators (Berkelman *et al.*, 1995) can be used. However, it is difficult to integrate most of these technologies into a lightweight and compact wearable haptic device, because even though the actuators themselves can be small, more components must be added on to the device in order to integrate the actuator with the

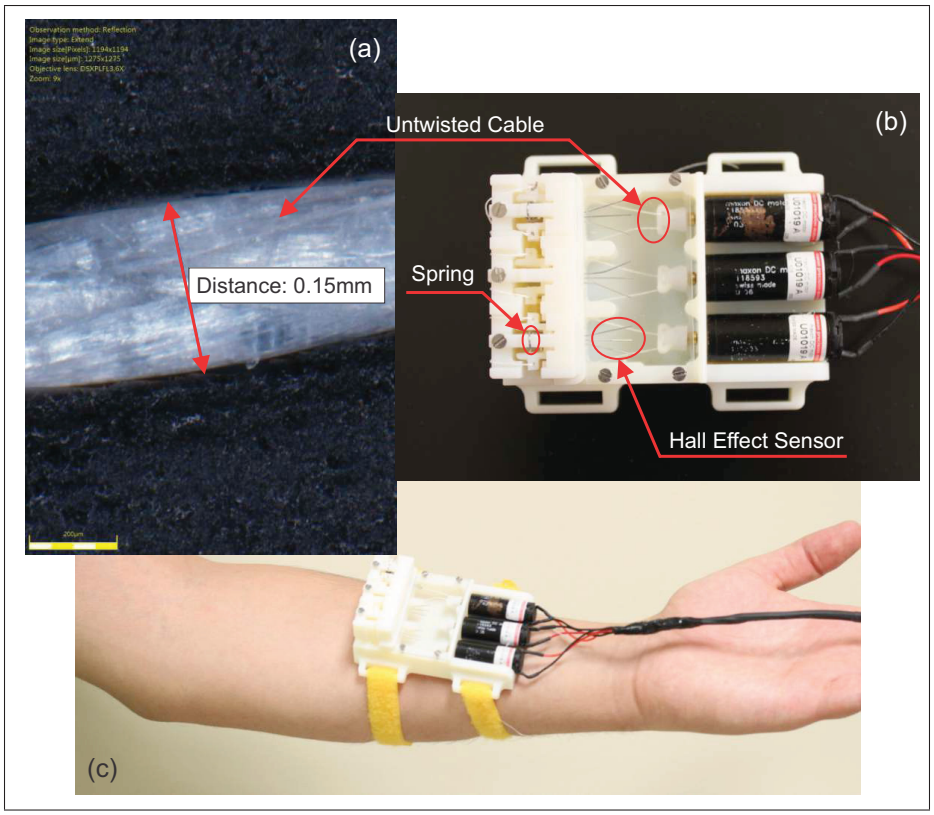

Figure 3.1 (a) Microscopic view of a synthetic fiber spectra; (b) Top view of the haptic device using three Maxon DC motors, hall effect sensors and load springs; (c) Wearable haptic device placed on the glabrous skin of the human forearm

sensor (Duchaine and Rana, 2014). To circumvent this problem, we decided to use twisted wire actuators coupled with a compact direct drive conventional DC motor.

The principles behind the actuator's mechanism have, of course, been known for centuries. The wire actuator mechanism is based on the fact that when two wires are twisted together, their apparent lengths decrease. By fixing one end of the twisted wires to a motor shaft, and the other end to an object, it is possible to pull the object in a linear motion. More recently, a wire actuator was patented by Kremer (1989), and by Shoham (2005). Wurtz *et al.* (2010) that it is possible to mathematically predict the non-linear motion that is caused when the wires begin double-twisting. Double-twisting occurs when high rotational stress causes the fully twisted

wires to re-twist around each other. However, although it is possible to predict the effects of double-twisting in theory, in reality it is almost always too complex.

In the field of robotics, twisted wire actuators first appeared in the literature by Kawamura *et al.* (1995), when they developed a high-speed mechanism for cable-driven robots by using wires to reduce the vibration of the system. In rehabilitation robotics, Godler *et al.* (2010) presented a wire actuator for controlling an under-actuated robotic finger, followed by an entire robotic hand.

Since twisted wire actuators feature elastic compliance, they are safe for direct contact with human skin even when they are operating at a very high transmission ratio. Furthermore, twisted wire actuators are ideal for use in haptic interfaces because the twisted wires prevent backlash from occurring. This means that when the end effector reaches the maximum distance it can travel when applying pressure to the user's skin, the twisted wires prevent the effector from moving backwards, and no distance is lost as the effector simply stays put.

However, most of the twisted wire actuators used by past researchers are limited in terms of their wire length, and the resulting transmission ratios are low. In all the solutions that were presented in previous studies by Suzuki and Ichikawa (2005); Sonoda and Godler (2010), the length of wire that can be twisted was specified by the distance between the movable parts of the mechanism and the motor shaft. As shown by Wurtz *et al.* (2010), this allows a maximum displacement of just 46% of the untwisted wire length before double-twisting occurs. All of these results show that this type of mechanism, where the length of the wire is held constant, results in a low transmission ratio.

In order to improve the transmission ratio, we propose that the length of the wire should not be held constant; instead, the wires should be fed into the mechanism so that the length of the section of twisted wires can vary as necessary. This will result in both a higher transmission ratio and a more compact device. We present the kinematic and dynamic models of our modified twisted wire actuator in the following section.

3.3 Twisted Wire Actuator

3.3.1 Kinematic Analysis

The schematic view of the proposed mechanism is illustrated in Figure 3.2. The two ends of a wire are attached to the motor shaft and passed through the holes separated by a constant distance, A, from the center of the shaft (Figure 3.2. a). As the two components, the shaft and the holes, are fixed at the same position (y direction), when the mechanism is operating the distance d remains constant between the motor and the centers of the holes.

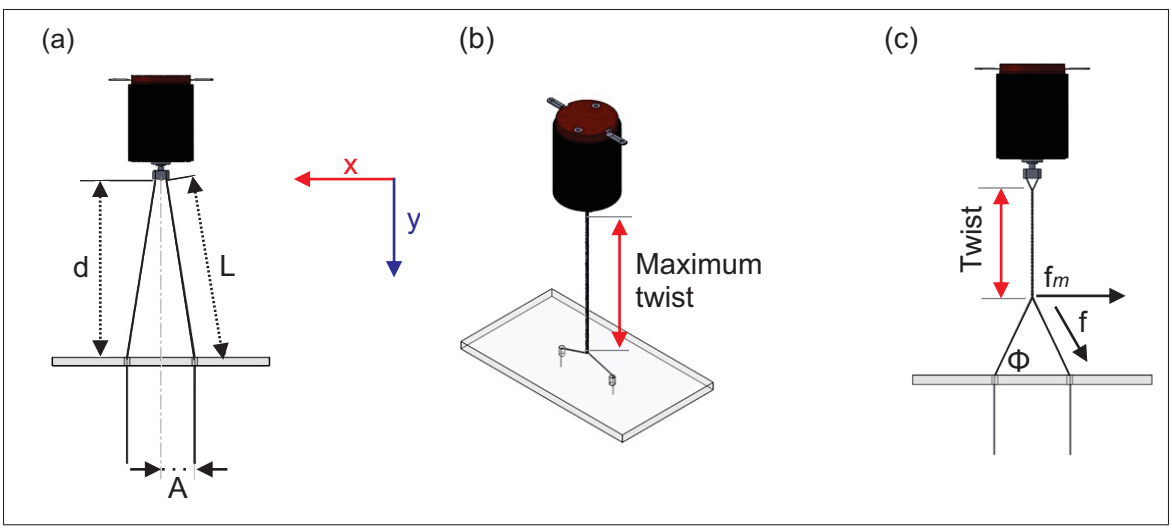

Figure 3.2 (a) Original cable placement before twisting. (b) Maximum twisting of cable, before double-twisting occurs. (c) Diagram showing the force from the motor

The distance d represents the fixed distance between the motor and the holes through which the wires pass. This distance is constant, as the positions of the motor and the holes remain fixed when the system is in action. L is the length of the wires between two points: the point at which they are attached to the motor, and the point at which they pass through the holes. Since the wires are twisting while the mechanism is in action, L is highly variable, as the twisting motion causes the wires to be pulled into the space of length d.

The planar projection of this process can be calculated using a triangle, shown in Figure 3.3 (a), that represents the geometry of the untwisted wire. Here, the lengths of d and L remain constant (similar to Figure 3.2), while the third side of the triangle represents the horizontal projection of the wire, based on its radius r, the angular position of the motor θ, and the distance between the two holes A.

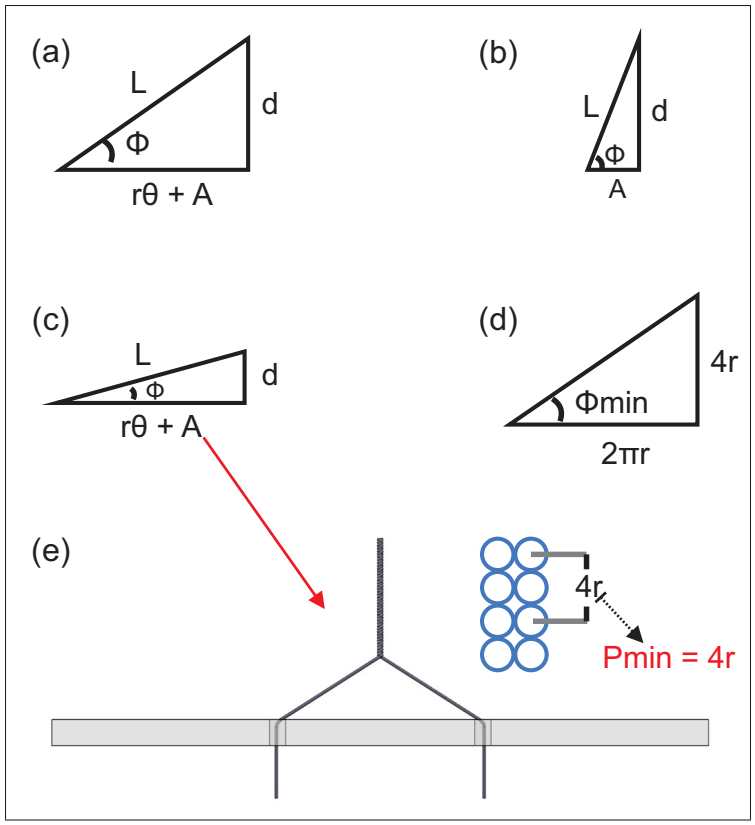

Figure 3.3 (a) Initial arrangement of the mechanism; (b) Secondary arrangement of the mechanism; (c) Triangle representing the final values of the system's variables; (d) Triangle representing the final values of the system's variables with the P_{min}; (e) View of the twisted wire in its final position

$$L = \sqrt{(r\theta + A)^2 + d^2} \tag{3.1}$$

In the initial condition, i.e., when the wires are not twisted and the rotation angle is equal to zero (Figure 3.3 (b), the wire length that corresponds to the hypotenuse of the triangle is called the initial length, L_0.

$$L_0 = \sqrt{A^2 + d^2} \tag{3.2}$$

Therefore, as the linear displacement given by the actuator is the result of the difference between the post-twisting length, L, and the pre-twisting length, L_0, this linear displacement can be represented as:

$$\Delta L = L - L_0 = \sqrt{(r\theta + A)^2 + d^2} - \sqrt{A^2 + d^2} \tag{3.3}$$

As mentioned earlier, after a certain number of twists the wire begins to re-twist on itself by double-twisting. When double-twisting occurs, the relationship between the motor angle and the resulting linear displacement is difficult to predict using simple equations. Therefore, to avoid this unpredictability, we define the maximum possible displacement given by our mechanism as the maximum number of twists in the wire that can occur without inducing double-twisting.

To find the maximum possible displacement before double-twisting occurs, a series of equations must to be calculated. First, we define the maximum number of twists that can occur before double-twisting begins, as shown in Figure 3.3 (c) and Figure 3.3 (e). This maximum occurs when the size of each node is equal to the sum of the diameter of the two wires.

$$P_{min} = 4r \tag{3.4}$$

We are now able to define the minimum twisting angle, ϕ_{min}, and the maximum angular position of the motor, θ_{max}. With our knowledge that each twist gives $P_{min} = 4r$, the minimum

twisting angle is illustrated in Figure 3.3 (d), and the maximum angular position of the motor is determined as:

$$\phi_{min} = \tan^{-1}\frac{4r}{2\pi r} = \tan^{-1}\frac{2}{\pi} \approx 32.5^{\circ} \tag{3.5}$$

$$\tan\phi_{min} = \frac{d}{r\theta_{max} + A} \tag{3.6}$$

$$\theta_{max} = \left(\frac{d}{\tan\phi_{min}} - A\right) r^{-1} \tag{3.7}$$

Equation 3.7 describes the relationship between the angular motor displacement and the length of the twisted wires. Note that at this stage we have not yet taken into consideration the values of the static parameters. These will be included in the next section.

3.3.2 Static Analysis

Here we calculate the static equations in order to define the relation between the actuator torque and the load force that can be delivered from the mechanism. We also present the modelling of the physical aspects of the entire mechanism.

We know the net tension of the applied force to ends of the wires, which, as shown in Figure 3.2 (c), allows us to verify the value of f_m. This value is a component of the force, f, and is perpendicular to the rotational access of the motor that creates the torque.

$$\sum F = 0 \tag{3.8}$$

$$f_m = f\cos\phi \tag{3.9}$$

By multiplying f_m by the given wire radius, the torque is equivalent to:

$$\tau_m = f_m r = f r \cos\phi \tag{3.10}$$

After replacing ϕ with the triangle elements shown in Figure 3.3 (b), the geometries of the untwisted wire and the motor torque are as follows:

$$\cos\phi = \frac{r\theta + A}{L} \tag{3.11}$$

$$\tau_m = f r \frac{r\theta + A}{\sqrt{(r\theta + A)^2 + d^2}} \tag{3.12}$$

Furthermore, as brand-name motors come with a pamphlet that gives the maximum torque (among other details), it is also useful to estimate the net load according to the rotation angle of the motor. Equation 3.13 gives the relationship between the motor torque and force, and Equation 3.14 gives the maximum force that can be applied by the mechanism.

$$R_m = \frac{r(r\theta + A)}{\sqrt{(r\theta + A)^2 + d^2}} \tag{3.13}$$

$$f = \frac{\tau_m \sqrt{(r\theta + A)^2 + d^2}}{r(r\theta + A)} \tag{3.14}$$

3.3.3 Validation Analysis

After developing the kinematic and static models of the twisted wire actuator, we must conduct an experiment to validate that the calculated formulas do indeed describe the exact behaviour of the proposed mechanism. To this end, we used a bench test to measure the linear motion

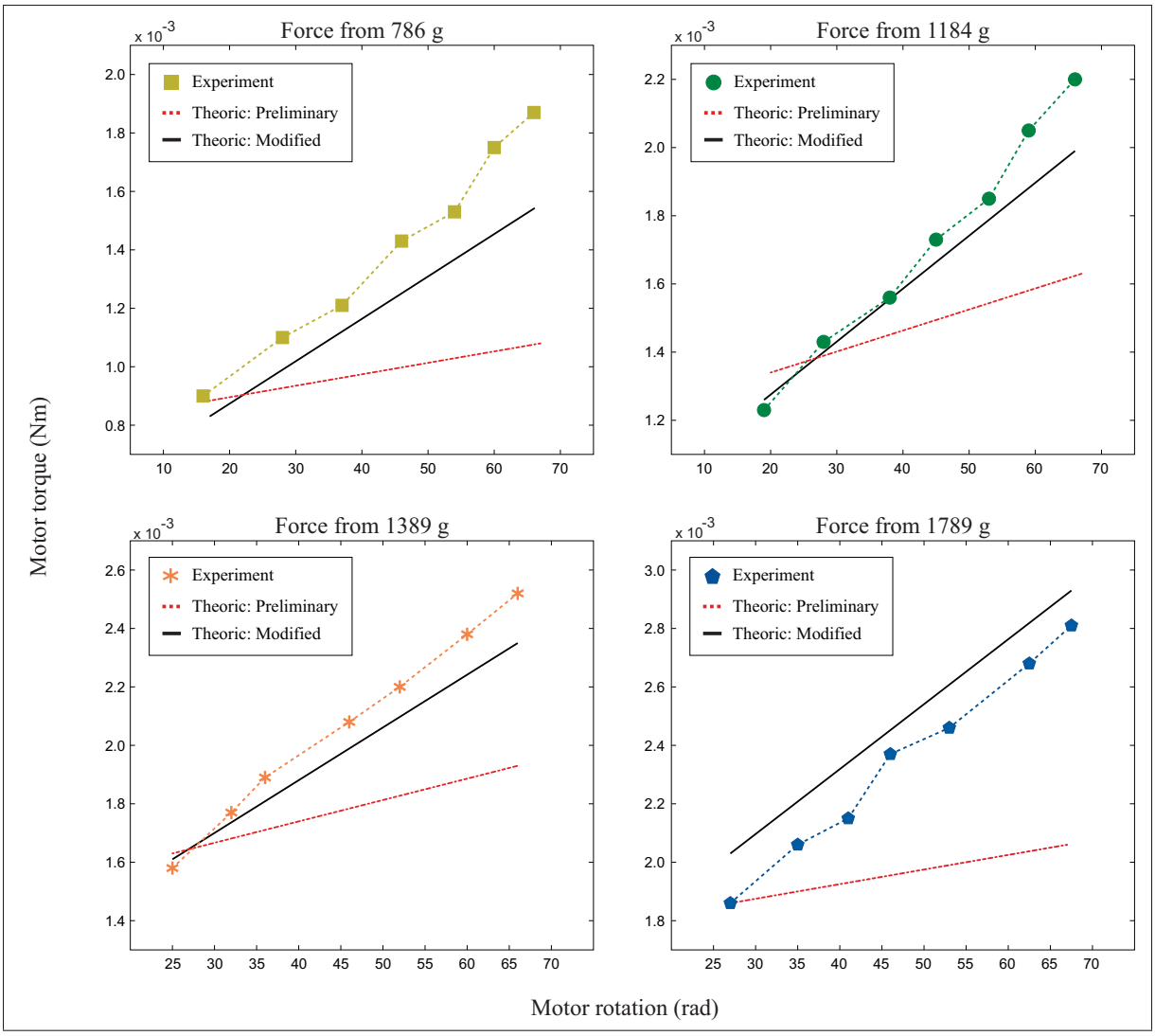

Figure 3.4 Static analysis for comparisons between the preliminary theoretical data, the results of the experiments, and the modified theoretical data. During the experiments, four separate tests were conducted using laboratory test weights of 786g, 1184g, 1389g and 1789g. Note that the modified theoretical data have been modified by taking the torsional stiffness ($k = 1.65$) into consideration

and the linear force that was generated by the actuator through the wire transmission. The schematic view of the motor, and the housing that was initially used in this experiment, are shown in Figure 3.5.

For the kinematic analysis, the relevant displacement of the prototype was determined as follows:

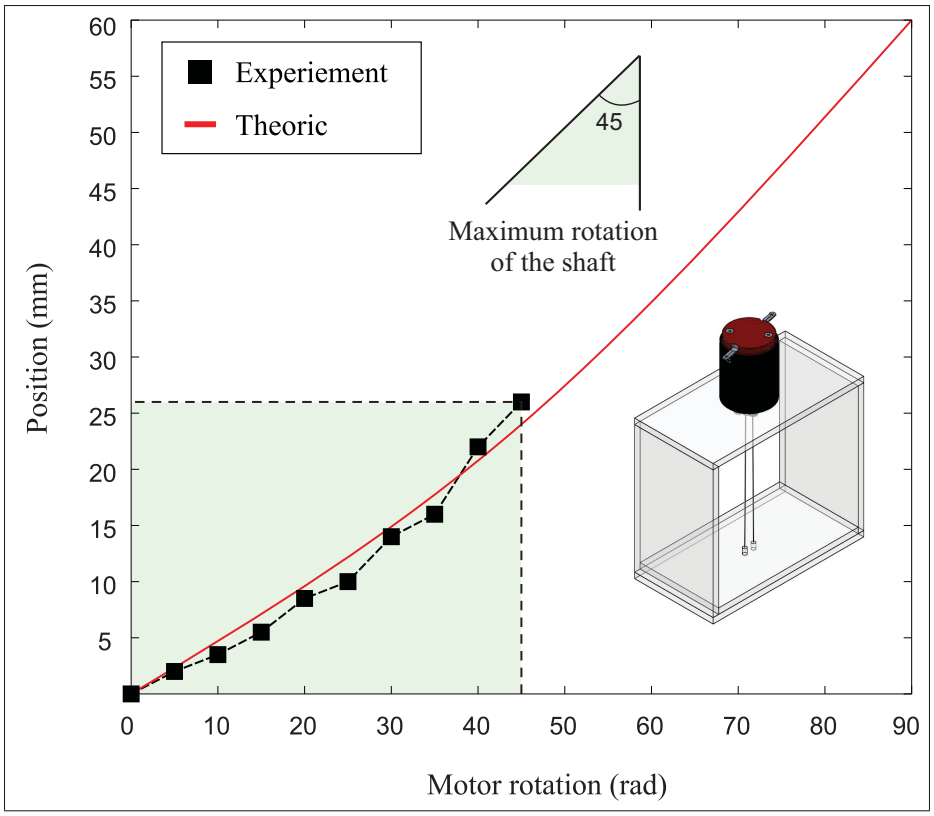

Figure 3.5 Comparison between two analyses, each of which represent the kinematic system as based on the position angle of the motor. The black line is the experimental analysis, and the red line is the theoretical analysis. These analyses were obtained using a bench test performed on the prototype shown in the bottom-right corner

- The shaft was manually rotated. After every $5rad$, the linear displacement was measured using a micrometer. Unlike in the theoretical calculations, according to which the number of turns stopped at the end of the procedure, here the data acquisition was performed up to $45rad$ due to the difficulty of manually exceeding this value for our prototype. In fact, because of the instability of this condition, it is difficult to obtain an accurate measurement of the displacement, especially after further turns.

- Turning up to $45rad$ provided an adequate number of data for the comparison of the theoretical values. The data represent the range in which the torque produces a significant usable force to the end effector. Figure 3.5 shows the relationship between the linear and

the angular displacements, as determined by the theoretical analysis (red line) and by the results of the experiment (black line). The highlighted area indicates that the trends of the two curves are nearly identical. From this result, we conclude that our kinematic model can be used for designing the final prototype.

For the static analysis experiment, we attached a test weight to the end of the moving part and measured the displacement. By imposing a linear force on the mechanism, and by measuring the maximum torque as well as the maximum displacement, we were able to solve Equation 3.14. The predictions we made using this formula are indicated by the red dotted line in Figure 3.4. However, our predictions clearly do not match the results of the experiment.

We believe this discrepancy was caused by the torsional stiffness of the wire. Our equation assumes 100% mechanical efficiency, which is not a realistic depiction of actual task-oriented conditions, as it does not take variables such as stiffness into account. When the wires are twisted, each wire exerts some force on the other wire. These forces act in the opposite direction to the rotational angle of the twisted wire. This rotational stiffness can be expressed as:

$$\tau_s = k\Delta\theta \tag{3.15}$$

As shown in Figure 3.6, by considering the stiffness of the wire, (f_{st}), we can obtain the corrected force, f, and the corrected torque, τ_c,

$$(f_m - f_{st}) - f\cos\phi = 0 \tag{3.16}$$

$$\tau_c = f.r\cos\phi + k\theta \tag{3.17}$$

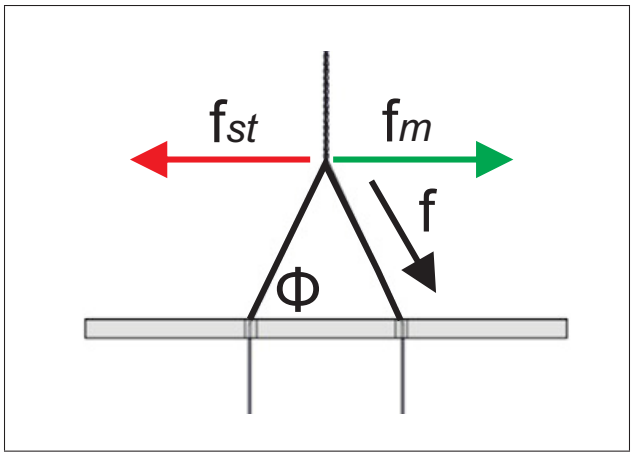

Figure 3.6 Major forces applied to the mechanism

We used trial and error to determine the stiffness factor, $k = 1.65$. The modified version of the static analysis, which is far more accurate, is illustrated by the black lines in Figure 3.4.

3.4 Mechanical Design

The core aim of the mechanical design is to create a device that can provide an orthogonal force by converting the rotary motion of the motor shaft into the linear movement of the piston. The pressure should then released using a spring. More specifically, an opposing spring force is continuously applied to the piston, which has the effect of moving the piston in the opposite direction. This results in the release of the twisted wires when the motor stops rotating. A miniature spring is placed on top of the piston, as shown in Figure 3.7, in order to generate the force that is needed to return the piston to its initial position.

Note that the piston must be able to apply up to 10 N of force to the user in order to convey a variety of static modalities. In our mechanism, this requires a piston travelling distance of approximately 10 mm.

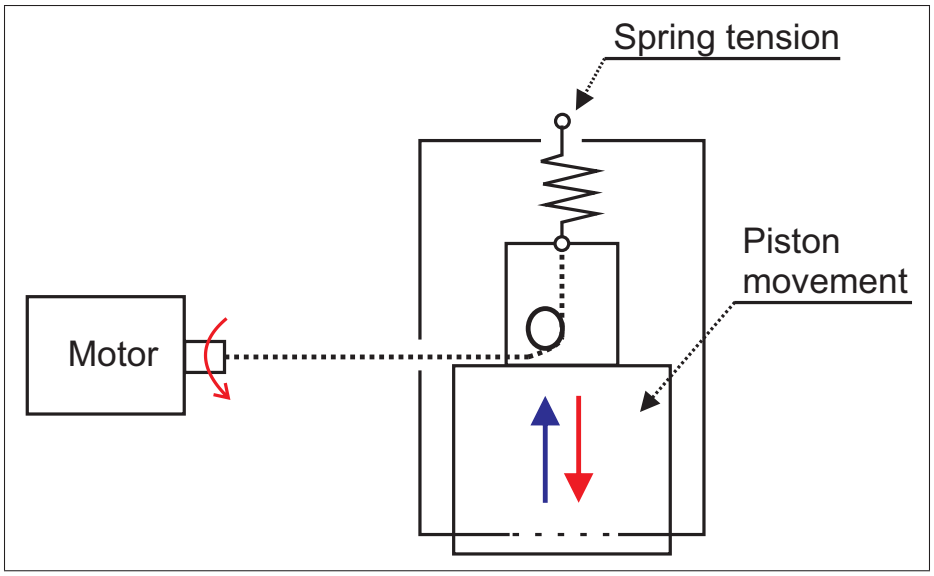

Figure 3.7 Load spring used to move the piston

3.4.1 Main Body of the Device

In order to create a wearable haptic device, our device should be able to apply static pressure ranging from 1 to 10 N, while being compact and lightweight. Furthermore, the device should not become unresponsive or uncomfortable for the user during long periods of operation.

We used CATIA V5 for drawing, modelling, and assembling the haptic device (Figure 3.8). We began prototyping after finding the critical parameters, such as the dimensions, lengths, edge curves, and the whole body structure. We used a rapid prototyping machine, Objet 24 from Stratasys, Ltd., to produce the main body and the piston in opaque white rigid plastic.

3.4.1.1 Motor

Here we calculate the motor torque, which corresponds to the displacement of 10 mm that requires about 10 N force. Our twisted wire actuator uses a set of three Maxon DC motors, each of which have a nominal voltage of 18 V, a load speed of 13000 rpm, a constant torque of 12.7 mNm/A, and a maximum force of 19 N. The motors are used to apply the additional force

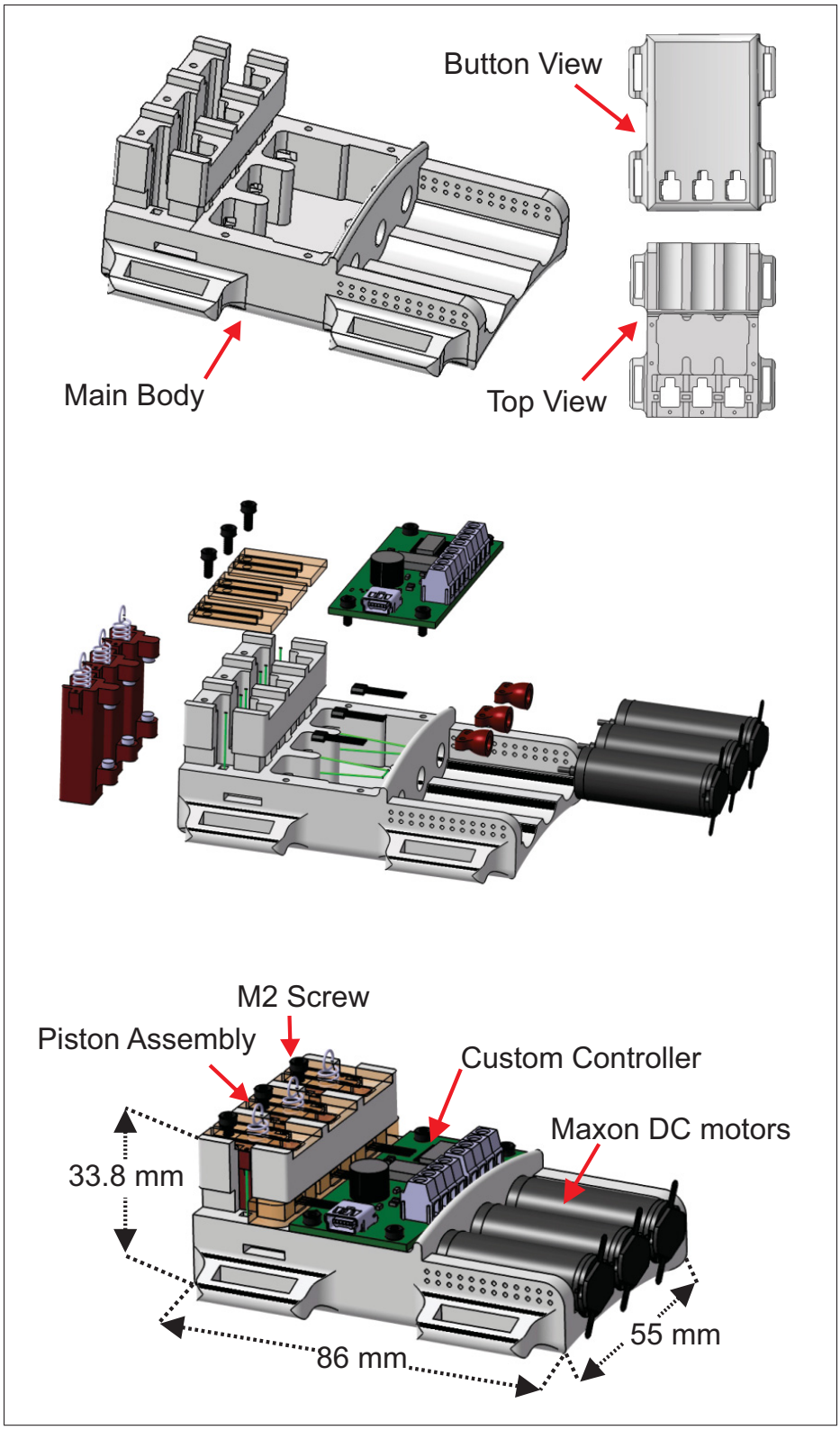

Figure 3.8 Schematic view of the haptic interface, including the twisted wire actuator

necessary to reach the desired position, after taking into consideration the opposing tension provided by the spring. The additional force to be applied by the motor is calculated as follows:

$$f_r = 0.334\ N/mm \times 10mm = 3.34N \tag{3.18}$$

We enter the following values into Equation 3.3: $A = 7\ mm$, $d = 35\ mm$ and the wire radius equals 0.15 mm. The motor shaft rotation will then be:

$$\Delta L = 10 = \sqrt{(0.15\theta + 7)^2 + 35^2} - \sqrt{7^2 + 35^2} \tag{3.19}$$

where:

$$\theta = 149.16\ rad \tag{3.20}$$

By adding all the given dimensions, including the spring force, the maximum applied force, and the corrected shaft ratio, we can obtain the Rcm and τ_m of the system,

$$\begin{aligned} Rc_m &= 1.7034 \\ &= 2.65\frac{0.15\theta + 7}{\sqrt{(0.15\theta + 7)^2 + 35^2}} - 0.0002 \end{aligned} \tag{3.21}$$

and the maximum torque,

$$\tau_m = (f_m + f_r) \times Rc_m \tag{3.22}$$

$$\tau_m = (10 + 3.34) \times 1.7034 = 22.72 \tag{3.23}$$

3.4.1.2 Wire

We used a synthetic fiber spectra that is sold under the name Dyneema. This wire has a very small diameter of 0.15 *mm*, but it is still highly flexible, durable, and rigid. Dyneema is typically used in the aviation industry, but it has also appeared in the field of robotics (Deschenes *et al.*, 2007; J-d Otis *et al.*, 2009).

3.4.2 Pistons

The pistons are the most complex aspect of the design, as they require many components to be integrated within their small casings so that they can safely apply pressure to the human subject. In our design, three pistons are embedded in the main body of the device. As can be seen from Figure 3.9, we designed the pistons to have extrusions on each side so that the wires could be threaded through the holes in the extrusions.

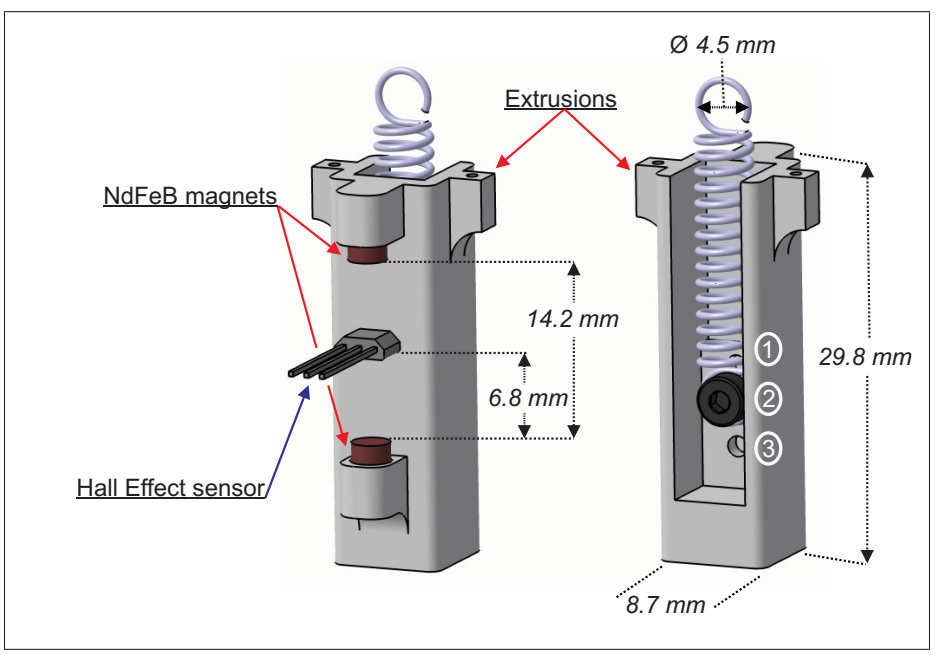

Figure 3.9 Pressure piston that is integrated with the haptic device

3.4.2.1 Sensor and Magnets

As there is no encoder in the system, the only way to know the position of the pistons is to use an external sensor to measure either the motor rotation or the pistons' movement. For this purpose, we used a linear Hall Effect sensor (SS495) made by Honeywell, Ltd. The 1 *mm* thick sensor is positioned in the middle of the 14.2 *mm* gap between the two small NdFeB neodymium N40 magnets (3.18 *mm* diameter $\times$ 9.53*mm* length), as presented by Kim *et al.* (2007). The sensor provides an accurate position of the pistons by sending a non-noisy analogue signal ranging between 0 and 5 V.

3.4.2.2 Springs

The size of the springs plays a critical role in determining how much force will be applied to the pistons to return them to their initial position. The main consideration when selecting a spring is usually the weight of the piston. However, in our case the pistons are so small that their weight is negligible, so we sought only to use the smallest springs possible. The strength of the springs does not matter, but they must be able to stretch to 10*mm*. We decided to use ultra-precision extension springs with loop ends from McMaster-Car, Ltd. These springs offer outstanding wear resistance, making them perfect for our applications. Figure 3.9 shows the three positions at which the spring may be set within the piston, as indicated by the numbers 1, 2, and 3. These three positions were implemented so that the spring's strength could be matched to the needs of the user. For instance, if the device is attached to the user's wrist, the spring should be set at position 3. There is not much fat at the human wrist area, so the looser spring will allow the piston to rebound more quickly from the hard surface. If the device is instead attached to a fleshier part of the person's forearm, the spring should be set at position 1, so the tighter coils will cause the piston to rebound more slowly, allowing the piston to sink further into the skin.

3.5 Evaluation of the Proposed Haptic Apparatus

In this section the haptic interface is evaluated using force and position tests. Both tests are conducted to determine the real-time positioning of the piston and the intensity of the applied forces. In task-oriented conditions, these two parameters play a critical role in the proper functioning of the mechanism.

3.5.1 Force Test

We hope that our haptic device will provide feedback to amputees so that they can have better control over their prosthetic limbs. This means that when a robotic hand grasps an object, the piston should apply orthogonal force feedback to the user that corresponds to the level of grasping force that is applied by the prosthetic fingers. Before we can test the accuracy of the device, we need to make sure it is capable of applying a certain range of forces to the user. To do this, we conducted a series of force tests.

The device was placed upside down and fixed on a force test stand (Mark-1 ES20), as shown in Figure 3.10. The force test stand was equipped with a digital force gauge (Mark-10 M4-10) capable of measuring forces from 0.5 N to 2500 N, and a digital displacement gauge (Mitutoyo 543-693) with $1\mu m$ accuracy. We carried out the experiment by running four input voltages into the device, of 5 V, 10 V, 15 V and 18 V. Although the manufacturer's description of the Maxon DC motor states that it performs best at a level of $12-15$ V for long-term operations, we wanted to test the device's performance at a higher voltage level. However, since our device is intended for long-term use, we will focus on 15 V in our discussion of the results of the test.

To start the test, the gauge effector is tangentially placed on top of the pistons so that the display indicates zero applied force. We then manually set the gauge effector at 1 mm above the initial position (Figure 3.11 top right) by very slowly turning the handle installed at the top of the force gauge. After 1 mm of displacement, the force applied from the pistons was measured using the force gauge. This experiment was continued for seven subsequent distances, rising

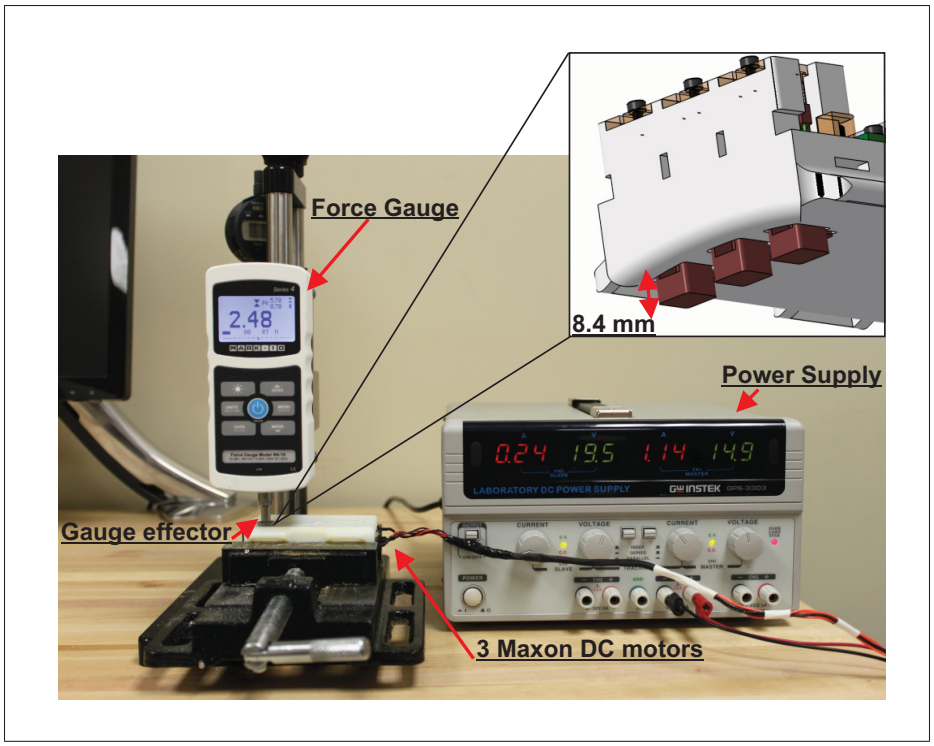

Figure 3.10 Setup of the force tests

by increments of 1 *mm*, until the displacement reached 8 *mm*, which is approximately the maximum possible displacement.

Figure 3.11 shows the input voltages, the applied forces from the piston, and the variance bar for each travelled distance. As can be seen, the haptic device is capable of applying forces between 2.9 *N* and 16.6 *N*, depending on the input voltage, before reaching the maximum position. This range of force seems sufficient to inform the user of the gripping force magnitude during low-intensity tasks, such as grasping a cup of tea or squeezing a soft ball. However, in order for the piston to reach its desired position, the haptic device must be applied to an area of the body that has a certain amount of rigidity (rather than, for instance, a cellulite-ridden thigh). Note also that Figure 3.11 shows that whenever the piston moves further away from its initial position, less pressure will be applied to the user.

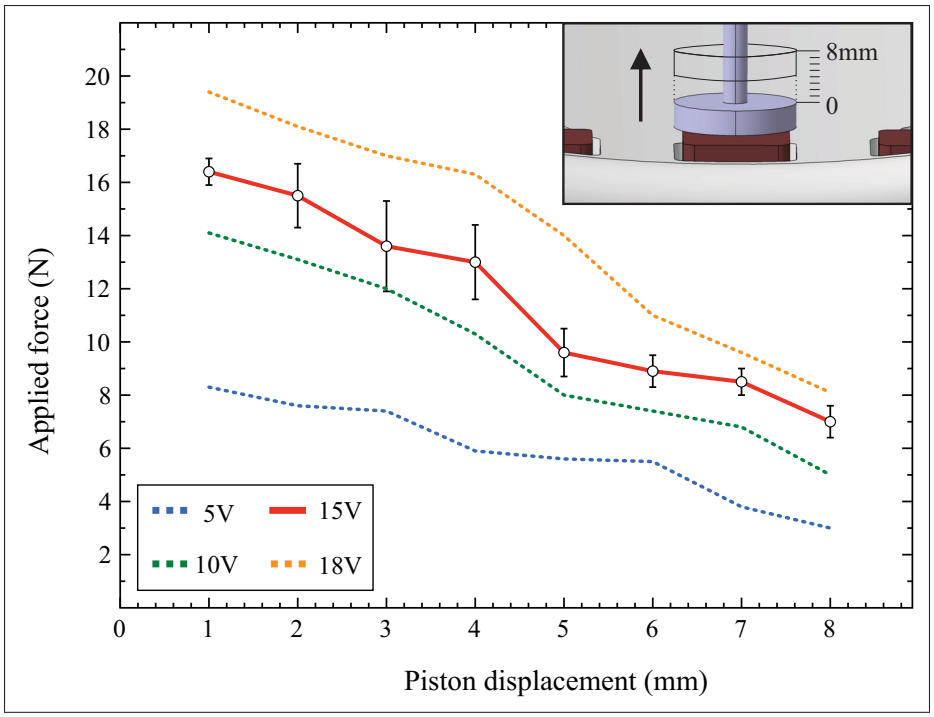

Figure 3.11 Results obtained from the force tests

3.5.2 Position Test

After determining the maximum force, it is important to estimate the positioning accuracy of the device during real-time operation. We used a GUI MATLAB interface, shown in Figure 3.12, and a PID controller with a sampling time of 0.1 milliseconds for this experiment.

For the test, the piston is positioned 1*mm* above its initial position, and three other displacement levels, of 7*mm*, 2*mm* and 4*mm*, were randomly given over a period of 15 seconds (taking the 2.5 *s* preparation time into consideration). The piston remained in the desired positions for 5 *s*, 5 *s*, and 2.5 *s*, respectively. The results are presented in Figure 3.13, where the blue line indicates the desired value, and the red line indicates the real-time positioning of the piston.

Based on the results we obtained, we can now define some of the critical features of the system: the time constant, the rise time, and the response time.

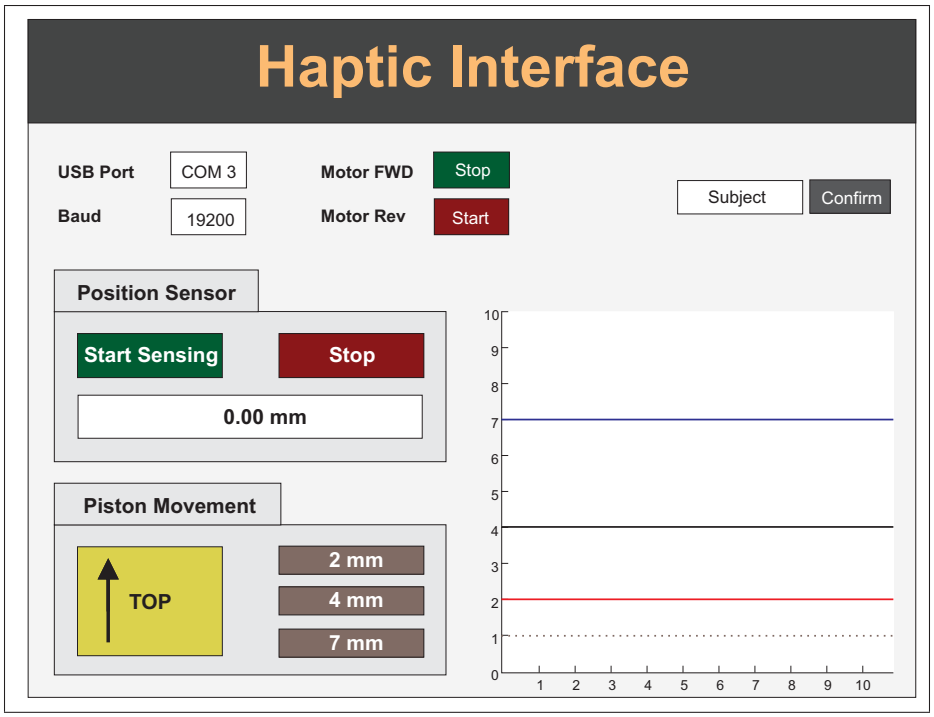

Figure 3.12 Haptic interface in GUI-MATLAB for real-time control over the positioning of the piston

3.5.2.1 Time constant

The time constant, λ, represents the time that it takes the piston to reach 1-1/e $\approx 63.2\,\%$ of the desired value. We calculate the positions at which λ occurs as follows:

$$Position_x = (x - x_{-1}) \times 0.63 + x_{-1} \tag{3.24}$$

In the test, we placed the piston at positions of $7mm$, $2mm$ and $4mm$. When we replace the value of x with these values, and consider $1mm$ to be the initial position, the formula tells us that the critical positions are $4.78mm$, $3.85mm$, and $3.26mm$. According to Figure 3.13, the three corresponding time constants are 0.48 s, 0.49 s, and 0.08 s. Therefore, the total processing times are 2.98 s, 7.99 s, and 12.58 s.

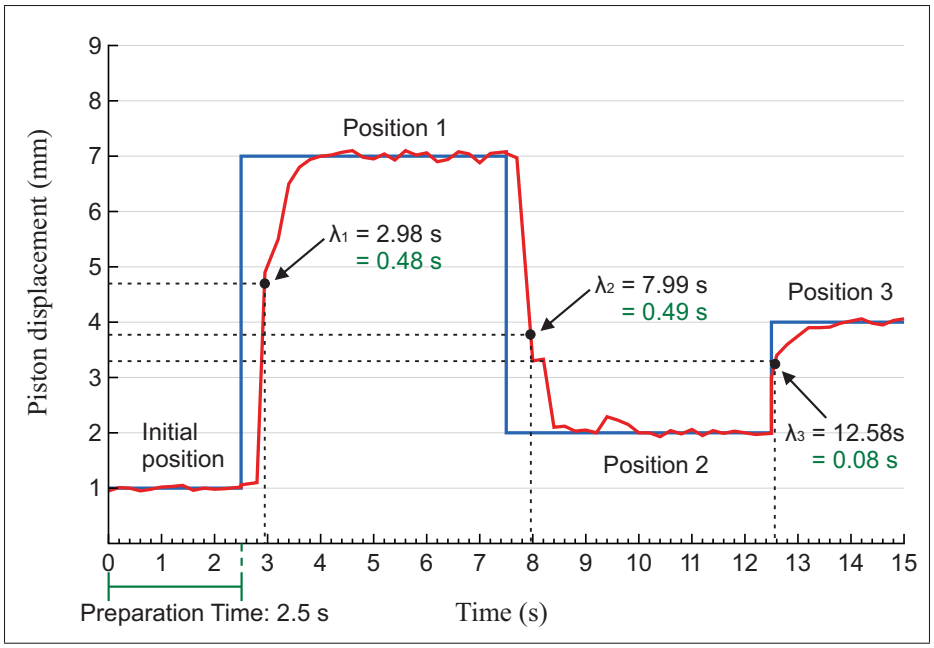

Figure 3.13 Desired and real-time positioning of the piston, along with the time constants

3.5.2.2 Rise time

The rise time (T_m) is the time taken by the piston to go from 10% to 90% of the desired value. In order to calculate the three values of T_m in our system, six positions should be used:

$$Position_x = (x - x_{-1}) \times 0.1 + x_{-1} \tag{3.25}$$

$$Position_{x_{+1}} = (x - x_{-1}) \times 0.9 + x_{-1} \tag{3.26}$$

After replacing the constant values, the six described positions are 1.6 *mm*, 6.4 *mm*, 6.5 *mm*, 2.5 *mm*, 2.2 *mm*, and 3.8 *mm*. Taking into consideration that $T_m = T_{90\%} - T_{10\%}$, Figure 3.14 shows that the first rise time is equal to 0.77 *s*, the second is 0.78 *s*, and the third is 0.23 *s*, with an average of 0.59 *s* for the whole system.

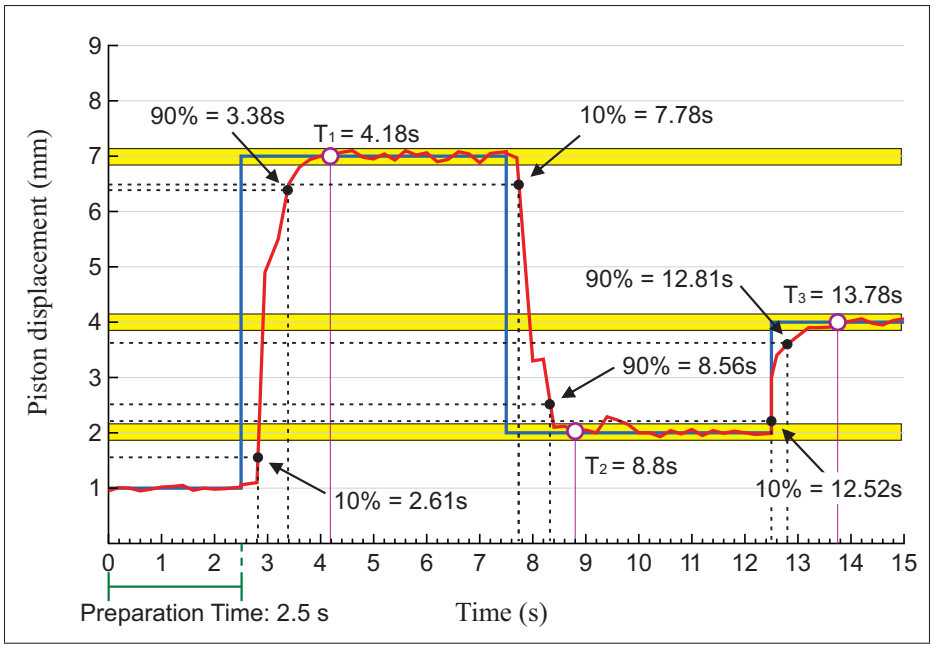

Figure 3.14 Desired and real time positioning of the piston along with the rise and response times

3.5.2.3 Response Time

The final critical feature of the PID controller is the response time, or the time that the piston takes to react to a given input. In Figure 3.14, the three yellow areas represent the range of $\pm 2\%$ for each given displacement level.

In the spatial interval of 6.86 *mm* and 7.14 *mm*, the system becomes perfectly stable at 3.9 *s*, which is 1.4 *s* after the initial rise shown in Figure 3.14. Then, in the second and third spatial intervals, the system becomes perfectly stable at 9.4 *s* and 13.1 *s*, respectively. For the second spatial interval, this is 1.9 *s* after the second rise time, and for the third spatial interval, this is 0.6 *s* after the third rise time. Overall, the response time of the haptic device requires an average of 1.3 *s* to attain $\pm 2\%$ of the desired stability level.

Our experiments proved that the piston is large enough to reach 8 *mm*, and that the required positioning features, including the time constant, the rise time, and the response time, are

sufficient for the proper operation of the mechanism. Therefore, our results confirm the functionality of the haptic apparatus.

3.6 Conclusion

This chapter presented the development of a novel haptic device based on a twisted wire actuator. Our main goal was to apply normal pressure, corresponding to the grasping force of robotic fingers, to the skin of the unimpaired human forearm. We conducted an investigation of this technique in which we calculated the model kinematic and static limitations. We thoroughly discussed the design process and the implemented equipment. Finally, we tested the apparatus through several experiments and verified its functionality.

In the next chapter we seek to integrate a vibrotactile actuator within our device. We want to investigate the impact of superposing vibrotactile and normal stress stimuli. Our current haptic device can apply pressure that corresponds to the grasping force that is applied when the prosthetic hand grasps an object such as a cup of tea. If the amputee uses the robotic hand to grasp a cup while the hand's fingers move across its surface, perhaps normal force and vibrotactile stimuli can be superposed so that the normal force represents the grasping force, and the vibrotactile stimulation represents the vibrations resulting from the fingers' movements.

CHAPTER 4

THE IMPACT OF SIMULTANEOUSLY APPLYING TWO DIFFERENT TYPES OF HAPTIC FEEDBACK UPON HUMAN SENSORY PERCEPTION

4.1 Introduction

The human sense of touch is composed of different types of mechanoreceptors that can localize contact, and that are sensitive to different modalities such as vibration, pressure or shear. Interacting with the environment, through actions such as grasping an object, involves the simultaneous stimulation of these different types of mechanoreceptors. This means that unlike some other applications of haptic feedback that require only one type of feedback, restitution of the sense of touch by direct mapping requires the simultaneous use of several types of feedback, such as normal stress, shear stress, thermal, or vibration. The impact of different types of haptic feedback on tactile receptors has been thoroughly discussed in previous studies (Stone, 2001; Caldwell *et al.*, 1997), and some teams have investigated the ability of different types of haptic feedback to restitute a given tactile modality and different tactile modalities (Jimenez and Fishel, 2014; Guiatni *et al.*, 2013). However, to the best of our knowledge, no study has yet investigated the impact of simultaneously applying multiple types of feedback upon the human ability to perceive a given one. The question we wish to answer is this: if an amputee grasps an object and the object moves in his or her hand, how does superposing stimuli that correspond to the fingers' movements and grasping force capabilities affect the subject's ability to perceive these capabilities?

After designing a haptic device in the previous chapter, this chapter tackles the specific problem regarding the impact of superposing two different types of stimuli on the human ability to perceive each of them separately. To address this problem, we conducted an experiment in which a normal stress was applied simultaneously with vibration upon each of our 14 subjects. We attempted to discover how the subjects' ability to perceive normal pressure on their forearms was affected by superposing vibration at two different locations. We then conducted the

experiment in reverse by superposing a normal stress feedback with vibration, to analyze how this impacts the subjects' perception of the vibration.

We present the details of this experiment in the following sections. We begin with a explanation of the setup of the experiment. We then explain the participants, and the experimental procedures. Finally, we present the results of our experiment and discuss their significance.

4.2 Materials and Methods

The experiment was performed under two feedback conditions, consisting of normal stress (i.e. normal pressure) and vibrotactile stimulation. These forces were applied perpendicular to the glabrous skin area of the human forearm.

The protocol of the experiment was approved by the Ethics Committee of Research (Comité d'éthique de la recherche - CÉR) at ETS University, Montreal, Canada.

4.2.1 Participants

The participants consisted of eight men and six women, the majority of whom were students recruited from ÉTS. They ranged in age from 21 to 35 years (mean: 27.8, SD: 4.07), and were all right-handed.

Participants were informed of the procedure prior to the start of the experiment. To enhance confidence in the test, participants were not aware of the order in which the stimulations and different pressure or frequency levels would appear, and during the experiment we randomly changed the order of the tests so that no two participants experienced them in the exact same order. All participants signed a form to indicate their consent to the procedure.

4.2.2 Apparatus

We designed a haptic device, shown in Figure 4.1, to apply vibration and orthogonal force to the skin. We then used a rapid prototyping machine, Objet 24 from Stratasys Ltd., to produce the main body structure of the device in a rigid, opaque white material.

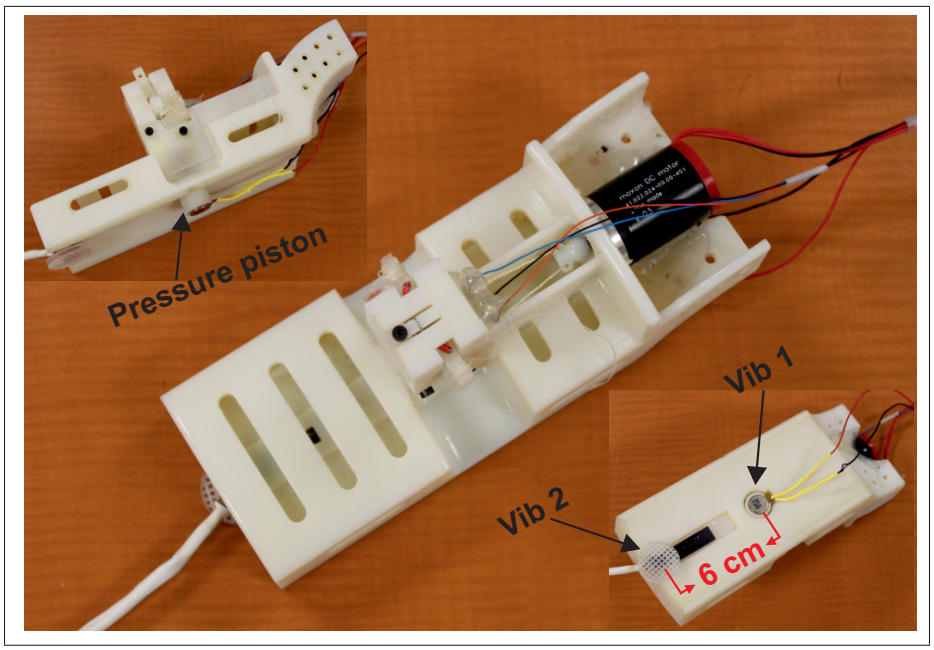

Figure 4.1 Haptic interface used for applying normal stress and linear vibration on the human participants. Vib 1 refers to the first vibrator motor, which is at the same location as the piston. Vib 2 refers to the second vibrator motor, which was used to apply vibrations at a location 6 cm away from the normal stress

A piston with a circular cross-section was integrated with the device to produce the normal stress stimulus. The piston's two extrusions were connected to a MAXON DC motor in order to apply a linear reciprocating force to the skin. This motor has a nominal voltage of 6 V and a maximum force of 18 N. The motor was also equipped with a linear Hall Effect sensor, the SS495 from Honeywell Ltd., to measure the rotation of the motor and the piston displacement. The sensor was positioned in the middle of the 14.2 mm gap that exists between the two small NdFeB magnets. As described in Kim *et al.* (2007), these magnets are located at the outer edges

of the piston. We used the sensor to measure the exact position of the piston, thus establishing that the haptic interface was capable of pushing or pulling a desired force across the entire piston length.

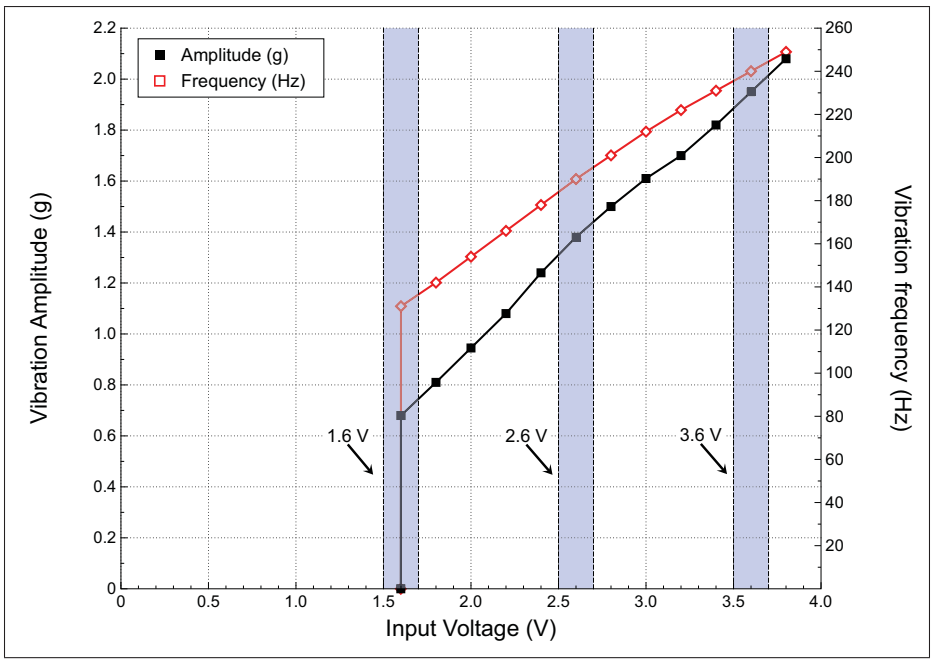

Figure 4.2 Vibrator motor performance characteristics. The three input voltages of 1.6 V, 2.6 V and 3.6 V were delivered into the cylindrical vibrator motor

Two shaftless cylindrical vibrator motors (MN: 310-113) from Precision Microdrives Ltd., were used to generate the vibrotactile stimulus. This particular model of motor was selected for two reasons. First, it is small in size, with a 3.4 mm body length and a diameter of 10 mm. Second, its sturdy casing protects the moving parts, making it possible to maintain direct contact with human skin. When an input voltage in the range of 2.5-3.8 V is applied, the motor rotates on a plane at 12000 rpm. Figure 4.2 shows the vibration magnitude and frequency based on the input voltage. In the haptic interface, the two vibrator motors were placed 6 cm apart. 3M industrial adhesive was used to mount one on the main body of the piston (Vib 1), and the other on the bottom surface of the device (Vib 2). Note that Vib 1 did not generate vibrations directly onto the participant's skin; instead, when testing the simultaneous

application of normal stress and vibration at the same location, the Vib 1 motor caused the piston to vibrate, and the piston applied the vibrations to the skin along with the normal stress.

A circular unit, 16 mm in diameter with a rough, grooved surface, was attached to the end of the piston to prevent the piston from coming in direct contact with the participant's skin. This was done in case the vibrator motor operated at a frequency that was higher than expected, in which case it could cause the piston to irritate the skin if it was applied directly. The circular unit also increased the cross-section of the contact area. The unit is depicted on top of the piston, as indicated by the red sign on the top side in Figure 4.3.

Figure 4.3 Participant applying pressure to the load-cell sensor while blindfolded and wearing the noise-removal headphones. The red arrow indicates a close-up view of the piston portion of the haptic device, with the circular unit attached to the top of the piston

4.2.3 Stimuli

Participants were exposed to two forms of stimuli: normal stress and linear vibration. Normal stress forces were delivered at three different levels, ranging from 2.8 N to 8.4 N (Figure 4.4).

We used an oscilloscope display to track the pressure magnitude at each level. The maximum distance that could be travelled by the piston was 9.6 mm, and the maximum load was a pressure of 8.4 N. Participants were not informed of these facts until after the experiments ended, in order to avoid influencing their responses.

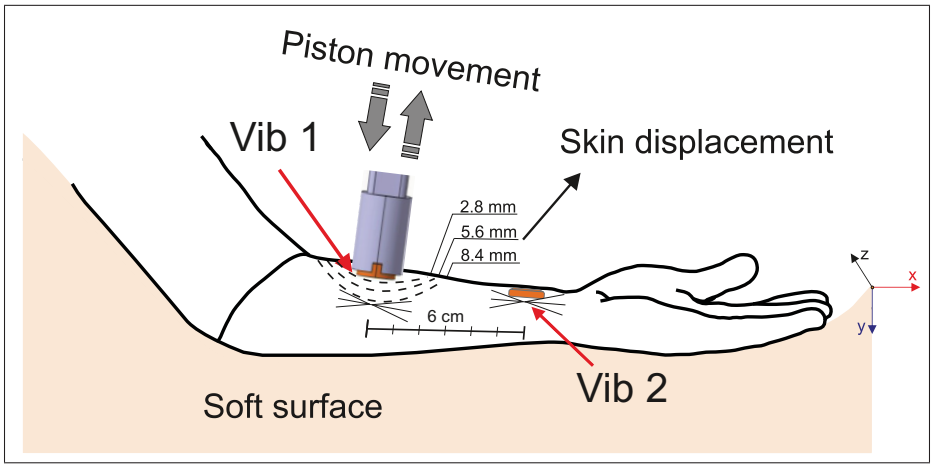

Figure 4.4 Method of stimulating the normal stress and the vibration onto the participant's forearm. Measurements in mm describe the piston's displacement from its original position

When testing the vibrotactile stimulus, the experiment was conducted using three input voltages: 1.6 V, 2.6 V and 3.6 V. As shown in Figure 4.2, almost no vibration below 1.6 V appeared in the system.

For each input voltage level, three tests were conducted: vibration alone, vibration with normal stress simultaneously at the same location, and vibration with normal stress simultaneously at a different location (6 cm away).

We will hereafter abbreviate each feedback condition as follows: P is normal force, PV1 is normal force with vibration at the same point, PV2 is normal force with vibration at different points, V is vibration, VP1 is vibration with pressure at the same point, and VP2 is vibration with pressure at different points.

4.3 Procedure

During the experiment, vibration was applied at the same time as pressure (at the same location, and then again at a different location) to observe whether the vibration improved the perception of pressure, as demonstrated by a comparison between the results of applying pressure alone, vibration at the same location as pressure, and vibration at a different location as pressure. The same process was done, in vice versa, to study the effect of using pressure to improve the perception of vibration.

At the start of the experiment, the participant was seated comfortably in front of a table and asked to place his or her dominant hand on an inflatable pillow, as shown in Figure 4.3. The haptic interface was strapped to the participant's forearm, above the wrist joint. The participant also wore a blindfold and noise-cancelling headphones (with a noise reduction rating of 28 decibels), to enhance concentration and to avoid the influence of environmental events.

To assist with force scaling, each participant was introduced to the range of force stimuli (from 0 to 9.6 N) through familiarization trials. During the familiarization procedure, each participant was given 15 minutes to interact with the device and test out the different types of haptic feedback by applying as much pressure as they desired to the load-cell sensor.

Here we will provide an overview of the experimental procedure. During the tests themselves, the feedback condition that was being tested (either P, PV1, PV2, V, VP1, or VP2) was first applied to the participant's arm for 25 seconds. Participants were instructed to pay attention to the relevant stimulus (i.e., normal stress during the P-tests, and vibration during the V-tests). Once the feedback had been applied, the participant had a few seconds to rest so as to avoid numbing the skin.

The participant was then asked to press on the button of a load-cell force sensor. For all the participants, the haptic device was attached to the right, dominant, hand, and they pressed on the load-cell force sensor button with the left hand. While the participant pressed the button, the haptic device generated the same type of feedback (i.e., the same feedback condition) onto

the skin, at a magnitude (for normal stress feedback) and frequency (for vibrotactile feedback) level that corresponded to the pressure that was applied to the sensor.

The idea was for the participant to estimate the level of feedback that the device had originally applied (during the first 25-second application) and attempt to reproduce this feedback, by pressing the sensor button with the correct amount of pressure to stimulate the same level of feedback from the haptic device. This phase also lasted 25 seconds—that is, the participant had 25 seconds to adjust the pressure that was applied to the sensor button, and to judge that the haptic feedback was at the correct magnitude/frequency level. Since the participants were blindfolded and wearing noise-removal headphones, the researcher set a timer for 25 seconds and tapped the arm of the participant when the time was up to let him/her know when to stop.

We will describe the specific details of the tests for each feedback condition in greater detail, but first we must note several aspects of the experiment that require further clarification:

- Randomization:

  The order in which these tests were conducted was randomized - and in fact, every part of the experiment, from the order of the magnitude and frequency levels to the order of the PV1, PV2, etc., tests, was randomized for each subject. We did this by creating a simple code that randomized the order of the tests, and kept track of each participant's ordering, to ensure that no two participants' test sequence was the same.

- Stimuli Application Time:

  The time of 25 seconds was chosen for two reasons. The stimuli had to be applied for over 10 seconds, to give the participants time to recognize and respond to it; and we could not apply the stimuli for over 25 seconds without the participants experiencing a numbing sensation, and losing the ability to concentrate on the stimuli. Therefore, we found that a time of 25 seconds was ideal. Note that we removed the first five seconds of each feedback section from the data, before analyzing the results, as the participants typically began their responses by pressing far too hard on the sensor, and then taking a few seconds to adjust.

- Estimation Scale:

  The participants used their own estimation scale to decide upon the amount of normal force that had been applied to their skin - i.e., they did this merely by sensing the differences between the amounts of force that were applied, rather than by being given an official scale, or by being told how much force was being applied each time. Participants also used their own estimation scale when pressing on the load-cell sensor button, when attempting to generate the same feedback level from the device as they estimated the device had initially applied to their skin.

We will now elaborate upon the specific feedback conditions, beginning with those of the normal stress tests. The stimuli of the normal stress tests were applied under three feedback conditions: P, PV1, and PV2. When testing the P feedback condition, we first used the haptic device to apply the normal force to the participant's skin, at a magnitude of either 2.8 N, 5.6 N or 8.4 N, for 25 seconds. Following this, we asked the participant to apply pressure to the load-cell for 25 seconds, to generate the same magnitude of pressure feedback from the device as he or she estimated the device had initially applied to the skin. This was repeated for each magnitude level.

The process was the same when testing the PV1 and PV2 feedback conditions, except that the randomly-selected pressure magnitude was stimulated while the relevant vibrator motor was rotating at its maximum voltage of 3.8 V (244 Hz). During the PV1 tests, the pressure and vibration were applied simultaneously at the same location using a vibrator motor (Vib 1) that we incorporated with the twisted-wire actuator haptic device. The device's piston was used to apply pressure to the participant's skin; and the vibrator motor was attached to the top of the device, so that the piston would apply the vibrations to the participantÕs skin at the same time as it applied the pressure. During the PV2 tests, of pressure with vibration applied simultaneously at a different location, the piston applied only pressure, while a separate vibrator motor (Vib 2) applied the vibrotactile feedback. Again, following the 25-second initial application period, the participants were asked to apply pressure to the load-cell sensor for 25

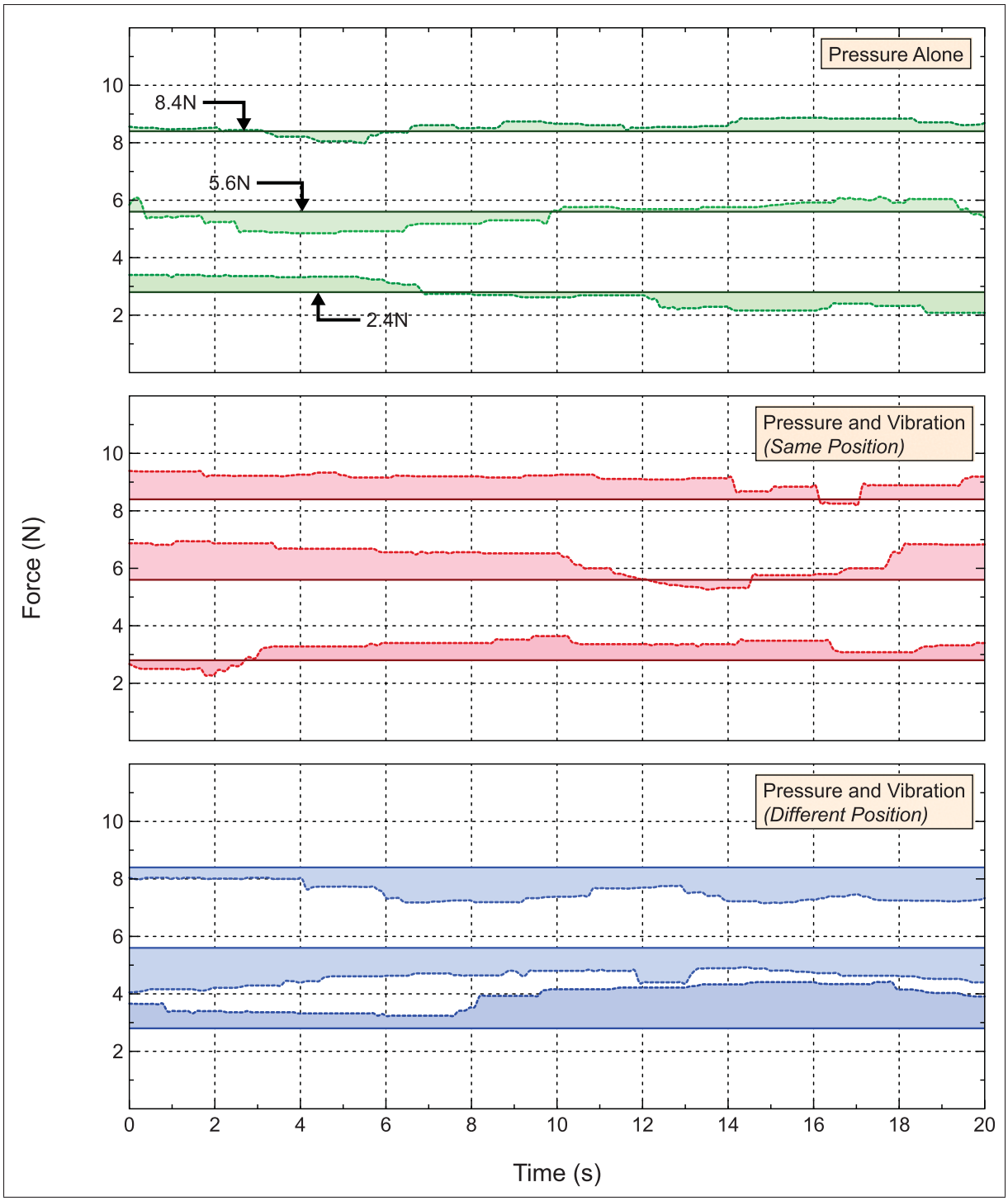

Figure 4.5 Feedback from one participant during the last 20 seconds of each test

seconds, to generate the same pressure as they estimated the device had initially applied to their skin.

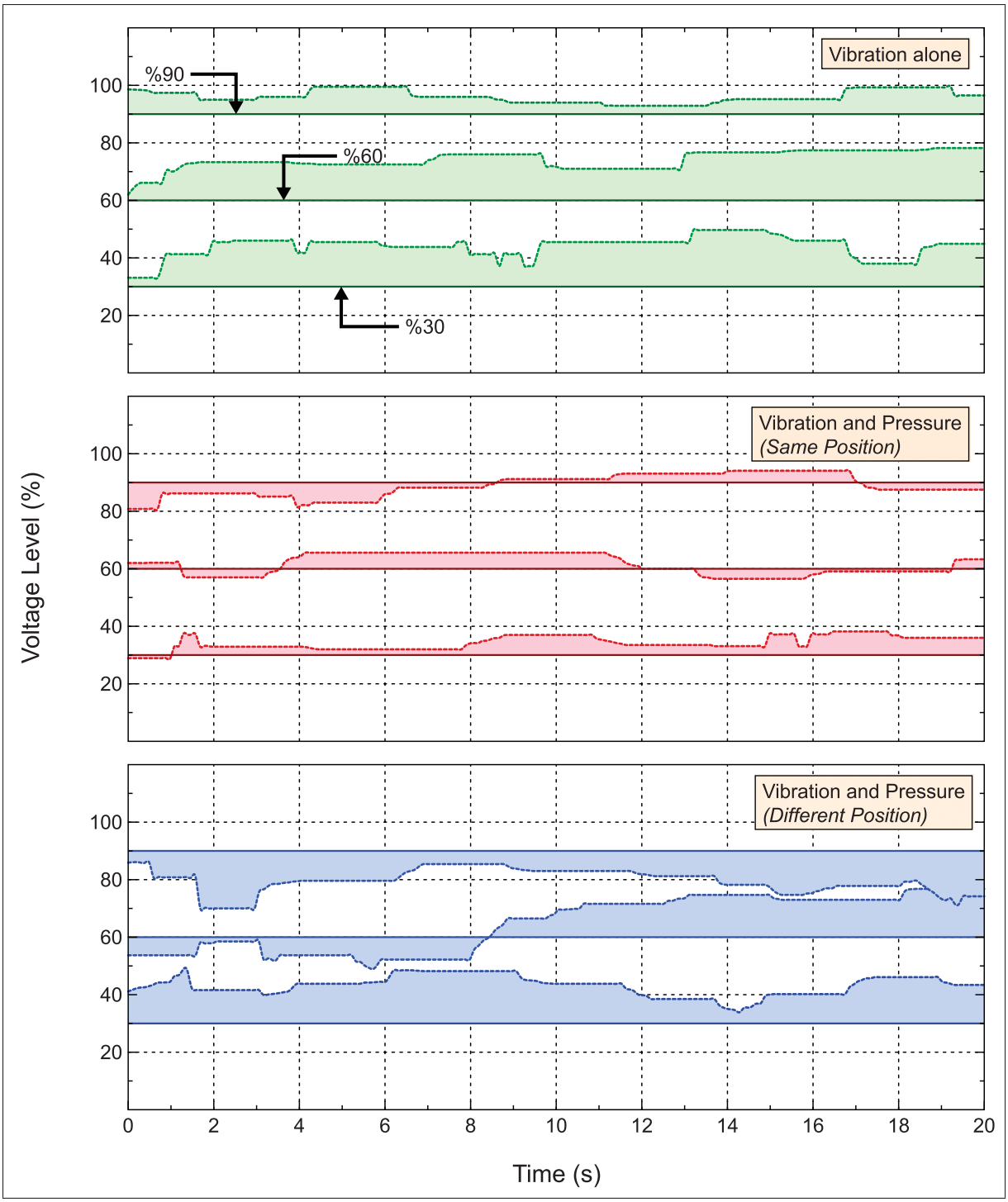

Figure 4.6 A subject's feedbacks from the vibrotactile stimulations in three input ranges during the last 20 seconds of the trial

The stimuli of the vibrotactile tests were also applied under three feedback conditions: V, VP1, and VP2. When testing the V feedback condition, we first used the haptic device to apply the vibrotactile feedback to the participant's skin, at a frequency of either 1.6 V, 2.6 V, or 3.6 V, for 25 seconds. Following this, we asked the participant to apply pressure to the load-cell sensor button for 25 seconds, to generate the same frequency level of vibrotactile feedback from the device as he or she estimated the device had initially applied to the skin. This sequence was repeated for each frequency level.

The process was the same when testing the VP1 and VP2 feedback conditions, except that the randomly-selected vibration frequency was stimulated from the Vib 1 motor (for VP1) or the Vib 2 motor (for VP2), while the piston applied a constant normal stress (the piston was at its maximum displacement distance of 9.6 mm). Again, following the 25-second initial application period, the participants were asked to apply pressure to the load-cell sensor for 25 seconds, to generate the same frequency level of vibrotactile feedback from the device as he or she estimated the device had initially applied to the skin.

Several more clarifications must be made regarding the tests. First, we did not track the amount of force that subjects applied when they pressed on the load-cell sensor. Instead, we tracked the magnitude of the normal stress (for the three normal stress feedback conditions, or P-tests), or the frequency of the vibration (for the three vibrotactile feedback conditions, or V-tests) that the haptic device applied to the participant, as it was this magnitude or frequency level that corresponded to the pressure that the participants applied to the sensor. The participants aimed to press on the sensor until they sensed that the normal stress (for the P-tests), or the vibrations (for the V-tests), felt the same as when they were initially applied. Therefore, we effectively measured the participants' ability to accurately perceive the stimulus itself, rather than simply the pressure they applied to the sensor button.

Second, it may seem that there was no difference between the two simultaneous-vibration-and-pressure tests. But we did not merely repeat the same procedure; during the vibration tests the frequency of the vibration changed for each test, while the magnitude of the pressure was held

constant; and vice versa for the pressure tests. Therefore, the repetition of the simultaneous-vibration-and-pressure tests was necessary in order to study the effects at each frequency or magnitude level.

Moreover, the main difference between the tests (i.e. the difference when testing the effect of vibration upon perceiving pressure, vs. the effect of pressure upon perceiving vibration), was in the type of feedback that the participants were asked to focus upon. So, when testing the effect of vibration upon perceiving pressure, the participant was focusing on the pressure; and when testing the effect of pressure upon perceiving vibration, the participant was focusing on the vibration. In addition, the type of feedback to be focused upon was the first type to be applied to the participant, before being followed by the additional feedback type. For instance, during the pressure-with-vibration tests, we first applied pressure alone for one second to allow the participant to focus on the pressure, before we added the vibration at the same location.

To give an example of the accuracy of the feedback generated by the participants, Figure 4.5 and Figure 4.6 depict the normal stress and the vibrotactile feedback from one participant. The straight lines represent the magnitude or frequency level that was initially applied by the haptic device, and the trimmed margins around the lines indicate the magnitude or frequency level that was generated by the participant when attempting to replicate it.

On the left, the participant's response is shown as force because this is the force that the piston applied to the participant, as the participant pressed on the force sensor. The participant was attempting to press on the force sensor to generate the right amount of pressure from the piston. On the right, the participant's response is shown as the voltage level percentage that was used by the vibrator motor as it conveyed vibrations (through the piston) to the participant's skin. The vibration frequency here corresponded to the amount of pressure that the participant applied when pressing on the force sensor. In the graph, the voltage is given in terms of the percentage of maximum possible voltage - that is why it shows 20, 40, etc., for 20%, 40%, etc., of the maximum voltage level of 3.6 V.

Overall, each of the three magnitude levels was tested for each of the three normal stress feedback conditions, and each of the three frequency levels was tested for each of the three vibrotactile feedback conditions, resulting in 18 numerical data per person and a total of 252 trials for all 14 participants.

Lastly, at the end of the experiment, the participants were asked simple questions about the performance of the system, such as how well the magnitude force corresponded to the feedback from each device. They were then shown graphs of the final results.

4.4 Result Analysis

The experimental data underwent a statistical analysis to determine the effects of normal stress upon the detection of vibration, and vice versa. The main parameters were the variances, and the corresponding norms of the numerical data, which were used to determine the relevant error of each stimulus. Our analysis considered the data collected from the last 20 seconds of each of the 14 participants' feedback. As described in the procedure section, we did not include the first five seconds of data from each experiment, as the participants needed a few seconds to adjust their responses. Note that in this section, we present the results as categorized by the type of test, which may make it appear as though the tests occurred in a standardized order for each subject. However, the testing order was entirely randomized; we have merely grouped the results together in this section for ease of analysis.

4.4.1 Normal Stress Stimulation

This section will investigate the impact of superposing vibration on the normal stress stimuli. As described above, the normal force was delivered to each participant's forearm under a randomly selected feedback condition of either P, PV1, or PV2, and magnitude of either 2.4 N, 5.6 N or 8.4 N.

Table 6.1 lists the key statistical parameters from the average feedback of all 14 participants. In calculating the standard deviation in Table 6.1, we took the average results of each participant

Table 4.1 Statistical analysis of the collected data for the normal stress tests

	P			PV1			PV2		
	2.8 N	5.6 N	8.4 N	2.8 N	5.6 N	8.4 N	2.8 N	5.6 N	8.4 N
Mean	3.168	5.922	8.489	3.439	4.841	7.993	3.543	6.480	9.184
Median	3.164	5.854	8.576	3.471	4.762	8.103	3.559	6.561	9.284
Standard Deviation	0.228	0.284	0.154	0.211	0.301	0.560	0.291	0.508	0.651
Manhattan Norm	0.412	0.559	0.546	0.725	0.822	0.668	0.704	1.050	0.868
Euclidean Norm	0.031	0.053	0.052	0.042	0.062	0.076	0.042	0.055	0.064

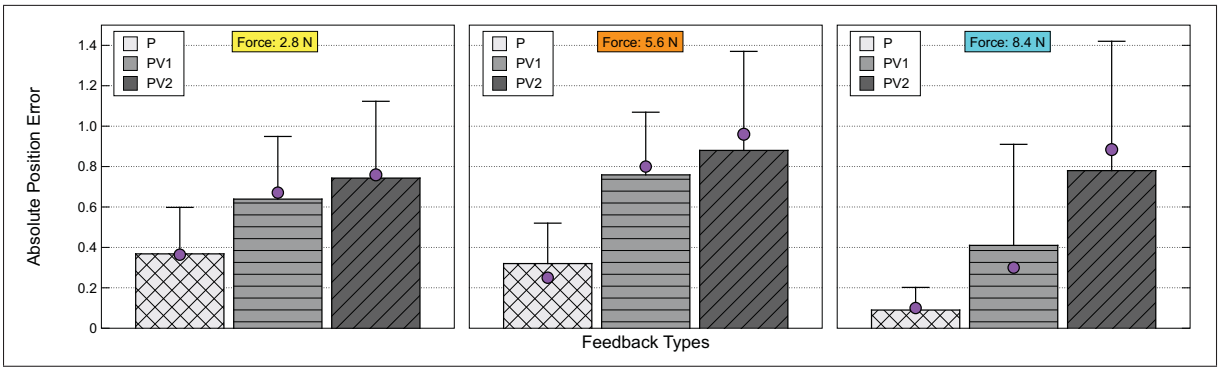

Figure 4.7 Participants' feedback under three types of normal stress stimuli (P, PV1, PV2). The grey rectangles indicate the mean, the bars with horizontal lines on top indicate the absolute error, and purple circles indicate the median

(i.e., the average of all of the individual participants' 20 second periods), and from this, calculated the standard deviation of the 14 participants' means. Each 20 second period included 203 data points. We calculated the other measures in the same way.

Figure 4.7 depicts the absolute mean, absolute error, and the median of all the subjects' results for each of the normal stress feedback conditions. Here, we use "absolute" to refer to the absolute difference between the pressure (measured in N) that we applied to the participants (through the haptic device), and the pressure that the haptic device applied to the participants after they had pressed on the load-cell sensor. Essentially, the absolute error measures the difference between the initial pressure applied by the device, and the pressure that the subjects generated later when attempting to replicate it, thus providing a measure of the participants' accuracy.

Table 4.2 Statistic analysis of the normal stress stimuli from the ANOVA table. Type A indicates P, PV1, and PV2. Type B indicates only PV1 and PV2

	Type	*SS*	*df*	F	$P-value$	$F_{critical}$
2.8N	**A**	**0.89 - 2.00**	**2 - 33**	**7.39**	**0.002**	**3.28**
	B	0.063 - 1.06	1 - 22	1.31	0.26	4.30
5.6N	**A**	**2.41 - 5.73**	**2 - 33**	**6.94**	**0.003**	**3.28**
	B	0.65 - 4.84	1 - 22	2.98	0.09	4.30
8.4N	**A**	**1.08 - 1.48**	**2 - 33**	**12.7**	**0.001**	**3.28**
	B	1.08 - 1.27	1 - 22	7.93	0.01	4.30

We infer from this graph that P alone is more accurately judged by the subjects than PV1 and PV2, at all three magnitude levels. Table 4.2 depicts the one-way ANOVA table that was used to determine whether or not the mean of the position error was significantly different at each level.

At the lowest magnitude level, 2.8 N, the difference between the means of P, PV1 and PV2 is clearly distinguishable (0.368 < 0.639 < 0.743), whereas the absolute error is nearly identical. This result is logical when one considers the low level of delivered force at 2.8 N, and thus the high level of skin sensitivity required to distinguish it from the vibrations. When testing our hypothesis that P is superior to PV1 and PV2, the test statistic shows the significant difference of the collected data by considering the $F-value$ ($F = 7.39$, $F_{.05;2,33} = 3.28$, $\alpha = 0.05$) and the $P-value$ ($P = 0.002$).

Next we determined the reliability of the data collected at 5.6 N. The $P-value$ of 0.003 and the $F-value$ of 6.94 (between all the feedback conditions) show the significant negative impact of vibration on the perception of normal stress. This result is a good reason to replicate the experiments at a higher magnitude level. Experimenting with higher magnitude levels might help determine a clear relationship between the level of force and the feedback errors. Of course, the level must not be so high that it causes pain or irritates the skin of the participants.

At the highest level of pressure, 8.4 N, analysis of the data again shows a significant difference between P and the other two stimuli, PV1 and PV2. At 8.4N, $F = 12.7 > F_{.05;2,33} = 3.28$, and the $P - value = 0.003$. This confirms our hypothesis that P provides superior functionality.

In further inspection of the normal stress stimuli, we recalculated the parameters between PV1 and PV2 to determine the effects of how the vibrating motors were positioned during each section of the experiment. In Table 4.2, Type B, the second row displays the $P - value$ and $F - value$ for 2.8 N, 5.6 N, and 8.4 N. As anticipated, at 2.8 N and 5.6 N we cannot determine whether PV1 or PV2 is superior. This is because the F-values, at $F_{2.8} = 1.31$ and $F_{5.6} = 2.98$, are very low compared to the $F_{critical}$ of 4.22 and the high $P - value$ of $P_{2.8} = 0.26$ and $P_{5.6} = 0.09$. We were able to obtain the desired result at 8.4 N. At this level there is a significant difference, as indicated by the $F_{.05;1,22} = 7.93$ ($F_{critical} = 4.30$) and the $P - value = 0.01$.

4.4.2 Vibrotactile Stimulation

This section examines the impact of normal stress stimuli upon the perception of vibrotactile feedback. During the tests, the input voltages of 1.6 V (130 Hz), 2.6 V (190 Hz), and 3.6 V (240 Hz) were each delivered to the vibrator motor for all the feedback conditions, of V, VP1 and VP2. In VP1 and VP2, the pressure piston remained at its maximum displacement (a distance of 9.6 mm).

We gathered the key parameters for the statistical analysis of the vibrotactile stimuli, the results of which are shown in Table 4.3. Here, we use “absolute" to refer to the absolute difference between the vibration (measured in Hz) that we applied to the participants (through the haptic device), and the vibration that the haptic device applied to the participants after they had pressed on the load-cell sensor. The absolute error measures the difference between the initial vibration applied by the device, and the vibration that the subjects generated later when attempting to replicate it, thus providing a measure of the participants’ accuracy.

Evidently there are differences between the means and the standard deviations of all three feedback conditions. Normal stress has a positive impact on vibration at VP1 and VP2 regardless of

Table 4.3 Statistical analysis of the collected data for the vibrotactile stimuli

	V			VP1			VP2		
	130 Hz	190 Hz	240 Hz	130 Hz	190 Hz	240 Hz	130 Hz	190 Hz	240 Hz
Mean	3.850	5.278	8.375	3.406	6.030	9.051	3.616	6.572	9.353
Median	3.886	5.300	8.424	3.419	6.022	9.071	3.607	6.305	9.366
Standard Deviation	0.294	0.478	0.557	0.226	0.218	0.198	0.364	0.329	0.412
Manhattan Norm	0.879	0.832	0.856	0.480	0.360	0.352	0.659	0.446	0.598
Euclidean Norm	0.065	0.063	0.065	0.039	0.027	0.027	0.050	0.038	0.046

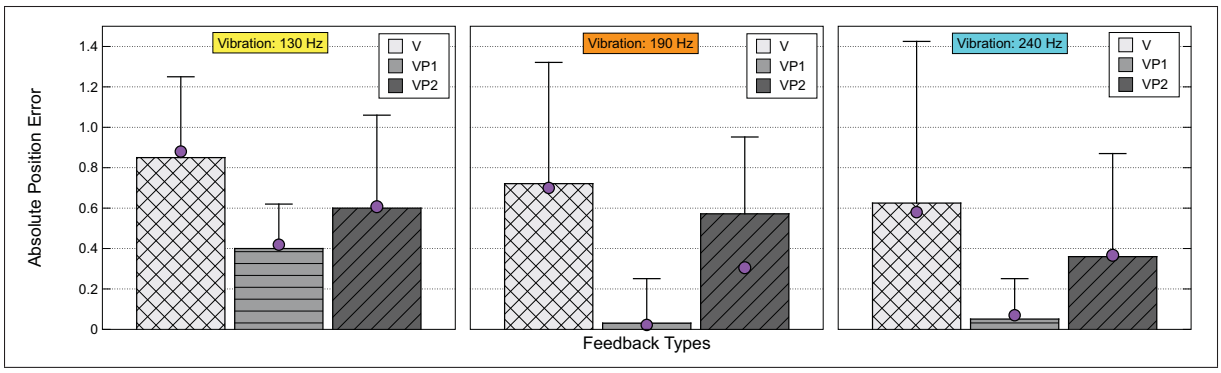

Figure 4.8 The fourteen subjects' feedback under three types of vibrotactile stimuli (V, VP1, VP2). Bars and lines show the absolute mean and the absolute error, and purple circles indicate the median across all tests

the level of force. This difference is more visible at the higher vibration amplitudes of 190 Hz and 240 Hz, which have respective means of $0.03 < 0.272 < 0.572$ and $0.05 < 0.525 > 0.353$. As shown in Figure 4.8, the absolute errors of the bars indicate a smaller error from the feedback of VP1 compared to the V and VP2 conditions. This alone may support our hypothesis of the superiority of VP1 in the vibrotactile test. However, our hypothesis must be confirmed using data from the ANOVA table.

As with our analysis of the normal stress tests, our next step was to compare the $F - value$ and $F_{critical}$ and to calculate the $P - value$. The result is shown in Table 4.4. This step allows us to determine whether or not the difference of the variance is significantly higher in VP1 than in V and VP2.

Table 4.4 Statistical analysis of the vibrotactile stimuli from the ANOVA table. Type A indicates V, VP1, and VP2. Type B indicates only V and VP2

	Type	*SS*	*df*	F	$P-value$	$F_{critical}$
1.6V	**A**	**1.13 - 4.98**	**2 - 33**	**4.44**	**0.018**	**3.28**
	B	0.37 - 3.77	1 - 22	2.60	0.118	4.30
2.6V	**A**	**1.01 - 3.47**	**2 - 33**	**5.71**	**0.006**	**3.28**
	B	0.98 - 3.28	1 - 22	5.65	0.025	4.30
3.6V	**A**	**1.96 - 4.94**	**2 - 33**	**7.74**	**0.001**	**3.28**
	B	1.19 - 4.52	1 - 22	6.61	0.019	4.30

At the lowest vibration magnitude, $1.6V$, the difference between the means is small. We used the feedback from V, VP1, and VP2 to calculate the $P-value$ ($P = 0.018$) and the $F-value$ ($F = 4.44$, $F_{.05;2,33} = 3.28$, $\alpha = 0.05$). The small size of these values proves that VP1 is superior. We confirmed the reliability of the data collected at the input voltage of $2.6V$ using the $P-value$($P = 0.006$) and the $F-value$ ($F = 5.71$, $F_{.05;2,33} = 3.28$, $\alpha = 0.05$). At the highest input voltage, $3.6V$, the $F-value$ ($F = 7.74$, $F_{.05;2,33} = 3.28$, $\alpha = 0.05$) between all feedback conditions, and the P-value of 0.001, show the significant difference of the variance. According to this result, normal stress, when applied at the same point as vibration, has a positive impact upon the perception of that vibration. As shown in Table 4.4, the input voltages are directly proportional to the $F-values$ and the $P-values$. This difference becomes more evident as the input voltage is increased.

We also compared the F and $F_{critical}$ between the V and the VP2 conditions to substantiate our claims of the superiority of one over the other. According to the results, shown in Figure 4.8, the absolute mean indicates VP2 as the second best feedback type at all input levels. The $F-value$ ($F_{1.6} = 2.60$), and the $F_{critical} = 4.30$, shown in Type B of Table 4.4, are not high enough to establish the reliability of the data collected at the input voltage level of $1.6V$. However, at $2.6V$ and $3.6V$ the $F-values$ ($F = 5.71$ and $F = 6.61$) and the $P-values$ ($P = 0.025$ and $P = 0.019$) demonstrate that the simultaneous application of normal stress, even at a point 6

cm away from the vibration, allows participants to perceive the vibration better than when the vibration is applied on its own.

4.4.3 Norms vs. Variances

To measure the error for each type of stimuli, we calculated the Manhattan and Euclidean norms shown in Table 6.1 and Table 4.3. The results of this process are illustrated in Figure 4.9, in which each participant's individual feedback, along with the average feedback for each stimulus from all 14 participants, is distinguished by its variance versus the Manhattan norm. We used norms to give a visual explanation of which tests had the lowest error. Since the graphs in Fig. 8 show norms plotted against variance, the type of tests in the lower-left corner are those with the least error.

Regarding the effect of superposing the normal stress stimuli with vibration, a clear upward trend from the lowest to the highest magnitude levels can be seen in the first row of Figure 4.9. At the highest magnitude levels, the variance and the norm are smaller, which leads to better restitution feedback and consequently less error in the system. At 2.8 N, the participants' responses to each type of stimulus have near-identical variance ranges; only the difference in the norm distinguishes one participant's feedback from another's. This gap between the average positions of P and the two others becomes more visible at 5.6 N, and at 8.4 N it reaches its maximum.

In the vibrotactile stimulations shown in the second row of Figure 4.9, we again witness an upward trend. Unlike the normal stress stimuli, however, here the superiority of one condition is clear even at the lowest voltage level. All three input voltage levels reveal the superiority of VP1 and the limited functionality of V, though it is especially evident at the highest levels, 2.6 V and 3.6 V.

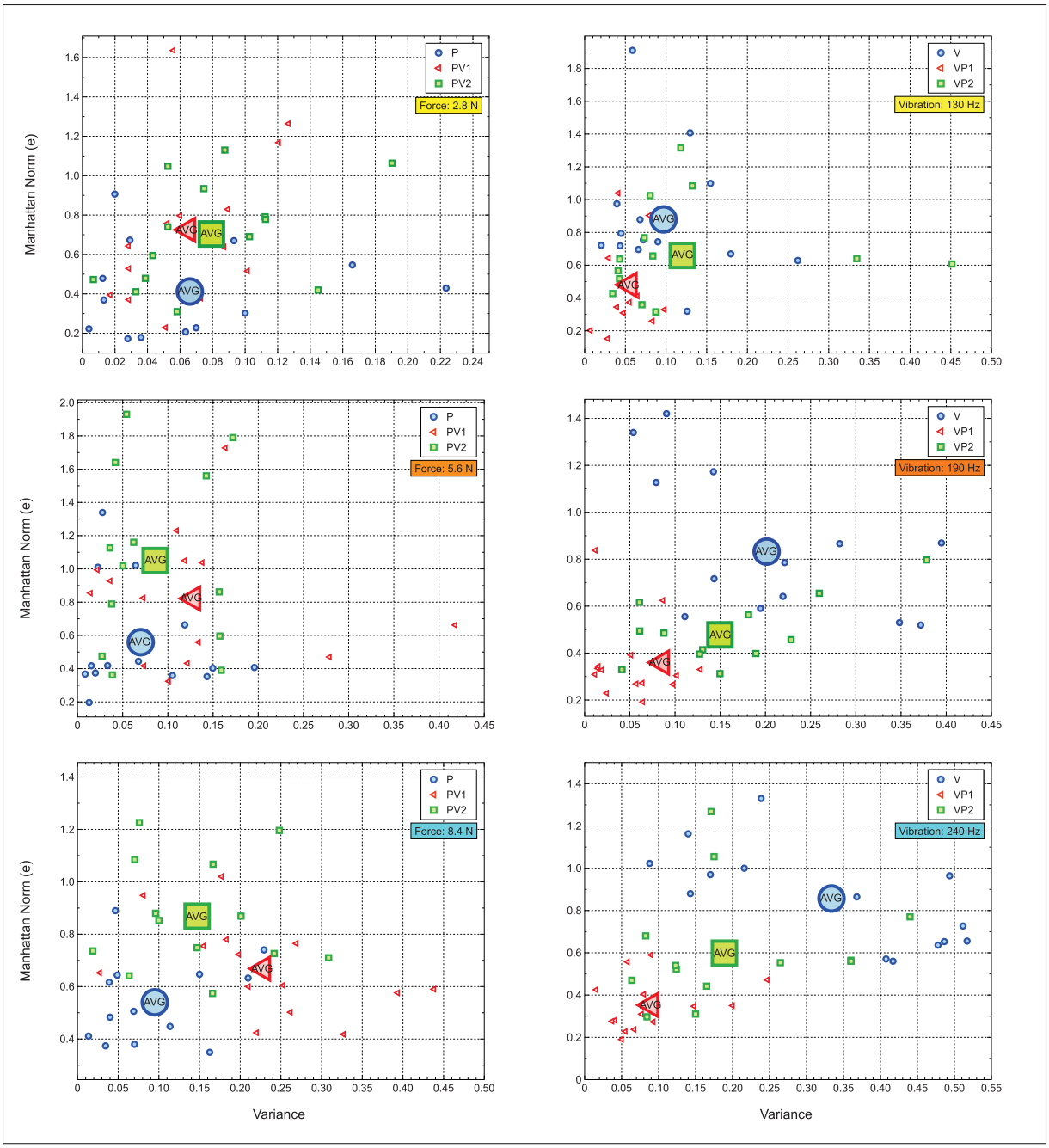

Figure 4.9 Static analysis of the Manhattan norm versus variances under different conditions. The first row belongs to the normal stress stimuli from the 2.8 N to 8.4 N and the second row belongs to the vibrotactile stimuli starting from 1.6 v to 3.6 v. Bigger rectangular, triangle and the circle indicate the average positioning result of all 14 subjects' feedback

4.4.4 Subjects Preferences

As mentioned in the procedure section, at the end of the tests the participants were questioned about which feedback system they preferred. Participants were asked to rank the feedback conditions by assigning a score between 0 (worst) and 1 (best).

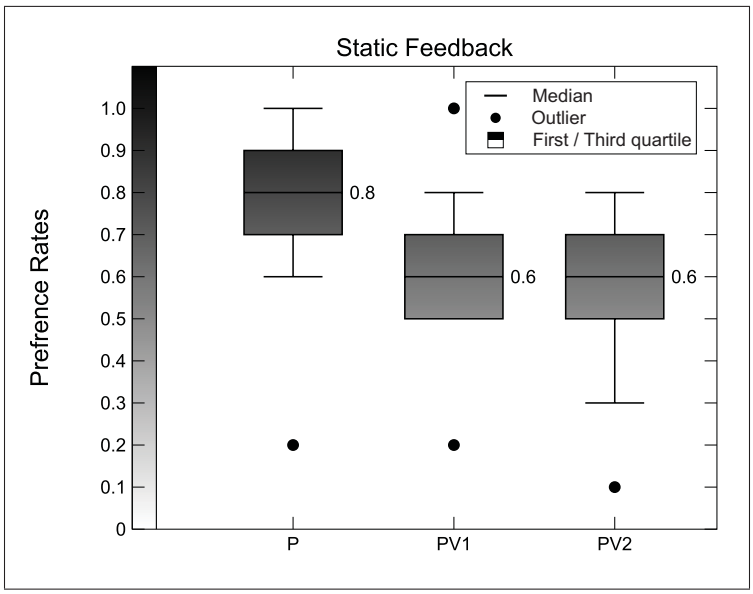

Figure 4.10 Preference rating in different feedback condition of the normal stress stimuli from the 14 participants

Figure 4.10 shows the participants' ratings regarding P, PV1 and PV2. Although participants gave a variety of scores to each feedback condition, the overall rates are surprisingly consistent with the results of our analysis of the collected data. All the participants but one ranked P as most-preferred, then PV1, and finally PV2 as least-preferred.

All 14 participants' preference rates for the vibration stimuli and its feedback conditions are shown in Figure 4.11. All the participants but two ranked VP1 as providing the best feedback, and V, the worst.

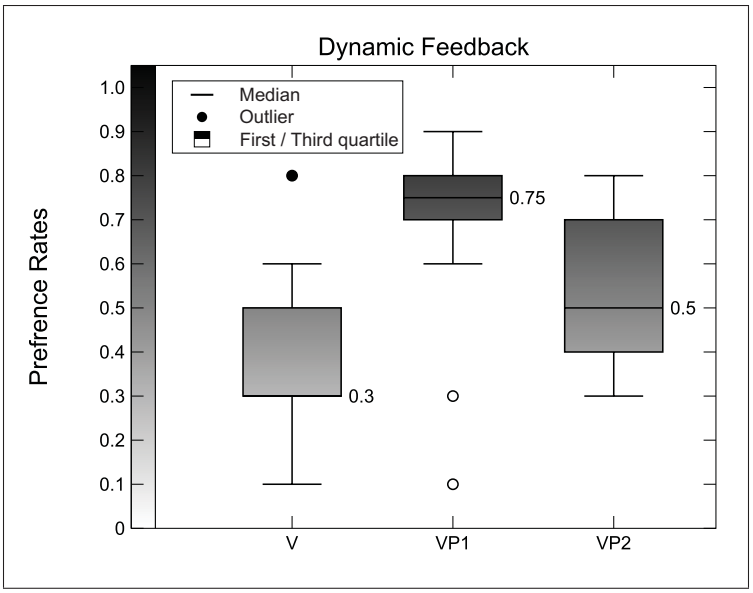

Figure 4.11 Preference rating in different feedback condition of the vibrotactile stimuli from the 14 participants

4.5 Conclusion

The purpose of this study was to simultaneously apply two different types of stimuli, at the same and at different locations, to see how this impacts the ability of humans to perceive a given stimulus.

Analysis of the errors and the variance obtained through our experiment suggests that normal stress alone provides a much more accurate restitution of exteroceptive sensation, compared to vibrations applied simultaneously at the same point and at a different location. Indeed, the negative impact of vibrations upon the subject's ability to perceive the applied normal stress, under both superposed and non-superposed conditions, is noticeable at all force levels. It seems that the dynamic stimulus blurs human perception of the applied stress. This conforms to our initial hypothesis. However, while the results support one of our beliefs, they contradict another one. The statistical results, as well as the subjects' comments presented in Figure 4.12, suggest that applying vibration at the same point as the normal stress is less distracting than when the vibration is applied at a distant location. We do not yet have a clear explanation for this. Our

current hypothesis is that even though the vibration blurs the normal stress signal, perception of the normal stress is higher when vibration is applied at the same location because the subjects can focus all their concentration on that one point.

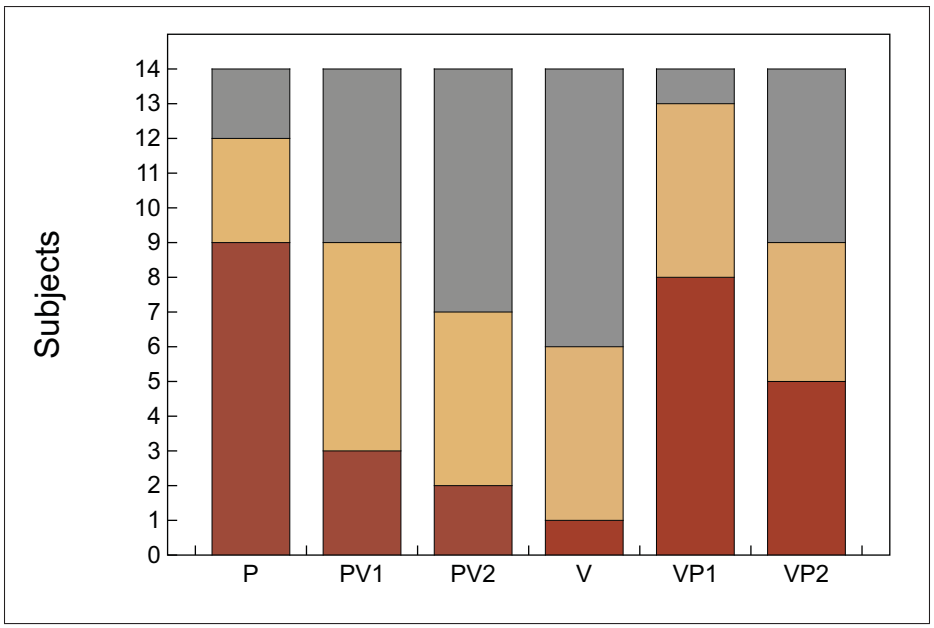

Figure 4.12 The overall subjects' feedback for all types of stimuli. The red part indicates the number of subjects that performed best with the specific stimulus, the grey part shows the number of subjects who performed worst, and the orange part denotes the number of subjects who were in-between

Our experiment aimed at quantifying the impact of applying a normal stress stimuli simultaneously with vibration upon the ability of the subject to perceive the vibration. At both the $2.6V$ and $3.6V$ input levels, the difference between the absolute means, and between the $F-values$ and $F_{critical}$, is significantly higher. This confirms our hypothesis regarding the superiority of VP1 over the other conditions. In other word, the subjects' perception of the applied vibration increases when we raise the level of normal stress between the subject's arm and the vibro-actuator. This was expected, as the vibration and the normal stress are synergistically coupled: the vibration transmission is a known function of the stress at the contact point. Less expected is the following: almost all our results show that subjects perceive vibration better when we

apply normal stress simultaneously and at a different location, than when we apply just the vibration alone. We have not yet developed an explanation for this.

In conclusion, these results give new insights on how the simultaneous application of different haptic stimuli to a compact space on the human arm impacts the ability to perceive each stimulus. Although previous haptic devices have used different modalities simultaneously, to the best of our knowledge, nothing in the literature to date has investigated the pairing presented in this study. This is one step towards using haptic technology to fully restitute a highly multi-modal sense of touch to hand amputees. In parallel to this study, we have also designed a new tactile sensor that can measure normal stress diffusion and magnitude as well as dynamic events. Next chapter will focus on merging these two endeavours to examine how both types of technology can be used to help amputees.

CHAPTER 5

TACTILE SENSATION TRANSMISSION FROM A ROBOTIC ARM TO THE HUMAN BODY VIA A HAPTIC INTERFACE

5.1 Introduction

This chapter presents a robotic system that was used to study the restoration of touch sensitivity. We endeavour to find out how humans can use multi-modal haptic feedback to recognize texture as well as the applied force from fingertips of the robotic hand. Here, a combination of tactile sensors, robotic fingers, and a haptic interface enabled us to undertake different types of experiments on human subjects. To this end, we have conducted two separate tests on eight human subjects in order to assess the effectiveness of the static and dynamic modalities in different detectable ranges of the skin sensitivity.

Several stimulation techniques, including electrotactile, vibrotactile, and mechanotactile, can be integrated with the haptic device. Antfolk *et al.* (2013) have thoroughly discussed these functionalities. As mentioned in previous chapter, Our haptic device uses a combination of vibration and mechanical pressure to transform the dynamic and static feedback, separately. Vibration is particularly useful in prosthetic applications due to its fast and convenient ability to restore a sense of motion Damian *et al.* (2011); Fortin *et al.* (2014). It can be applied directly to the skin, and patients can quickly recognize its effect. Furthermore, vibrotactile stimulation can provide a sense of motion and direction when multiple vibrator motors are placed on the skin Tan *et al.* (2003). Mechanotactile stimulation provides a way to recognize static events. Small mechanisms can be integrated with the haptic device in order to apply pressure and stimulate the SA receptors. In recent years different approaches have been tested to find the best way to apply pressure. According to Biggs and Srinivasan (2002), tactile receptors on hairy skin are more sensitive to the tangential force (shear), whereas the receptors on glabrous skin and the finger-pads are more sensitive to normal pressure. In our experiment pressure is applied vertically, since the goal is for pressure applied from the finger-tips to stimulate the proper feedback at the glabrous skin area.

In the following sections, we describe the materials and instrumentation that were used in this study. We then discuss the method used to investigate the impact of static and dynamic modalities on sensory fingers, the robotic hand control, and the haptic interface reactions regarding the desired stimuli. Finally, we present the end result and discuss the effectiveness of different types of stimuli under various input ranges.

5.2 Instrumentation

We used the system shown in Figure 5.1 to provide each subject with pressure and vibration sensations from a haptic device, measured by a tactile sensor.

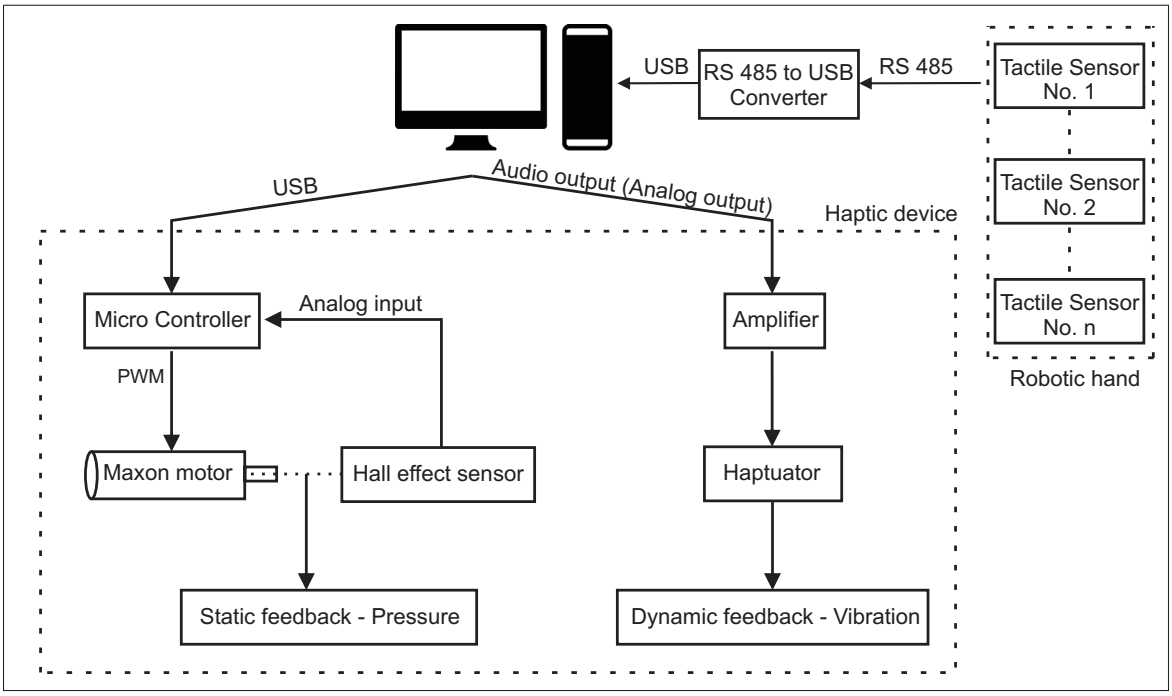

Figure 5.1 Architecture of the experiment setup

5.2.1 Tactile Sensor

Another group of researchers in our laboratory have developed a multi-modal capacitive tactile sensor (Figure 5.2). It was designed in our research laboratory, CoRo, at École de technologie

supérieure (ÉTS) and commercialized (patented - Duchaine and Rana (2014)) by Kinova, Inc. and Robotiq, Inc. Our sensor is unique in that it can perceive both pressure and speed of movement, based on data that were generated under both static and dynamic conditions, and that can be captured by the sensor at the same time and location.

Our research focuses on texture recognition, so we will only be using the dynamic sensing capabilities of the sensor. However, the static sensing capabilities are described as follows for the reader's information. Figure 5.2 shows various elements of our tactile sensor, including a close-up view of its sensitive surface (made using an SEM diagnosis microscope). The sensor has a resolution of 3×4 taxels per phalange with a sampling frequency of about 25 Hz. It uses two layers of micro-structured silicone dielectric filled with nano-particles of ferroelectric ceramic, which give the sensor a wide range of measurement and a high sensitivity to lightly-applied forces (10^{-4} N per taxel).

We were able to conduct our experiments under dynamic conditions because our sensor is able to determine variations in forces at a very high frequency. Each texture generates unique data because each texture features a different depth and pattern of an engraved motif, which generates unique vibrations when moving over the sensor's surface. The sensor detects these vibrations and transmits the information about the textures' movements to the vibrator motor, which then applies a corresponding type of vibration to the user's skin.

The modality we are measuring in these experiments is the stress rate that is applied to the sensor's surface. Dynamic sensing is achieved here using a transimpedance amplifier that only goes out of its equilibrium in response to variations in the sensor capacitance. This make it highly sensitive to any dynamic event, such as vibration, and allows us to have a sampling frequency that is considerably higher than what is used for static measurements (1000 Hz vs. 25 Hz).

We used a vibrotactile transducer to ensure that the sensor was adequately sensitive to vibration in terms of frequency. In fact, even though our sensor's range of acquisition ($50 - 500$ Hz) is the same as the range within which humans can distinguish frequencies, the results of numer-

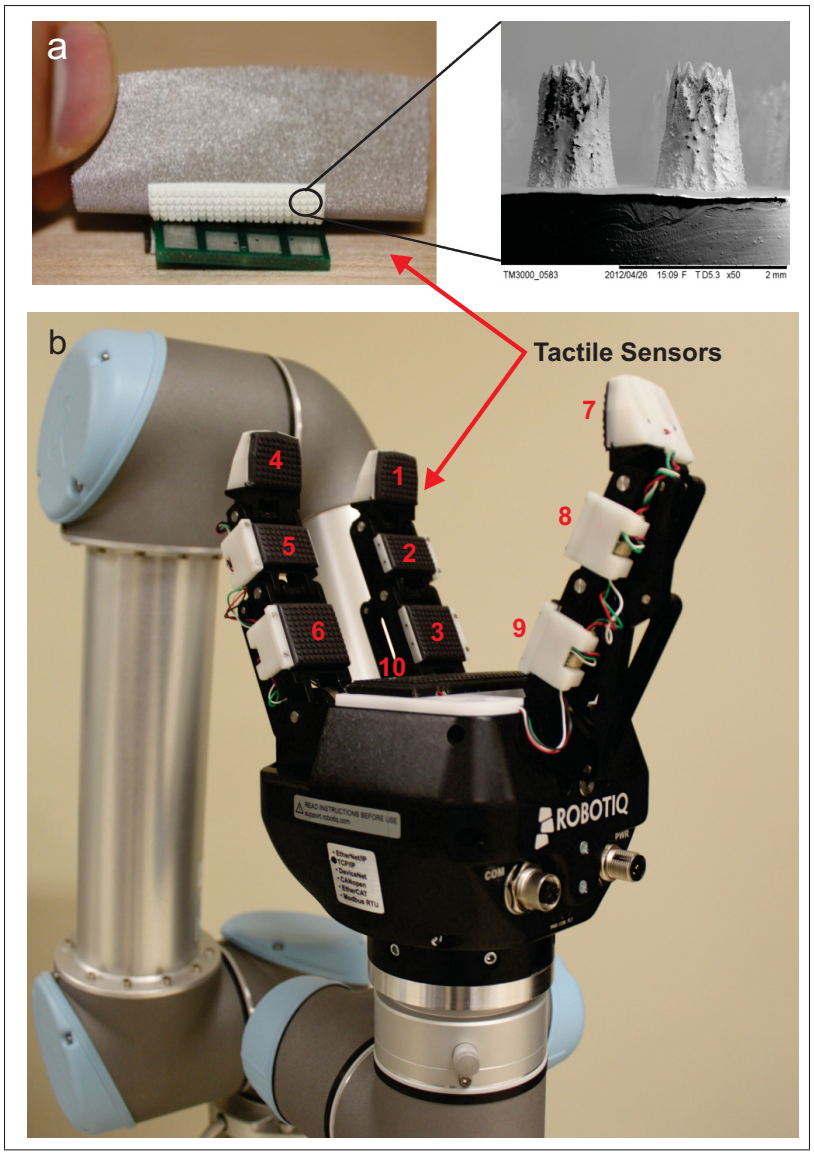

Figure 5.2 Robotic components of the haptic system. The sensors provide normal stress measurements (10^{-4} N – 20 N per taxel) as well as dynamic sensing capabilities. (a) Foam used between the two plates of the capacitor, from Rana and Duchaine (2013). (b) Three-finger adaptive robot gripper from Robotiq, Inc., equipped with 10 tactile sensors and mounted on a UR5 Universal Robot

ous tests conducted during its development show that our sensor exceeds human sensitivity to mechanical vibratory frequency.

A simple experiment, conducted on 10 subjects, determined the optimal frequency for human sensitivity to be 250 Hz. This value is consistent with the range of $200-300$ Hz that has been identified in the literature. We then set the Haptuator to vibrate with a frequency below this level. The FFT of the sensor signal was still able to display a clear peak amplitude, proving that the sensor can detect certain vibrations even when humans cannot.

5.2.2 Robotic Hand

We placed an adaptive 3-finger adaptive robot gripper from Robotiq, Inc., on top of the Universal Robot manipulator, UR5 (Robot, 2012). The gripper has a maximum payload of 7.5 kg (2.5 kg for each fingertip), and a gripper stroke of 155 mm. The combination of the robot gripper and the UR5 resulted in a system that functions almost similar a real human hand.

5.2.3 Haptic Device

We used a wearable haptic apparatus (Figure 5.3), which is almost the same as the one that used in chapter 4. The only difference is that instead of two ordinary vibrator motor, the device equipped with a cylindrical vibrator motor shown in Figure 5.3 to generate the vibrotactile stimulus. Our cylindrical vibrator motor was the Haptuator Mark II, made by Tactile Labs, Inc. The Haptuator is a vibrotactile transducer with a bandwidth of $90-1000$ Hz and typical impedance of 5.5 Ω, and it depends on frequency as well as voltage for the oscillation of mass in its formation (Figure 5.4). We used a signal source to supply a sine/square wave with different frequencies and amplitudes, in order to ensure better performance.

5.2.4 Software

A Qt-based graphical user interface (GUI) was created specially for this experiment. This software was responsible for acquiring the static and dynamic data from the tactile sensor via a USB 2.0 port at a constant rate of 20 Hz and 1000 Hz, respectively. During static conditions, it forwarded static data to a micro-controller that commands the piston of the haptic device

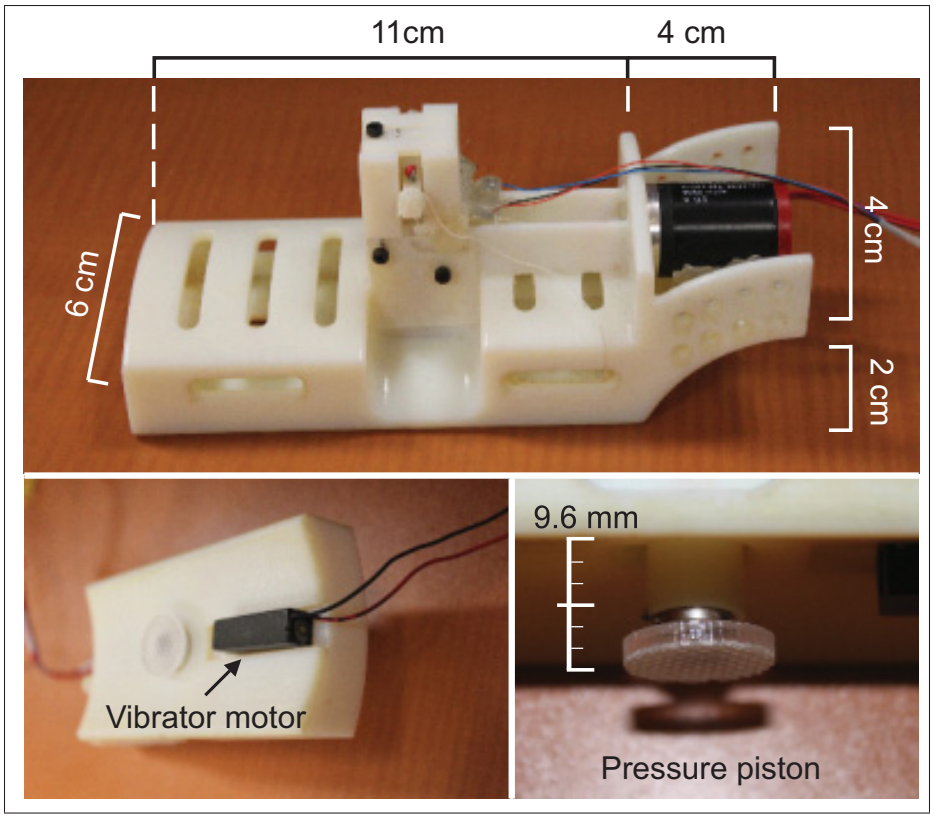

Figure 5.3 The haptic interface used to apply normal stress, along with a linear vibrator motor (Haptuator Mark II)

through PID control. During dynamic conditions, it sent the vibration signals to the Haptuator's amplifier, directly from the audio analogue output.

5.3 Experimental Procedure

The experimental procedure was conducted in two separate phases. Both phases examined the transmission of touch sensitivity, but phase one was under a static condition, whereas phase two was under a dynamic condition. Both phases used the haptic interface to simulate the given tactile feedback upon the skin.

The protocol of the experiment was approved by the Ethics Committee of Research (Comité d'éthique de la recherche - CÉR) at ÉTS, Montréal, Canada.

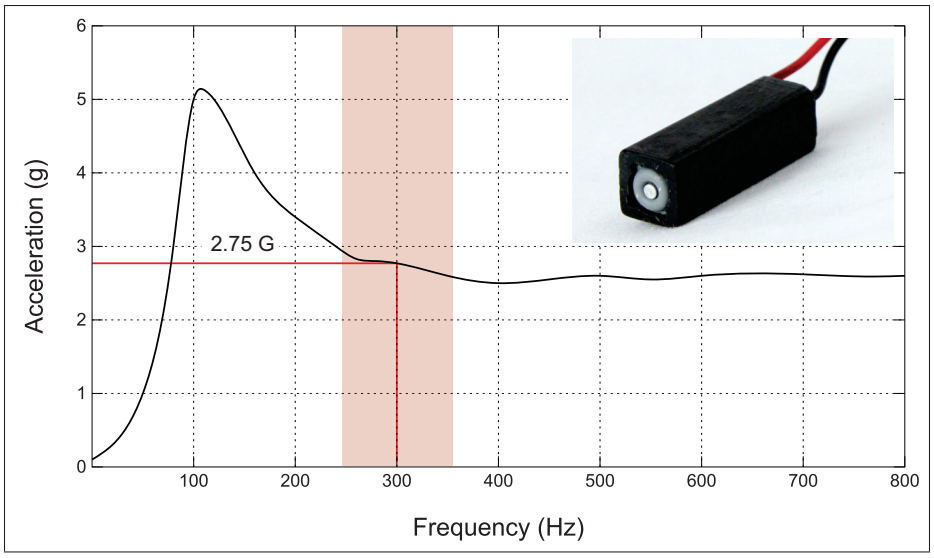

Figure 5.4 Normalized acceleration of the Haptuator Mark II (linear unbalanced vibrator motor) for $1V$ of input

5.3.1 Participants

We recruited four women and four men, aged 21 to 35, from the student body of ÉTS. Before beginning the experiment we informed each subject of the experimental procedures, and they each gave their legal consent by signing the participation form. At the start of the experiment, participants were seated comfortably and the haptic device was strapped to the forearm of their dominant hand, above the wrist joint. The subjects wore noise-cancelling headphones and their eyes were covered by blindfolds to allow them to concentrate on their tasks, and to avoid the influence of environmental events.

Once the participants had finished their tasks, they were asked simple questions about the performance of the device, and about the magnitude force corresponding to the feedback of each task. At the end of the experiment, all participants were shown graphs of the results they had helped to obtain.

5.3.2 Normal Stress Under Static Conditions

We used a static test to determine the influence of different pressure magnitudes upon the communication of the tactile sensor with the haptic device. The simple task of holding an egg reflects the importance of this experiment. For an amputee, proper force regulation is critical when attempting to successfully hold an egg in his or her prosthetic hand. The prosthetic hand must meet two criteria to accomplish the task. First, the eggshell must not be broken because of an overload of pressure. Second, the egg must not slip out of the hand because of insufficient pressure. In either case, the force ratio from the sensor should be proportional to the pressure feedback from the haptic device in order to provide reliable sensitivity to the user.

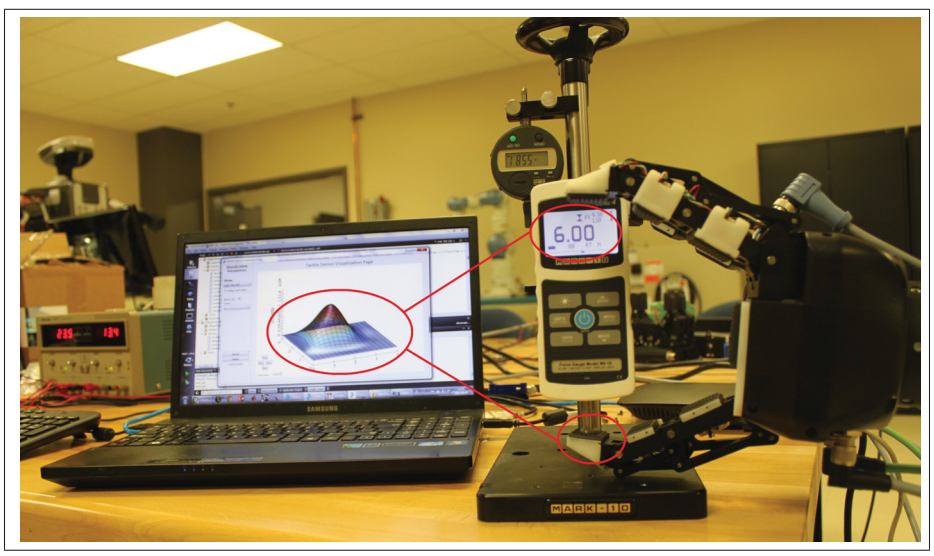

Figure 5.5 Calibration of the tactile sensor and the haptic interface under normal pressure. The force gauge shows 6 N for the force applied to the tactile sensor. The graph shows the real-time response corresponding to the measured force

We began the procedure by applying a normal stress of 2 N to a tactile sensor on a robotic finger. At the same time, the haptic device, which was connected to the tactile sensor, applied the equivalent pressure feedback to the glabrous skin area of the subject's forearm. We maintained this feedback for 20 seconds. We then removed the stress and asked the subject to replicate the external stimulus by applying pressure to the tactile sensor, by turning the handle (Figure 5.5).

We asked the subjects to stop pressing on the sensor once they felt they had reached the same pressure as before, and to inform us once this occurred. We repeated this procedure for 4, 6 and 8 N, and for each subject. The subjects chose their own estimation scale for this task. Meanwhile, the experimenter overseeing the procedure tracked and recorded the real-time pressure data of the sensor using software developed for this experiment, as shown in Figure 5.5.

We conducted familiarization trials to assist with the force scaling. During these trial sessions, subjects were introduced to the force stimuli ranges, starting from zero and increasing in intervals of 2 N, up to 10 N. In order to apply an accurate force, we used a digital force gauge, the Mark- 10 M4-10. This was equipped with a digital displacement gauge with $1\mu m$ accuracy, the Mitutoyo 543-693.

5.3.3 Pattern Recognition Under Dynamic Conditions

In the next phase, we determined the impact of linear and rotary motion while the dynamic feedback was transmitted from the haptuator to the skin. We used six customized textures for the experiment. As shown in Figure 5.6, these textures were engraved to depths of either 0.2 or 0.5 mm. Each piece was compared with five other pieces, resulting in fifteen data per subject and 120 data in total (Figure 5.7).

Here, the dynamic feedback varied according to the characteristics of each texture. As the textures were rubbed on the tactile sensor, it recorded how fast, and for how long, the engraved motifs moved across the sensor's surface. This caused the tactile sensor to produce signals that were unique to each texture's movement. These signals were then converted into input voltage levels, and transmitted to the Haptuator (note that during this process there was some variation in the transmission times of the signals). The Haptuator applied vibration to the skin according to the given voltage level. In other words, the speed of the vibrations, and the length of time for which they were applied to the skin, corresponded to the individual qualities of each texture, as measured while they were rubbed on the tactile sensor.

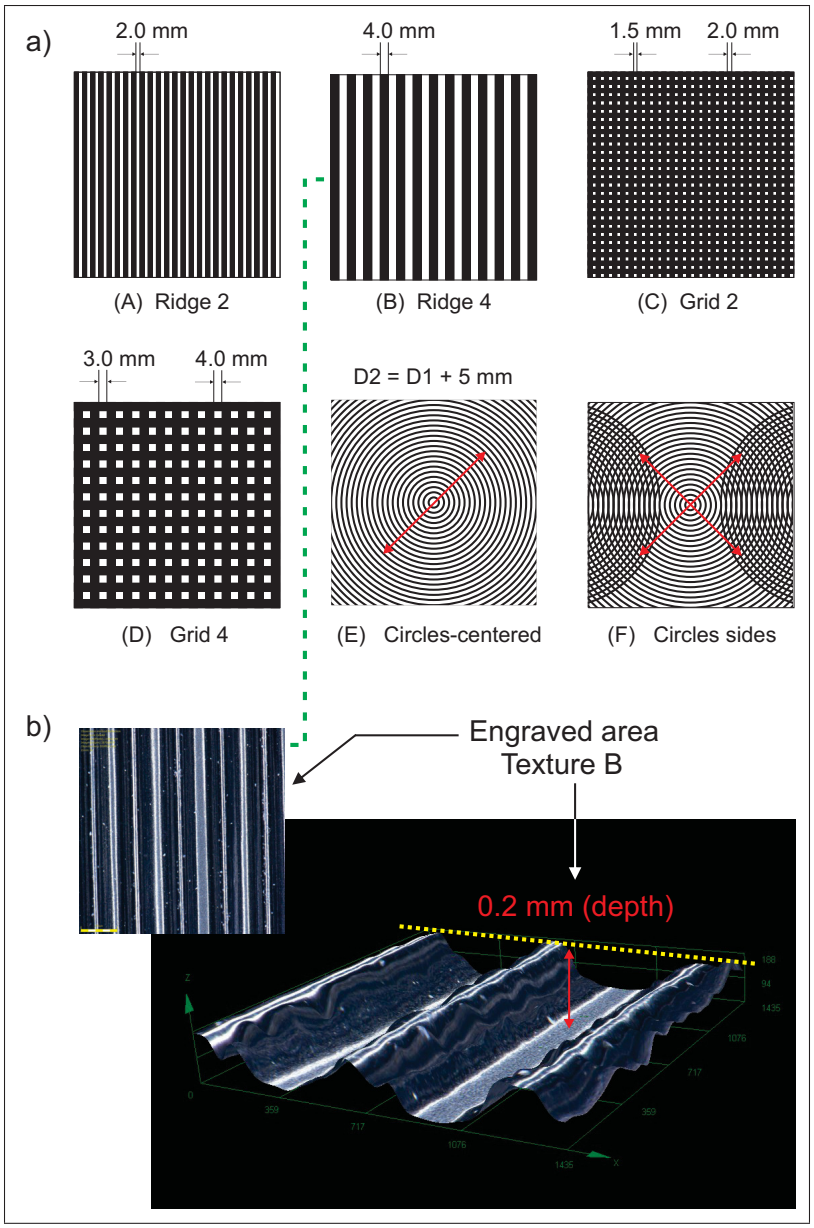

Figure 5.6 (a) Acrylic textures for the dynamic test. A, B, and C were each engraved to a depth of 0.2 *mm* and D, E, and F were each engraved to a depth of 0.5 *mm*. (b) 3D view of the engraved area showing depth of texture B (as an example) with an opto-digital microscope (OLYMPUS DSX100)

We began this phase by choosing a pair of textures at random and rubbing the pieces, one by one, on the tactile sensor for 10 seconds. The haptuator vibrated while this occurred, providing

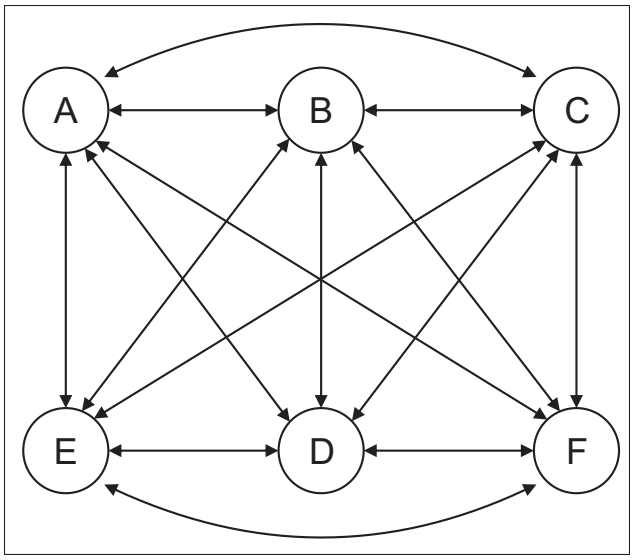

Figure 5.7 Comparison of the acrylic textures. The arrows represent the 15 groups

real-time feedback of the movement. The frequency and amplitude of the vibrations corresponded to the degree of roughness or smoothness of the pieces, as well as to the speed of reciprocating motion on their surfaces. While this took place, the subjects were blindfolded and were wearing noise-cancelling headphones. They concentrated on their task, and tried to remember the vibrational behavior of each piece. Once the initial rubbing process was complete we rubbed the pieces again and asked the subjects to identify the order in which each texture appeared, based on the vibrational feedback.

We randomly changed the order of stimulations and the range of forces for each subject in both phases, in order to enhance confidence in the test. The participants were not informed of the actual number of stimuli, the magnitude of the forces, and the order of each stimulus until all the tests were completed.

5.4 Results

When determining the functionality of the proposed mechanism under laboratory conditions, we considered the feedback obtained from all eight subjects. However, a different analytic

procedure was used for each, due to the dissimilarity of the test methods and, consequently, the differences in the numerical results.

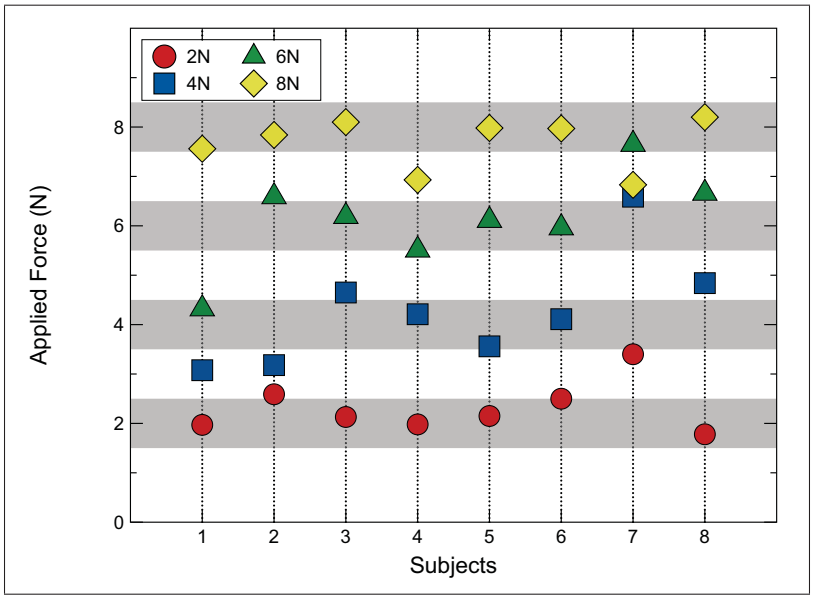

Figure 5.8 Static feedback of the subjects based on the applied forces. ± 0.5 is considered the safety margin for each level

We began our analysis of the results obtained under static conditions with a comparison of each feedback result based on the magnitude of the applied forces. As shown in Figure 5.8, the feedback placements follow distinguishable patterns across the range of magnitudes. The safety margins for acceptable feedback, of about ± 0.5, are indicated by the horizontal gray areas on our graph. At the lowest magnitude level, 2 N, six subjects are in the safety margin, and one subject, No. 2, is close to reaching the desired value. When the force magnitude is increased to 4 N, the detection accuracy drops to three subjects. At 6 N, it changes to four subjects. Finally, at 8 N, we again witness an increasing trend of success up to six subjects.

Figure 5.9 shows the key statistical parameters for the average feedback from all eight subjects. As can be seen across all levels, the static feedback was relatively well-detected by the subjects. More precisely, however, there is a better restitution feedback at both the lowest (2 N) and highest (8 N) magnitude levels. These levels had a success rate of 75%, while the middle two

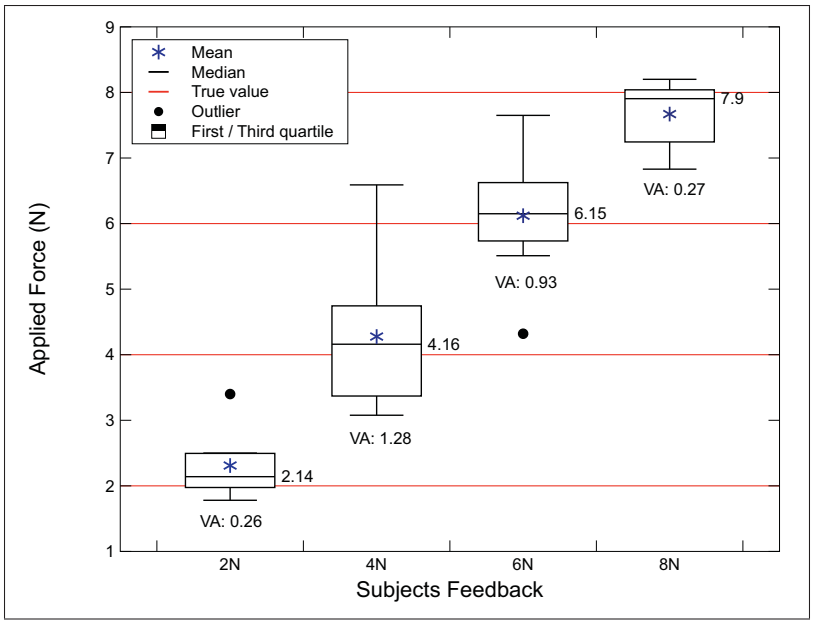

Figure 5.9 Key statistical parameters from the subjects' feedback under a static condition. VA represents the variance

levels (4 N and 6 N) had a 43% success rate. Furthermore, the variance of the given feedback is higher in both middle ranges ($2N : 0.26,\ 4N : 1.28,\ 6N : 0.93,\ 8N : 0.27$). This may be due to the difficulty of proper force recognition at some of the in-between levels.

In the pattern recognition task, as opposed to the static condition, each group of samples is compared separately. Table 6.1 shows the collected results for this experiment along with their success rates.

The efficiency of our device to sense and transmit vibrations according to textures, combined with the subjects' ability to feel and remember this information, has an overall success rate of 78.33% for all experiments. Some pairs of samples appear to have been differentiated more easily than others, as shown in Figure 5.10a. For example, in the case of pairs $A-B$, $B-C$, $C-F$ and $D-F$, subjects were able to distinguish between textures 100% of the time. Meanwhile, pairs $A-D$ and $B-F$ were only differentiated in 37.5% of all trials, which was even lower than the statistically expected value. Overall, the subjects' success ratio ranges from 66.67% to 86.67%, with an average of 78.33% and a standard deviation of 8.54%. Figure 5.10b shows

Table 5.1 Results from the dynamic test

	Subjects								
	1	2	3	4	5	6	7	8	%
A - B	✓	✓	×	✓	✓	✓	×	×	62.5%
C - A	×	✓	✓	×	×	✓	✓	✓	62.5%
D - A	✓	×	×	×	✓	×	×	✓	37.5%
A - E	✓	✓	✓	✓	✓	✓	✓	✓	100%
F - A	✓	✓	×	✓	×	✓	✓	✓	75%
C - B	✓	✓	✓	✓	✓	✓	✓	✓	100%
D - B	✓	✓	×	✓	×	✓	✓	✓	75%
B - E	✓	✓	✓	✓	✓	✓	✓	×	87.5%
F - B	×	✓	✓	×	✓	×	×	×	37.5%
D - C	✓	✓	×	✓	✓	✓	✓	✓	87.5%
E - C	✓	×	✓	✓	✓	✓	✓	×	75%
C - F	✓	✓	✓	✓	✓	✓	✓	✓	100%
D - E	✓	✓	✓	✓	×	✓	✓	✓	87.5%
D - F	✓	✓	✓	✓	✓	✓	✓	✓	100%
F - E	✓	✓	✓	✓	✓	✓	✓	×	87.5%

the percentage of successes when a particular sample was involved in an experiment, shedding light on the question of which samples are most and least easy to sense.

Although textures A, B and C were engraved at different depths from those of D, E, and F (2 *mm* and 5 *mm* respectively), this did not seem to have a significant effect on pattern recognition. In fact, it is hard to determine what factors have caused some pairs of samples to be more easily differentiable than others. Given the results of Table 6.1, there is no clear correlation between success and either the engraving depth difference, or the pattern's motif.

5.5 Conclusion

In this study, we attempted to create a functional loop between the main components of the proposed robotic system. The long term objective of our research group is to give amputees a sense of touch that is as similar as possible to that of unimpaired people. This work is a step towards this objective, and has the potential to partially restore some tactile-based capabilities to hand amputees, including texture recognition and grasping force sensibility. Although the

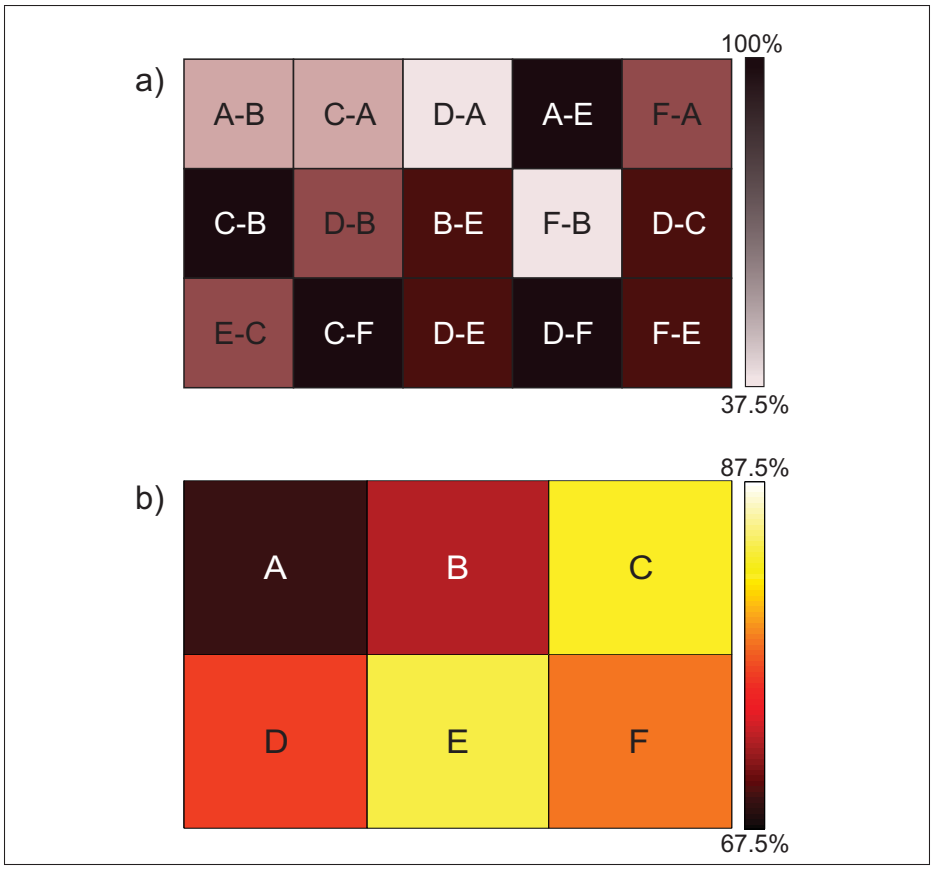

Figure 5.10 a) Subjects' correct answers under the dynamic test. More intense color indicates a better detection ratio. b) The best patterns, based on the subjects' feedback

performance of each component showed some deficiencies and neglected errors, the overall results are very promising.

While the restoration of touch sensitivity under a static condition was the main priority, over 80% of participants received a reasonable amount of feedback at each level of the applied force. This positive trend was also present for the restitution of touch sensitivity under a dynamic condition. More than 70% of the participants could easily distinguish different textures using the dynamic feedback that they received from the vibrator motor.

CHAPTER 6

THE USE OF VIBROTACTILE FEEDBACK TO RESTORE TEXTURE RECOGNITION CAPABILITIES, AND THE EFFECT OF SUBJECT TRAINING

6.1 Introduction

This study presents a vibrotactile haptic feedback system for use under dynamic conditions, verifies its functionality, and shows how results may be affected by the amount of training that subjects receive. We hope that by using vibrotactile feedback to distinguish between different textures, upper-limb amputees may be able to partially compensate the sense of touch. During a previous experiment mentioned in chapter 5 (Motamedi *et al.*, 2015), we noticed a correlation between how familiar the subjects were with haptic systems, and how well they were able to use the haptic system to accurately identify textures. This observation lead us to conduct a second experiment, the results of which are the main focus of this chapter. We began with a group of subjects who were completely unfamiliar with haptic systems, and tracked the improvements in their accuracy over a period of four weeks.

In general, despite the multi-modal functionality of vibrotactile stimulation, most researchers have not yet examined the use of vibration under dynamic conditions. In previous studies of vibrotactile feedback, the haptic systems were designed only to convey a quantity of force or pressure to the user (Witteveen *et al.*, 2012; Chatterjee *et al.*, 2008; Pylatiuk *et al.*, 2006). Most of the previous research in this area focuses on detecting grasp quality because the sensors used in previous studies were mainly designed for static sensing (Brown *et al.*, 2013; Godfrey *et al.*, 2013). However, while grasp quality is an important part of the sense of touch, the ability to recognize texture is also a key component. A great deal of research has been done on pressure recognition under static conditions (Aggarwal *et al.*, 2015; Ben Porquis *et al.*, 2013; Bhattacharjee *et al.*, 2012), but there has not been much focus on texture recognition under dynamic conditions. We propose a haptic feedback system that will allow users to recognize textures based on a corresponding type of vibrotactile feedback. We are presently able to study vibrotactile feedback under dynamic conditions thanks to the development of an innovative

tactile sensor (Duchaine and Rana, 2014; Rana and Duchaine, 2013). Of course, the ideal haptic system must be adaptable to both static and dynamic conditions, but this is still a long way from being realized. This chapter, which focuses solely on texture recognition under dynamic conditions, is therefore but another small step towards a grander ideal.

Our main goal in this study is to verify that our proposed system is a functional haptic feedback loop for texture recognition during active touch sensing. We hope to prove its ability to convey the properties of different textures to humans through vibration, so that our system can be used in further research. This objective cannot be achieved without studying the effects of volunteer training as well. Therefore, in the pursuit of our main goal, we also endeavour to find out how providing subjects with further training can enhance their recognition of different textures using dynamic feedback.

This chapter will proceed according to the following organization. We begin by describing the technological components of our experiment, specifically the tactile sensor and software that we developed, as well as the robotic hand and vibrotactile actuator that we used. We then discuss the procedure of the experiment, including the participants and the exact method that was used to achieve texture recognition under dynamic conditions. Next we present our results and explore the effect that the participants' level of experience had upon their success rates. Finally, we conclude with a discussion of the factors influencing our results, and how future work might improve upon our current haptic system.

6.2 Instrumentation

All of our experiments used the setup shown in Figure 6.1. The robotic components consist of a set of sensory robotic fingers mounted on a robotic arm. This robotic limb is connected to a vibrator motor, which generates vibrations corresponding to the signals it receives while the robotic fingers are feeling a texture. These vibrations are then applied to the skin at the back of the volunteer subjects' necks, stimulating the FA tactile receptors in their skin and allowing

the subjects to recognize textures based on the vibrations. We also used the same tactile sensor and robotic arm packages that were described in chapter 5.

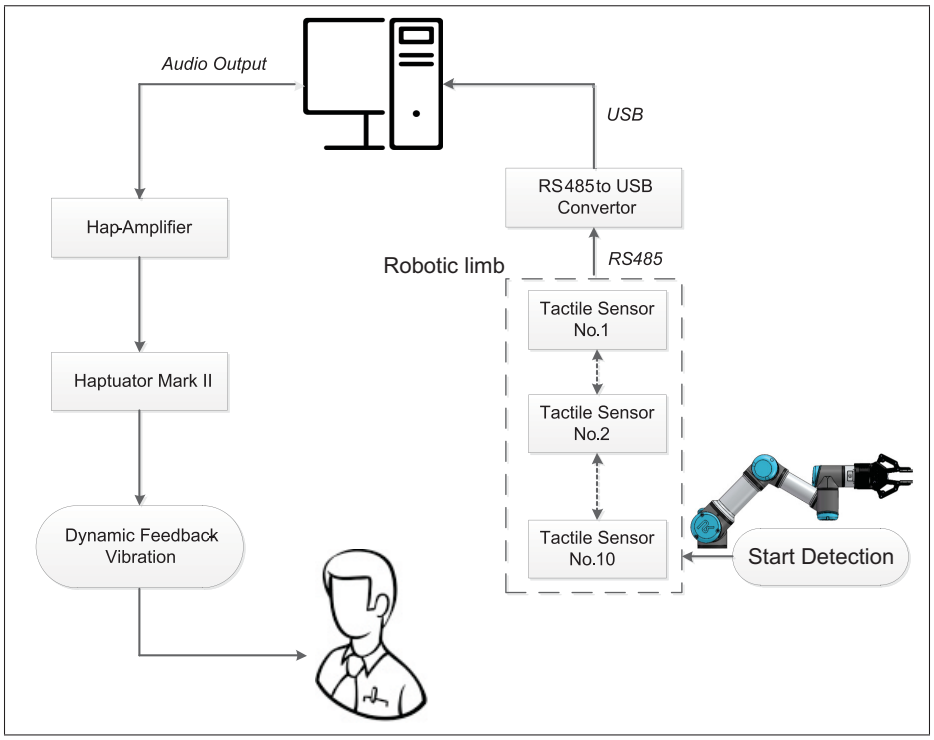

Figure 6.1 Architecture of the experiment setup

6.2.1 Vibrotactile System

For the vibrotactile stimulation package, we used the same Haptuator mark II, which is the one that we already used in our previous experiment. But, we also constructed a small, conformable, and highly adhesive casing to protect the vibrator motor. This casing was composed of a series of layers, of which the sticky outer layer was the softest, to ensure that users remain comfortable while the device is in contact with their skin.

First, we designed a hard plastic enclosure for the Haptuator. This was printed in clear resin with a FormLabs Form1+ stereolithography 3D printer. Then, we created a soft dual-layer

silicone elastomer skin to cover the hard casing. The skin was made by spin coating two platinum cure silicone elastomers, with coatings added multiple times at low speed.

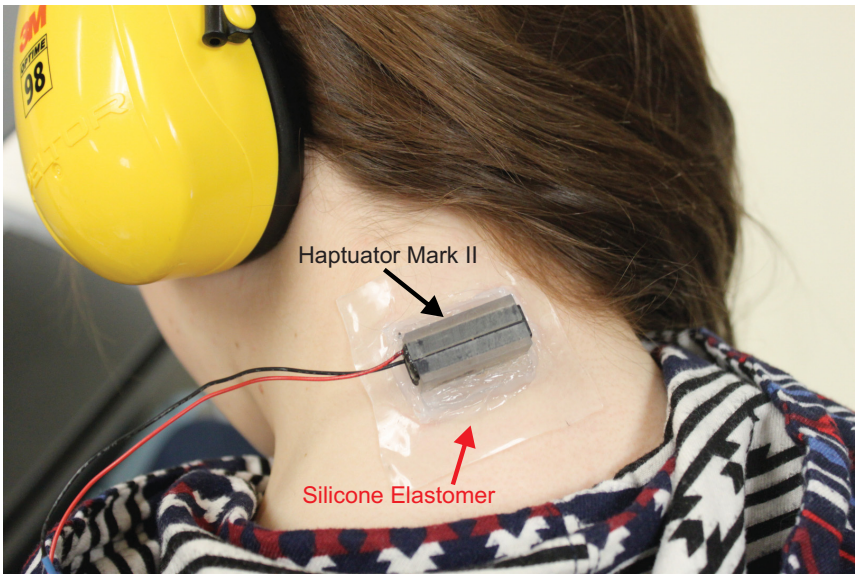

Figure 6.2 Soft dual-layer silicone elastomer used to attach the Haptuator to the subject's skin

The material for the first layer is the commercially available Ecoflex® GEL from Smooth-On, Inc. This silicone rubber gel is extremely soft ($000-35$ shore hardness) and very tacky. The second layer was also spin coated. This thicker second coating was made by mixing in equal amounts of two silicone elastomers, (EcoFlex® GEL and Ecoflex® Supersoft Silicone). Both silicones have extremely low levels of hardness ($000-35$ and $00-10$ shore hardness, respectively) and high elongation at break (800% or more).

The final skin measured approximately $1mm$ in thickness, making it highly conformable. It was very tacky on one side due to the Ecoflex® GEL, with a less tacky body due to the use of the silicone mix. Finally, this skin was glued onto the hard plastic case using a silicone adhesive, Sil-Poxy®, of intermediate mechanical properties ($A-40$ shore hardness, 750% elongation at break) and fast curing time (12 min).

We hope to further test these types of silicone skins in future work on haptic devices, as we believe they provide a robust, comfortable, and easy-to-manufacture alternative to straps and elastic bands. Our silicone skin is ideal for use in a vibrotactile haptic feedback system where the vibrator motor is placed at the back of the subject's neck. Usually, the vibrator motor is attached to the subject's arm. This makes sense considering the traditional method of attachment; with the straps and bands method, it is much more comfortable to have a strap around one's arm than around one's neck. However, the arm is not the ideal location, as the skin there is less sensitive than at the back of the neck. Furthermore, when designing a haptic feedback system for use with robotic limbs, one should keep the needs of the user in mind. Fortunately, the use of an adhesive silicone casing for the vibrator motor makes it much easier to attach it to the neck. Since the casing does not involve glue/solvent-based bonding, it is not affected by sweat or water, and it does not leave any sticky residue on the skin after it is removed.

6.2.2 Software

A Qt-based graphical user interface (GUI) was created specially for this experiment. This software was responsible for acquiring the dynamic data from the tactile sensor via a USB 2.0 port at a constant rate of 1000 Hz. During the procedure, it sent the vibration signals directly from the audio analogue output to the Haptuator's amplifier. The signals were transmitted in real time at a rate of 1 KHz.

6.3 Procedure of the Experiment

6.3.1 Participants

Twenty-one subjects in total participated in the experiments that we conducted (the first experiment being prior to the two that were specifically for this study). There were nine female and twelve male subjects, ranging in age from 20 to 35. Subjects were informed of the experiments' procedures prior to their participation, and they each signed the participation form to indicate their legal consent.

At the start of the experiments, each participant was seated comfortably and the vibration motor, the Haptuator, was attached to either the participant's forearm in the case of the first experiment, or to the back of the participant's neck in the case of the second experiment. After all the results had been obtained, the participants were shown graphs depicting the outcomes of the experiments.

The protocol of each experiment was approved by the Ethics Committee of Research (Comité d'éthique de la recherche, or CÉR) at ÉTS, Montréal, Canada.

6.3.2 Texture Recognition Task

We wished to determine the impact of linear and rotary motion while dynamic feedback was being transmitted from the Haptuator to the skin. To study these effects, we used six customized textures for our experiments. The six patterns are shown in Figure 5.6. They were engraved in acrylic with a laser cutter, to depths of either 0.2 or 0.5 *mm*. Each piece was compared with five other pieces, resulting in fifteen data per subject and 315 data in total. Figure 5.7 depicts all the possible texture pairings to be compared during the experiments. Although the number of different textures is not large, the textures we selected are generally very similar to one another. The fact that they are so similar means that the vibrations produced by the Haptuator must be an exact match to the information recorded by the sensor. If the Haptuator produced vibrations that were too similar, it would not even be possible for subjects to distinguish between the different vibrations, and there would be no hope that they could then identify the textures using our haptic feedback system. We could have avoided this potential difficulty by using a wider variety of textures or using real ordinary textures and materials. However, we have deliberately embarked on this challenge under the assumption that if we can prove that our system works when using very similar textures, it will be easy to distinguish between more varied textures later on. Preliminary experiments support this assumption.

During the experiments, the tactile sensor recorded the vibrations caused by the textures' motifs as they moved across its sensitive surface. The frequency, amplitude, and intensity of the signal

varied according to the characteristics of each texture, causing the sensor to produce a different signal for each texture. The software then converted these signals into input voltage levels, and varied the Haptuator's voltage to match the input. Therefore, when the Haptuator applied vibrations to the subject's skin, the frequency of the vibrations corresponded to the textures' unique amplitude and frequency profile, as measured by the tactile sensor.

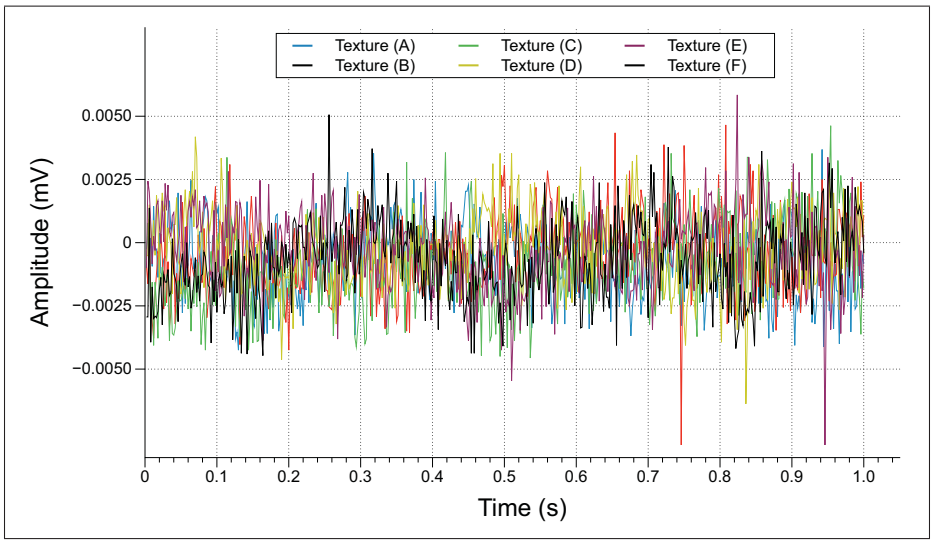

Figure 6.3 Input signals for each texture, of which the amplitude is proportional to the variation in the movements of the textures that were applied to the sensor's surface. Notice that all the input signals are within roughly the same range

We began this test by choosing a pair of textures at random and rubbing the pieces, one by one, on the tactile sensor for 10s. As shown in Figure 6.3, the Haptuator vibrated while this occurred, providing real-time feedback of the movement. The frequency and amplitude of the vibrations corresponded to the degree of roughness or smoothness of the pieces, as well as to the speed of the textures' motifs as they moved across the sensor's surface. To enhance the subjects' concentration, and to prevent the results from being affected by environmental events, the subjects wore blindfolds and noise-cancelling headphones during the process. They concentrated on their task, and tried to remember the vibrational behavior of each piece. Once the initial rubbing process was complete we rubbed the pieces again and asked the subjects

to identify the order in which each texture appeared, based on the vibrational feedback. We randomly changed the order in which each pair of textures appeared in order to enhance confidence in the test. The participants were not informed of the actual number of textures and the order of each pairing until all the tests were completed.

6.4 Results

6.4.1 Initial Observations

While conducting an experiment to be used for a previous study (Motamedi *et al.*, 2015), we noticed a correlation between the participants' familiarity with haptic systems, and their ability to use our system successfully. Subjects who were already knowledgeable about haptic systems prior to the start of the experiment were able to recognize textures based on the corresponding vibrations with much greater accuracy than the subjects with no previous knowledge of haptic feedback. This can be seen from a comparison of the results obtained by each group of participants, as shown in Figure 6.4.

Ten subjects in total were involved in the experiment we conducted for our previous study. Of the ten subjects, four were completely unfamiliar with the idea of haptic feedback. The four novices had an average success rate of 61%. They seemed unsure as to which textures the vibrotactile stimuli were meant to represent, and thus found it more difficult to accurately distinguish the different textures. Three of the other subjects were each somewhat familiar with haptic systems, and they had an average success rate of 77.6%. The final three subjects had extensive experience with testing this haptic system, which surely contributed to their much higher average success rate of 86%.

Besides our consideration of the subjects' prior levels of experience, our previous study also required us to take another parameter into account: the amount of similarity between certain textures. We intentionally designed some of the textures to be nearly identical to others, in order to test the Haptuator's ability to create vibrations that correspond to each separate texture. How

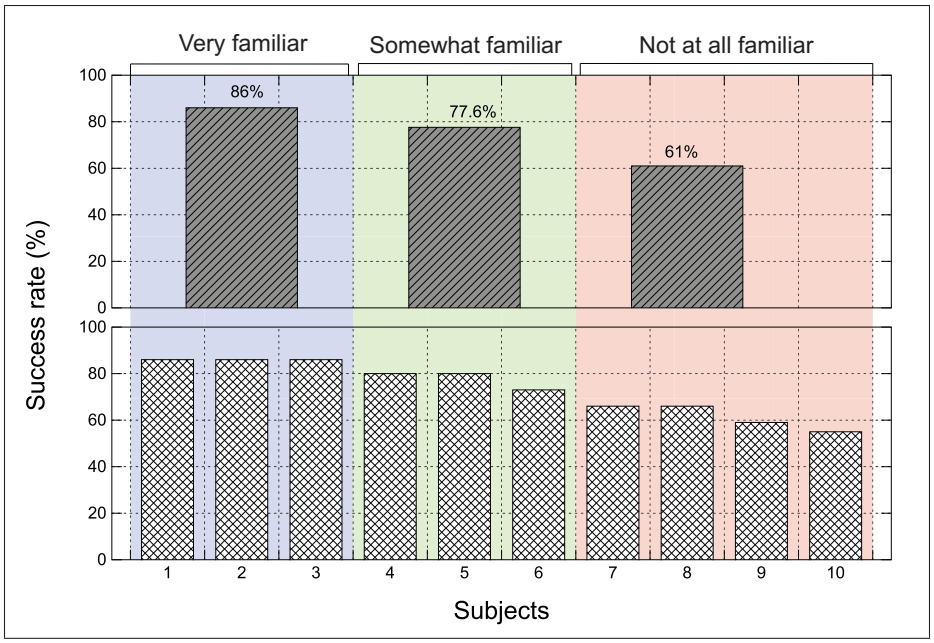

Figure 6.4 Subjects' success rates, grouped according to their initial level of familiarity with vibrotactile feedback

well the Haptuator was able to do so had a strong effect on each subjects' capacity to accurately differentiate between the textures using the given vibrotactile feedback.

Figure 6.5 gives the overall success rates for the recognition of each texture. This chart shows that almost all of the inaccurate responses occurred when the near-identical textures A and B were involved. As all of the subjects had trouble distinguishing between A and B, regardless of their level of experience, it is clear that subjects' training is not the only factor affecting texture recognition. Any discussion of the effects of volunteer training will also need to consider how the subjects' tasks were made more or less difficult by the degree of similarity between the textures they were asked to identify.

Ultimately, the main point of our previous study was to successfully verify the functionality of the haptic system we designed. But we also found the differences between the success rates of subjects to be a promising area for further research, and thus the inspiration for the present work.

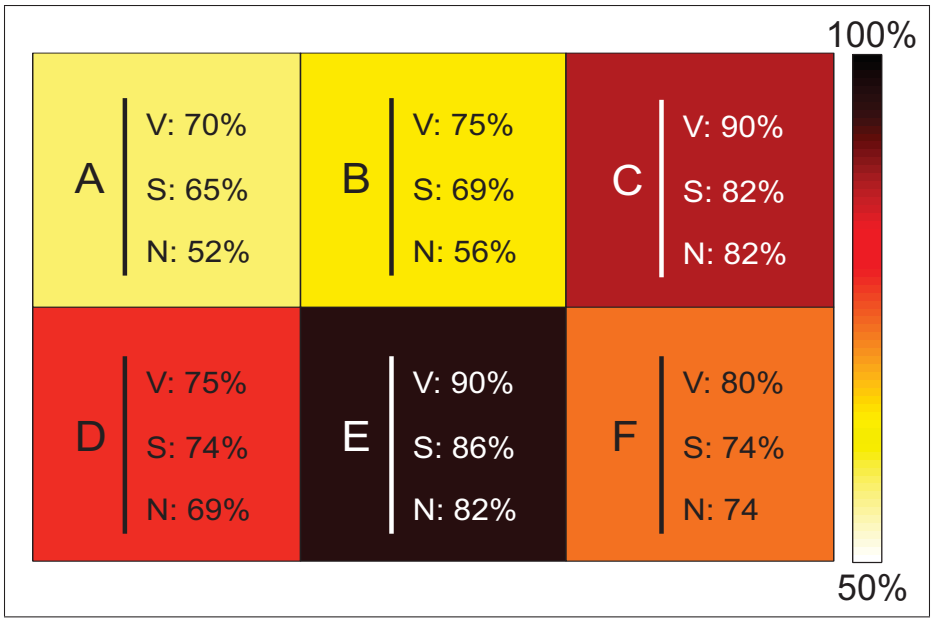

Figure 6.5 Rate of successful identification for each individual texture, according to subjects' level of familiarity. V indicates subjects that were very familiar with the haptic system, S indicates somewhat familiar ones, and N indicates the subjects that were not at all familiar with the haptic system

6.4.2 The Effect of Training

We conducted a second experiment to further examine the functionality of our proposed system. This experiment also served to verify our hypothesis regarding the effect of training on subjects' accuracy. It was conducted over a period of four weeks (two days per week in 30 minutes per subject) using 11 subjects, all of whom were completely unfamiliar with haptic systems at the start. Here we will present the results of how our vibrotactile device performed during these tests, as well as how the accuracy of the subjects improved as they gained more experience.

From our first experiment, we noticed that the amount of familiarity each subject had with haptic systems had a strong influence on the subjects' success rates, i.e., the ability of our haptic device to convey a sense of texture recognition to users through the use of vibrotactile feedback. Over the four weeks that the tests were conducted for the second experiment, the volunteers

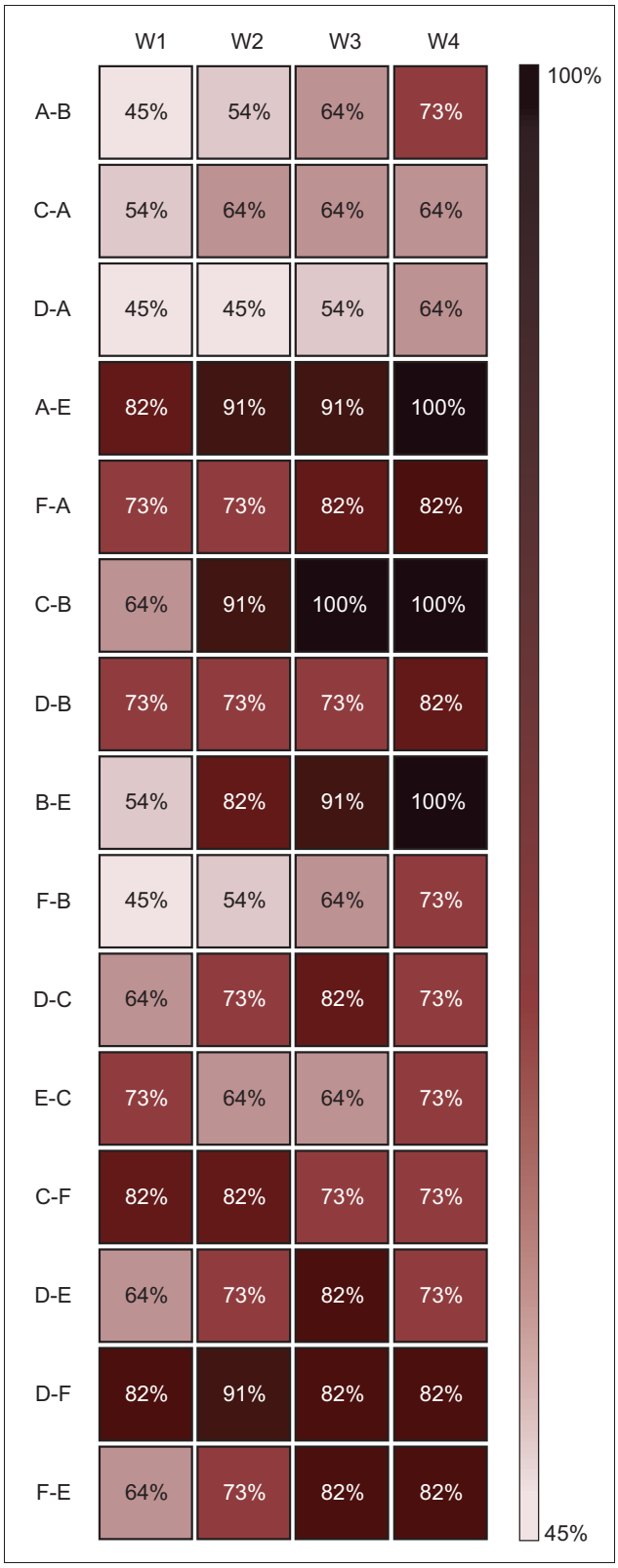

Figure 6.6 The average of the success rate for each particular pair of textures, over the four weeks of the experiment

gradually accumulated more experience with the device, becoming more adept at linking the type of vibrotactile feedback they received with the texture it was meant to represent.

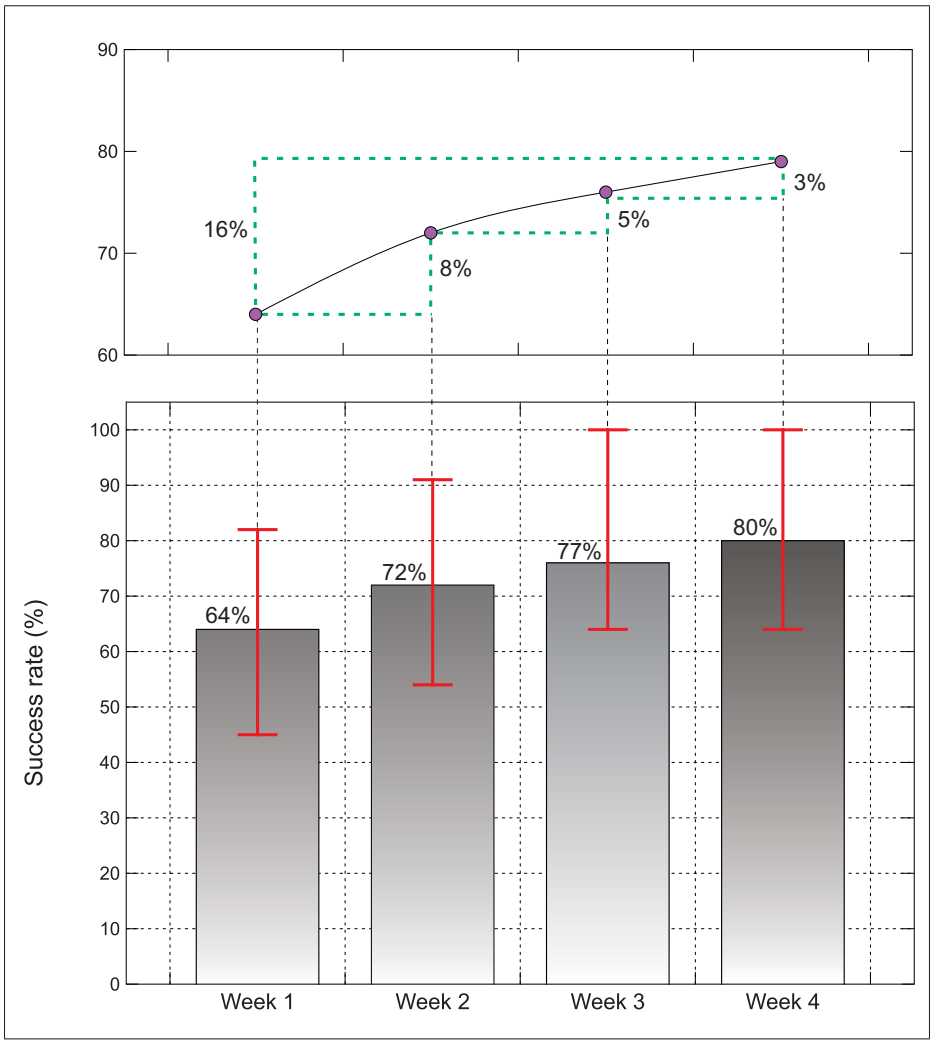

Figure 6.7 Subjects' success rate and the trend of success during four consecutive weeks. The red bars indicate the variance

As shown in Figure 6.6, the textures of every pair of samples were individually compared each week. The illustrated results show the outcomes of these tests based on the rates of successful identification. Certain sample pairings were more easily differentiated than others. For example, in the first week alone subjects were able to distinguish between textures in pairs $A-E$, $C-F$, and $D-F$, 82% of the time. Meanwhile, the textures in pairs $A-B$, $D-A$, and

$F-B$ were only differentiated in 45% of all trials, which was even lower than the statistically expected value. However, as we anticipated, there was generally an increasing trend of success as the volunteers gained experience. For instance, the pair $B-E$ began with a 54% success rate, but gradually progressed up to 100%. While a 100% success rate was only achieved for three pairs in total, 12 of the 15 pairs showed improvement over time. When we take all the pairs into consideration, the rate of successful texture recognition displays a clear positive correlation with the subjects' level of training.

The overall rate of success was 64% at the end of the first week, and by the end of the fourth week it had reached 80%. In general, as can be seen in Figure 6.7, we were able to increase the success rate of our subjects, when distinguishing between different textures using vibrotactile stimulation, by about 16%. Within each individual week, the subjects' feedback also shows a positive trend in the success rate.

Although the success rates had always increased by the end of each week, there was a decreasing marginal rate of gain in the success rate from one week to the next. This intuitively follows from the fact that novice subjects can greatly improve after just a short amount of training, but experienced subjects have less room for improvement. The success rate of 64% was established after the first week. Subjects improved their success rate by 8% after the second week of participation, by 5% after the third week , and by 3% after the fourth week. Table 6.1 depicts the one-way ANOVA table that was used to determine whether or not the mean of each week's success rate was significantly different from that of the previous week.

Table 6.1 ANOVA Table showing statistical parameters for the subjects' success rates

SS	df	MS	F	$P-value$	$F_{critical}$
19 - 95	3 - 56	66 - 17	3.88	0.013	2.76

We also compared how the success rates for each particular texture changed between the first and fourth weeks, to show the effect of the volunteers' gains in experience. The results of this comparison are shown in Figure 6.8, which sheds light on the question of which samples are most and least easy to sense. Of course, the overall success rate for each texture depends on its pattern and the depth of the engraved motif. However, the trend of increasing success is observable for each texture, even those within the most similar of pairings.

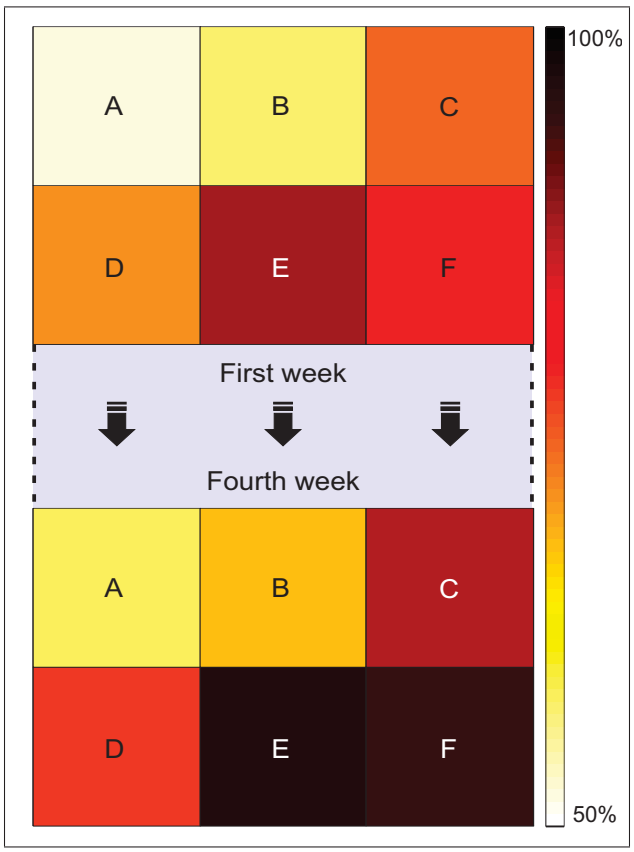

Figure 6.8 Overall improvement in the success rate for each particular sample, as shown by a comparison of the results from the first and fourth weeks

Although we achieved a success rate of 80% after four weeks of training, this may seem relatively low. Indeed, it appears there is still a lot of room for improvement. However, one must also consider that no system is perfectly accurate. Even when humans use their own fingers to

identify our textures, they cannot identify the textures correctly every time. We discovered this by conducting another experiment using the same textures, in order to determine the real level of touch sensitivity in humans. This time, we took the same group of subjects, who by now had each accumulated four weeks of experience from the previous experiment, and asked them to distinguish between the textures using the mechanoreceptors in their own hands (Figure 6.9).

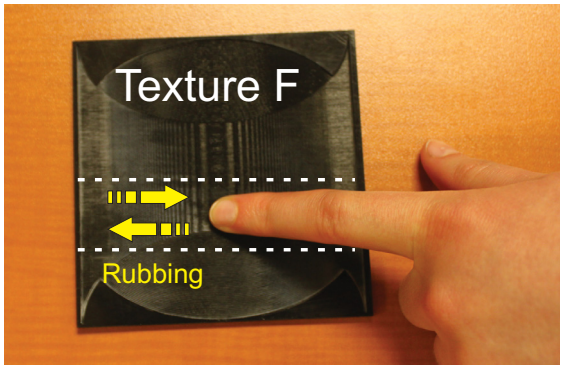

Figure 6.9 Subject identifying a texture using her index finger

For each pair of textures, the subjects were presented with first one texture, and then the other, and were allowed to view and touch the textures. They were then blindfolded and asked to identify which of the two textures had appeared first by using their index fingers to rub each texture for 10*s*.

The textures were arranged in the same pairings, and the pairings were presented in the same order, as they had been during the previous experiment. Despite having had weeks of experience with these textures, however, the subjects were still not able to distinguish between texture A and texture B with complete accuracy. Although textures A, B and C were engraved at different depths from those of D, E, and F (2 *mm* and 5 *mm* respectively), this did not seem to have a significant effect on pattern recognition. In fact, it is hard to determine what factors have caused some pairs of samples to be more easily differentiable than others. Given the results

of Figure 6.6, it seems there is no clear correlation between success and either the engraving depth difference, or the pattern's motif.

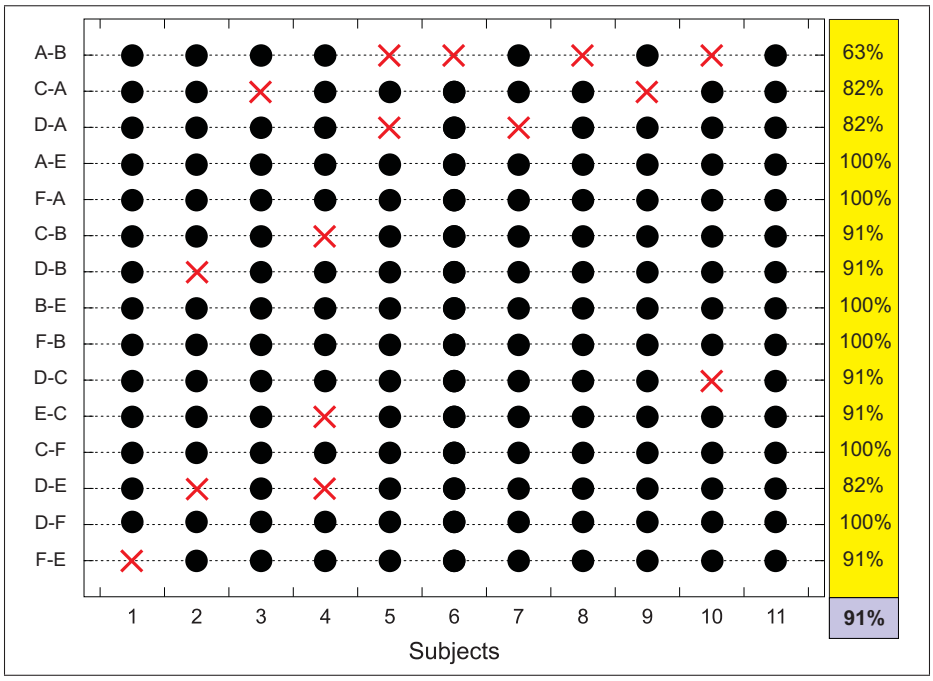

Figure 6.10 Subjects' feedback for each particular texture, when attempting to recognize textures using the mechanoreceptors in their fingers

As can be seen from Figure 6.10, the average success rate for all subjects, across all textures, was 91%. Thus there is only an 11% difference between the average success rate of our system, and that of humans, far less than the 20% difference we imagined previously when comparing our system's success rate to that of the illusory ideal.

6.4.3 Conclusion

This study presented a method of using vibrotactile haptic feedback to recognize textures, and discussed the effect of participants' training. The long term objective of this research is to give amputees a sense of touch that is as similar as possible to that of unimpaired people. During our main experiment, we attempted to increase the participants' ability to recognize different

types of textures by training them over four consecutive weeks. We found that it is not enough to develop a viable haptic system; volunteers must be properly trained in order to complete the feedback loop.

After the first week of our experiment testing subjects' improvements, the subjects had reached an overall success rate of 64%. This did not seem promising, as it was not much higher than the statistically significant minimum of 51%. However, by the end of the fourth week subjects achieved an 80% success rate. This improvement of 16%, after just three additional weeks of training, is even more impressive considering that the subjects themselves only reached a 91% success rate when using their own fingertips to identify the textures.

CHAPTER 7

THE USE OF HAPTIC FEEDBACK WHEN ACCOMPLISHING EVERYDAY TASKS

7.1 Introduction

So far, we have conducted several tests on human subjects to determine the impact of different stimulation methods, and to enhance the effectiveness of haptic feedback. Here, in the last chapter of this thesis, we will continue this process by comparing the performance of a robotic haptic system with that of the human vision system, when operating under conditions that one might encounter when completing various tasks. These tasks were selected based on their similarity to the conditions humans face during manipulation tasks in their everyday life.

The experiment was conducted in three phases. The first phase of the experiment was a slippage detection test. We compared the performances of the subjects during this test, when they used either their vision, static pressure feedback, or vibrotactile feedback, to detect when an object began to slip out of the grasp of the robotic gripper.

In the second phase of the experiment, we conducted a contact-detection test to compare the subjects performances when using either their vision or vibrotactile feedback.

Finally, the third phase of the experiment was a grasp precision test. We compared the performances of the subjects when using either their vision alone, static pressure feedback alone, or vision and static pressure feedback together, as they attempted to use the robotic gripper to move an object between two prespecified points.

7.2 Materials and Participants

The general architecture of the experiment setup is almost the same as the one that was presented in Chapter 5 (in the section on Instrumentation). The robotic arm and the gripper, as well as the haptic device and the vibrator motor, that were used during this experiment, were

Figure 7.1 Objects used during the experiment

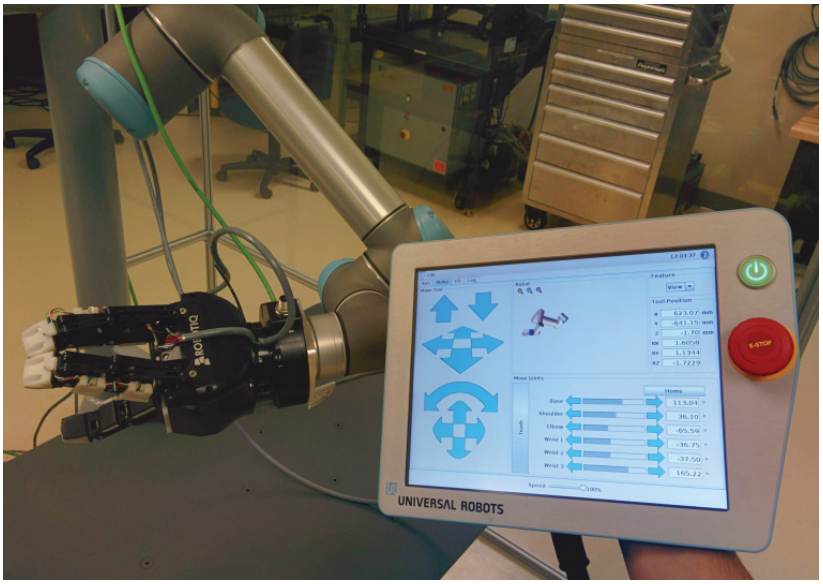

Figure 7.2 UR5 controller used to direct the robotic hand

Figure 7.3 Subject controlling the movement of the robotic fingers, while undergoing familiarization process for the static pressure test

also introduced in previous chapters. The novel aspect of this experiment comes from the objects that we used. In previous experiments, we engraved our own textures in different depths and lengths (for the dynamic condition tests), or we applied pressure to the load-cell or tactile sensors (for the static condition tests). Although these materials were useful for the texture recognition tasks, they cannot exactly be considered as textures or surfaces that are encountered in everyday life. That is why, as can be seen from Figure 7.1, we gathered different objects that can be easily found, at any places, in order to have a real test on real objects. This helped us to determine the functionality of the proposed mechanism, since we are trying to compensate for the lack of touch sensitivity and need for continuous visual attention during the accomplishment of routine tasks.

Twelve subjects (seven men and five women), aged 20 to 35, participated in this study. These subjects were already familiar with haptic feedback, and with the procedure of our experiments, from having participated in our previous tests. At the start of the experiment, participants were seated comfortably and the haptic device was strapped to the forearm of their dominant hand. Subjects wore noise-cancelling headphones and their eyes were covered by blindfolds (except

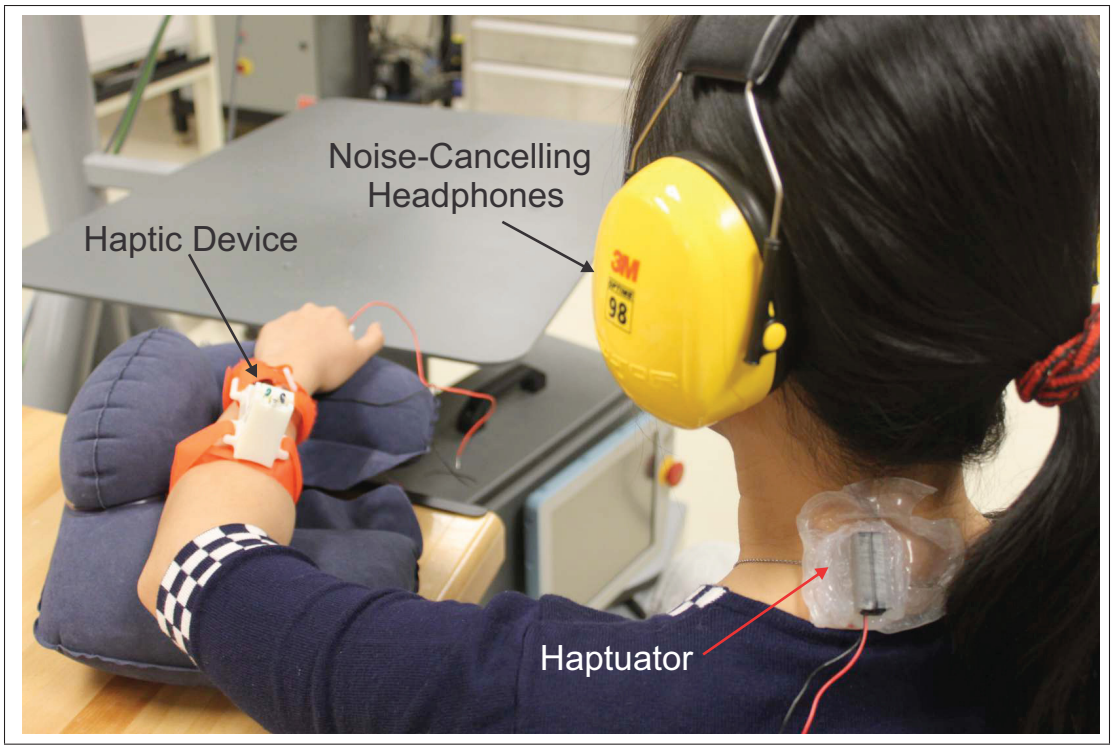

Figure 7.4 Soft dual-layer silicone elastomer used to attach the Haptuator to a person's skin

during the vision test) to allow them to concentrate on their tasks, and to avoid the influence of environmental events (Figure 7.3 and Figure 7.4). The protocol of the experiment was approved by the Ethics Committee of Research (Comité d'éthique de la recherche, or CÉR) at ÉTS, Montréal, Canada.

We also designed a new wearable haptic device (Figure 7.5), which is smaller and more preciese compare to what we have designed so far, in order to orthogonal forces to the participants during the experiments.

A Qt-based graphical user interface (GUI) was created specially for this experiment. This software was responsible for acquiring the data from the tactile sensor via a USB 2.0 port. The data were acquired at a constant rate of 20 Hz for the static data, and 1000 Hz for the dynamic data. Under static conditions, the software forwarded the data to a micro-controller, which commanded the piston of the haptic device through PID control. Under dynamic conditions,

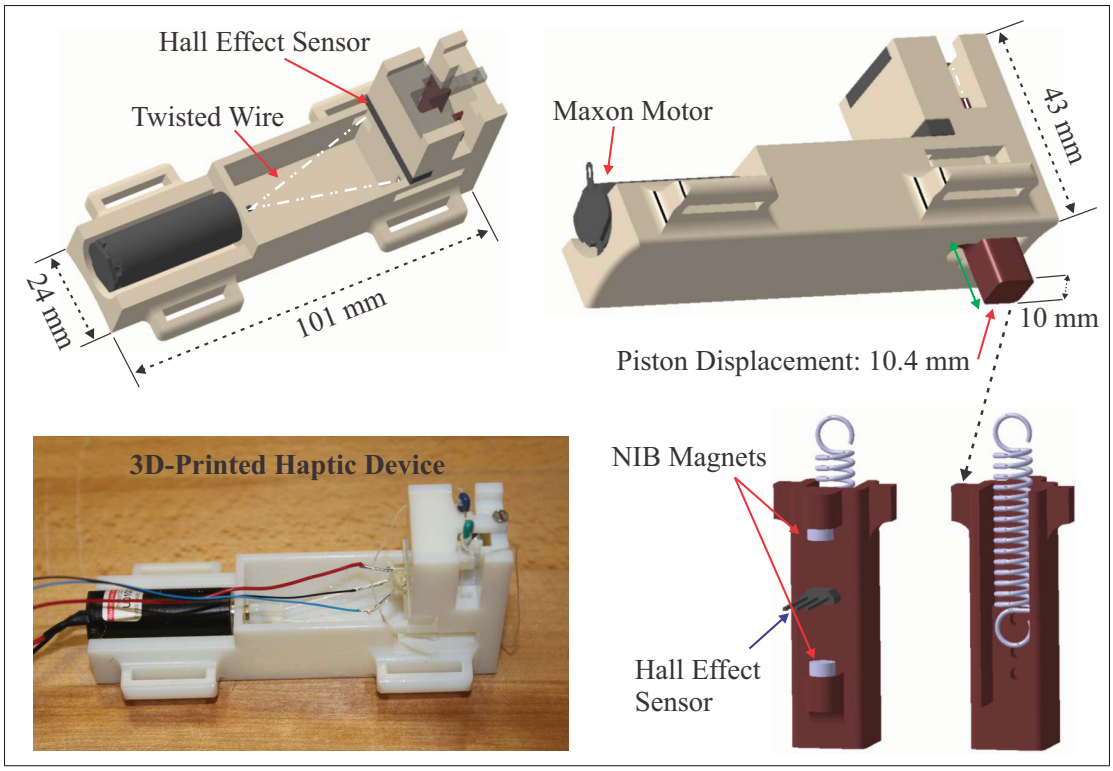

Figure 7.5 Global view of the haptic device, and close-up view of its components

the software sent the vibration signals to the Haptuator's amplifier, directly from the audio analogue output.

7.3 Experimental Procedure and Results

7.3.1 Slippage Detection

When we hold an object in our hand, after some time we may feel slippage between our fingers and the object. This detection mostly comes from the touch sensitivity of our fingers, which alerts us to an external event. In this phase of the project, we compared the performances of subjects when using their own vision, with their performances when using vibrotactile stimulation, and pressure feedback, in order to determine the relative effectiveness of haptic feedback

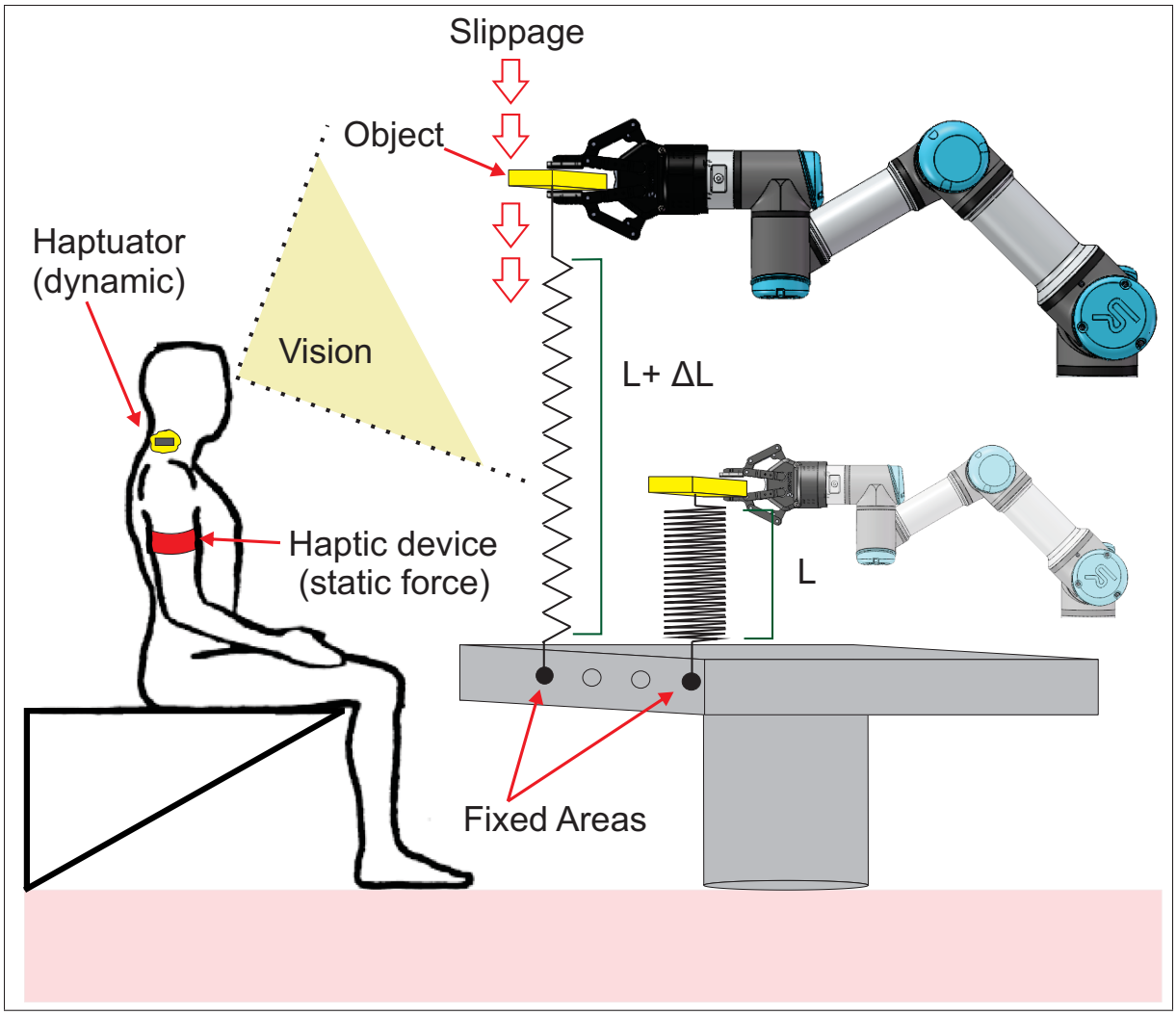

Figure 7.6 Subject detecting slippage, using vision, dynamic feedback, and static feedback

for detecting object slippage. We hoped to find our whether it is possible to replace our vision with either pressure or vibrotactile stimulation during slippage detection tasks.

We began the procedure by selecting one of the objects at random and placing it between the fingers of the robotic gripper. One side of the object was attached to the extension spring, which was screwed to the table to remain constant during the procedure. Once the object had been grasped, we asked the subject to move the robotic arm, using the controller, in an upwards direction from its initial position (L), until they either observed the slippage, or felt the

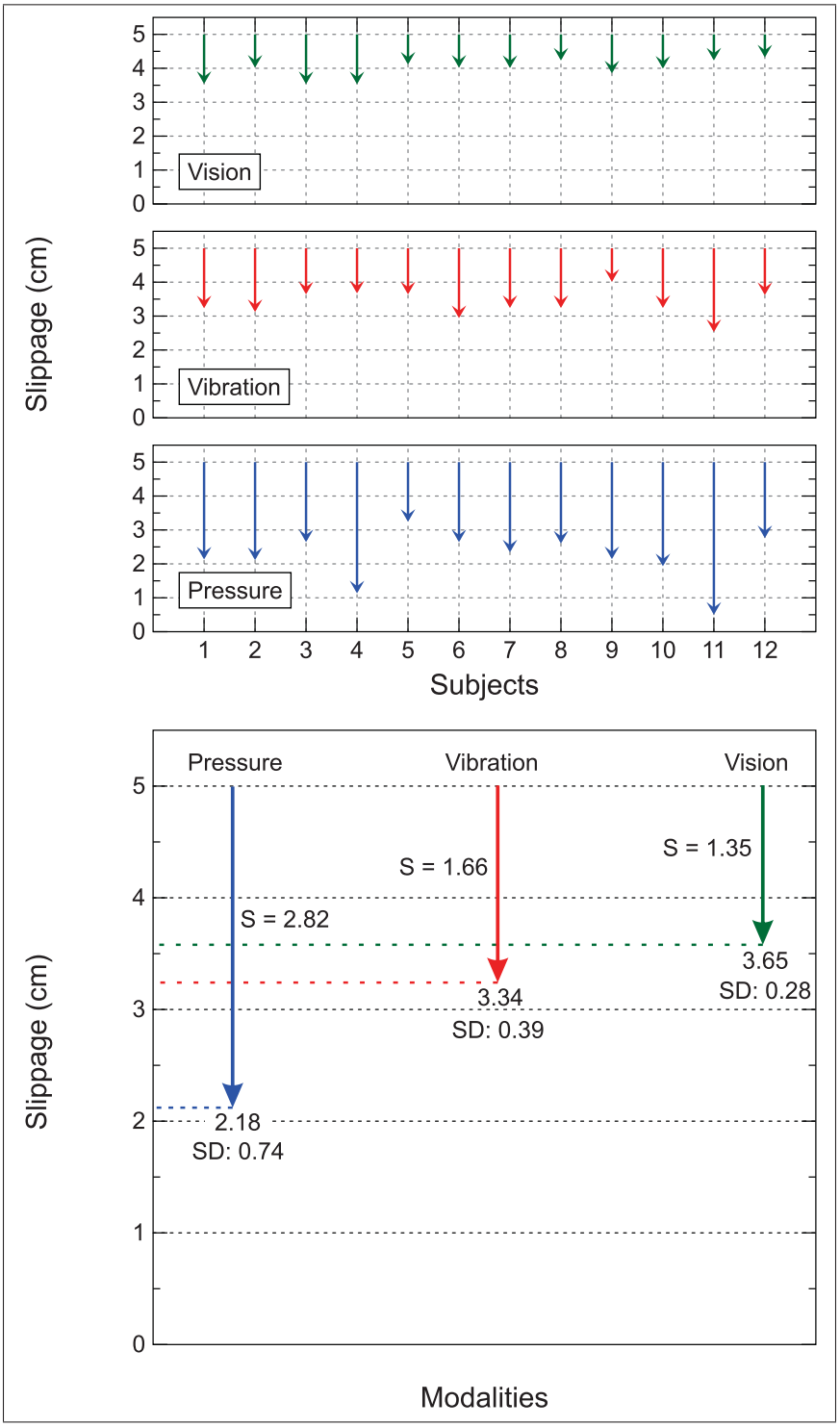

Figure 7.7 Results of the slippage detection task, based on the average of the twelve subjects' results. S indicates the distance of the slippage that occurred during the experiment and SD indicates the standard deviation

haptic feedback. The speed of movement was pre-adjusted at $20mm/s$. As can be seen from Figure 7.6, the Haptuator was placed at the back of each subject's neck and the haptic device was strapped onto his or her forearm. Under static conditions, the process was as follows: once the object reached the maximum distance at which slippage can occur, the haptic device, which was connected to the tactile sensor of the robotic finger, applied pressure to the subject's forearm. We asked the subjects to click on the stop button of the controller as soon as this occurred. The experimenter overseeing the procedure tracked and measured the slippage distance with a ruler that was implemented on the surface of each object. We repeated this procedure for the visual and dynamic feedback tests. During these tests, the subjects halted the movement of the robot (by pressing the stop button of the controller) as soon as they either observed the slippage, or felt the vibrations.

Figure 7.7 shows the results of the test. It also gives the distance of slippage for each object, and the average distance of each object's slippage, for each modality, before it was detected by the subjects.

Although human vision was more accurate than both types of haptic feedback, vibration was only slightly less effective than vision. The overall distance of the slippage that occurred during the vision test was $1.32cm$, compared to $1.66cm$ during the vibration test, and $2.82cm$ during the pressure test. In addition, the vision and vibration tests exhibit similar standard deviations: 0.28 for vision, and 0.39 for vibration. These results allow us to conclude that vibration is indeed a good candidate for the replacement of the visual attention during slippage detection tasks.

7.3.2 Contact Detection

The main goal of this phase was to compare the effectiveness of vibrotactile stimulation with the human visual system, while subjects attempted to detect the moment of contact between the robotic gripper and an object. We aim to determine whether vibrotactile feedback could be

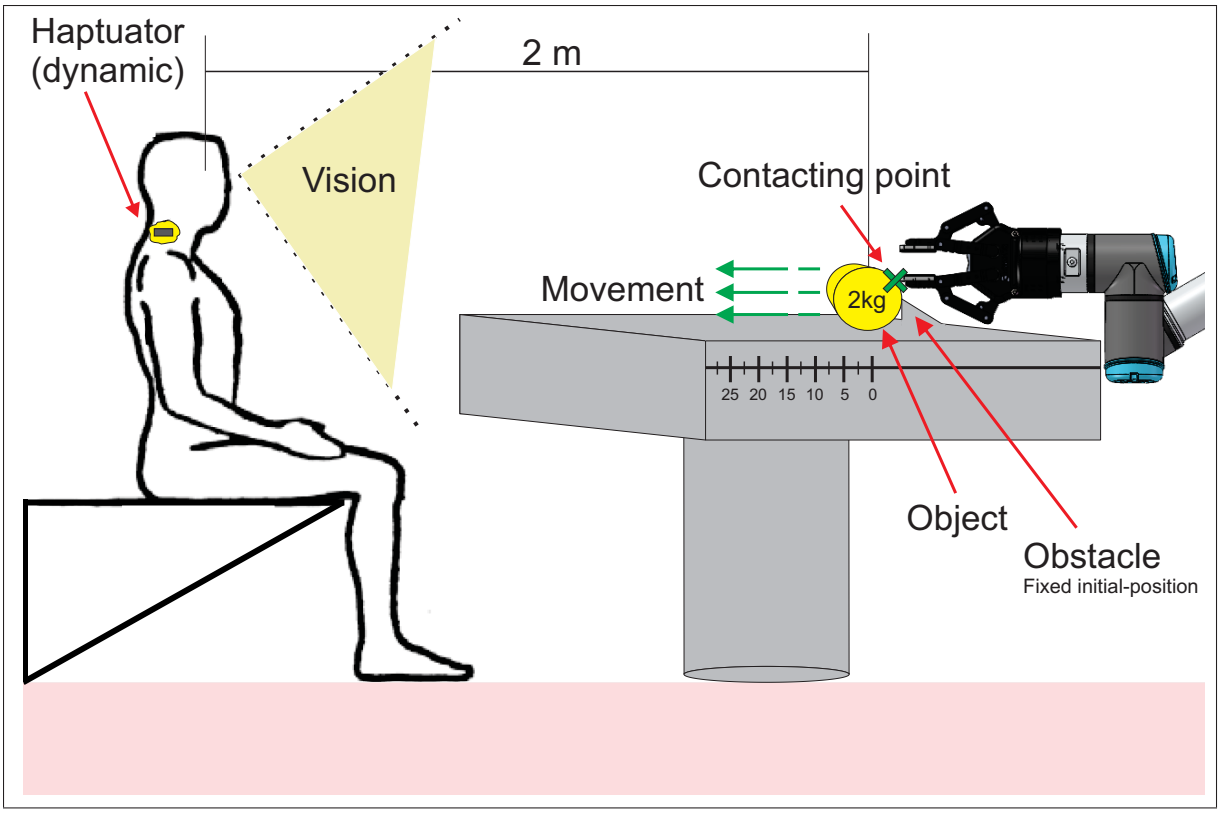

Figure 7.8 Subject detecting contact between the robotic fingers and the object, using either vision or dynamic feedback

used to replace vision, so that users of prosthetics may eventually be able to complete a task using only vibrotactile feedback while their visual attention is focused on something else.

For the experiment, we used seven objects, ranging in weight from $380g$ to $2.0kg$. We used objects of varying weights in order to validate the system's performance for a wide range of objects. As can be seen from Figure 7.8, we fixed the initial position of each object on the table before the process began. The subjects' task was to press the controller button that would halt the motion of the robotic fingers as soon as they observed (or felt) that the fingers had made contact with the object.

We began the experiment by having the twelve subjects detect the moment of contact using their vision. We then proceeded with the vibrotactile stimulation tests, in which the haptic device applied vibrations to the subject's neck once contact was made.

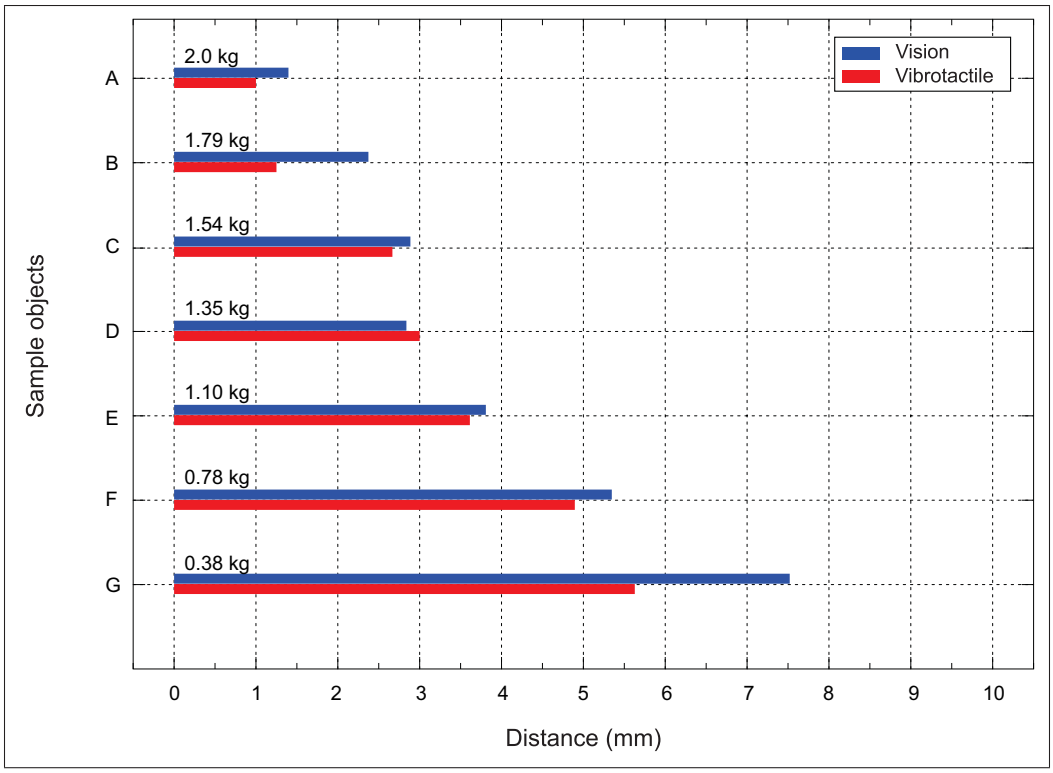

Figure 7.9 Results of the contact detection tests, based on the average of the twelve subjects' results

Figure 7.9 shows the average of the twelve subjects' results.

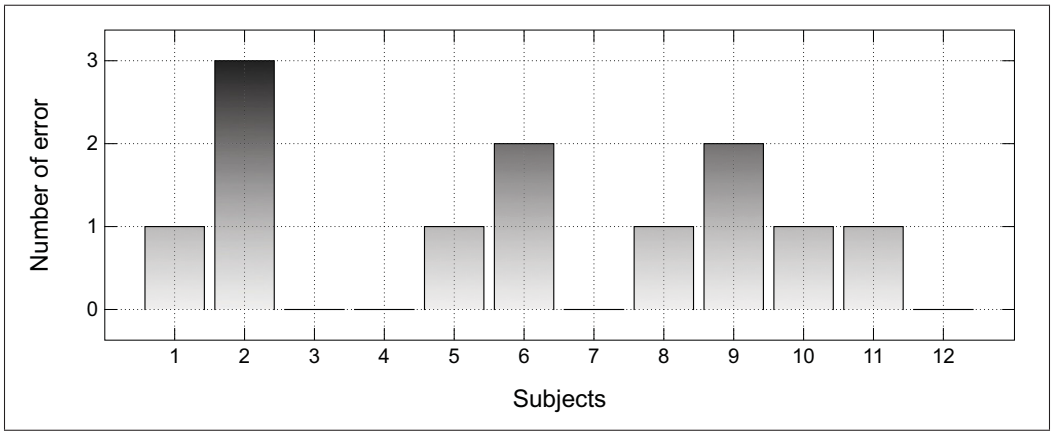

Figure 7.10 The number of errors that occurred during the test of contact detection using vision

The main parameter we used to evaluate the subjects' performance was the distance that the object travelled as a result of pressure applied by the robotic fingers. Therefore, a distance of 0 would be considered the optimal result, as it means that the subject detected the moment of contact at exactly the right time.

For almost all the objects (the exception was object C), vibrotactile stimulation proved slightly superior to visual attention. This result may seem strange at first glance, but it makes sense when we consider the details. As the subjects were seated at a distance of $1.1m$ from the robotic gripper and the object, it was difficult for them to observe the moment of contact. It was much easier for them to stop the robot's movement at the correct time when they simply had to sense the vibration on their necks. As can be seen from Figure 7.10, many errors occurred in the vision test. This was due to the subjects' difficulty with sensing the moment of contact through vision alone, as they frequently halted the movement before the robotic fingers had even made contact with the objects. As a result, 85.7% of the time the subjects were more accurate when using vibrotactile stimulation. This clearly demonstrates the viability of using vibrotactile feedback to replace vision for contact-detection purposes.

7.3.3 Grasp Precision

In the third and final phase of the experiment, we asked the subjects to move an object from one position to another location, $50cm$ away, by controlling the robotic gripper. Figure 7.11 illustrates this process. The subjects' goal was to accomplish this as quickly as possible, while commanding the robotic gripper to exert a sufficient (but not excessive) level of pressure on the object. During this process, we evaluated the performances of the subjects while they used their vision alone, static pressure feedback alone, and the two in combination.

We began the experiment by asking each subject to look at the object, and, with the robot controller shown in Figure 7.2, to use the robotic fingers to move the object from position one to position two. We then repeated the procedure, except this time we strapped the haptic device to the subject's forearm, and asked him or her to repeat the task using the pressure

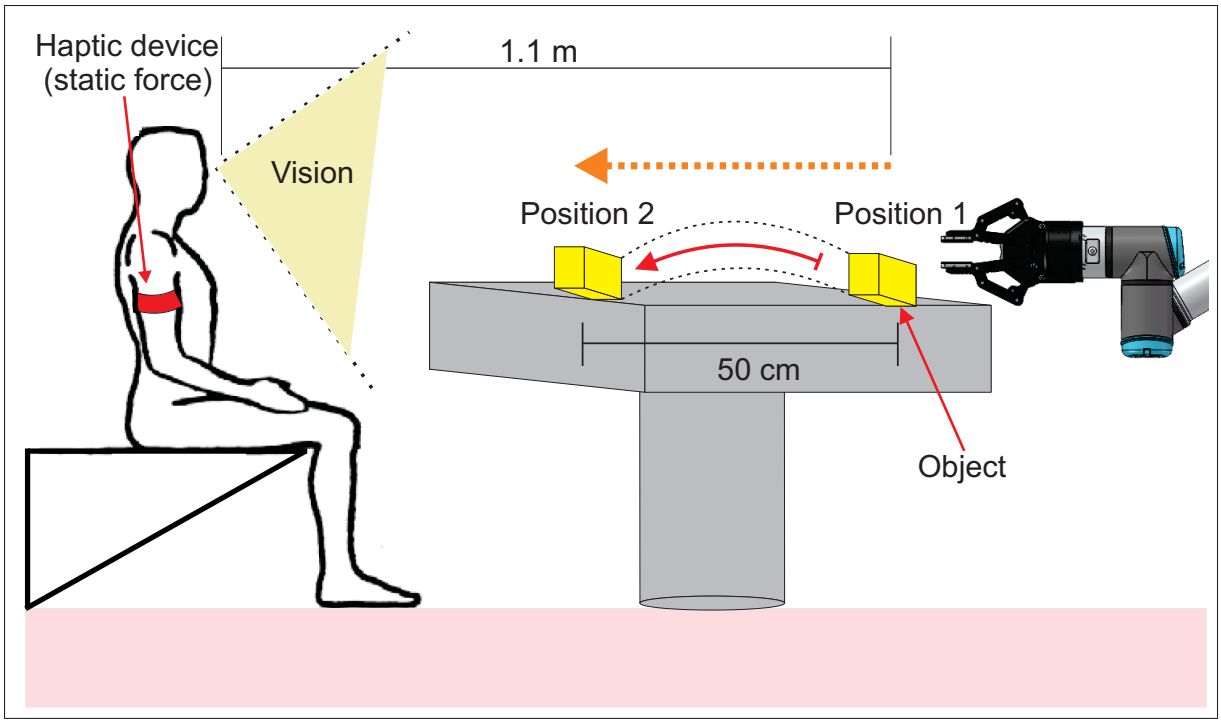

Figure 7.11 Subject performing the grasp precision task using vision and pressure feedback

feedback, representing the grip force, as well as their vision. Finally, the participants were asked to repeat the process while blindfolded, so that the pressure feedback was their only source of information for the task. The twelve subjects went through all three stages of the grasp precision experiment using three different objects, weighing $1.12kg$, $1.63kg$, and $2.0kg$.

In Figure 7.12, we gathered the subjects' results for each object when using vision, vision with pressure, and pressure alone. For example, the results of object A show that when subjects were asked to rely only on their vision, they were able to move the object more quickly, but with a higher amount of force applied by the robotic gripper to the object, than when they used pressure feedback alone. By contrast, when subjects were asked to use both vision and pressure feedback, both the moving time and the applied pressure were dramatically reduced. This trend was present in the results of all three objects.

The results indicate that when the subjects relied on their vision alone, they were able to complete the task more quickly, but they were also more likely to use excessive force. By contrast,

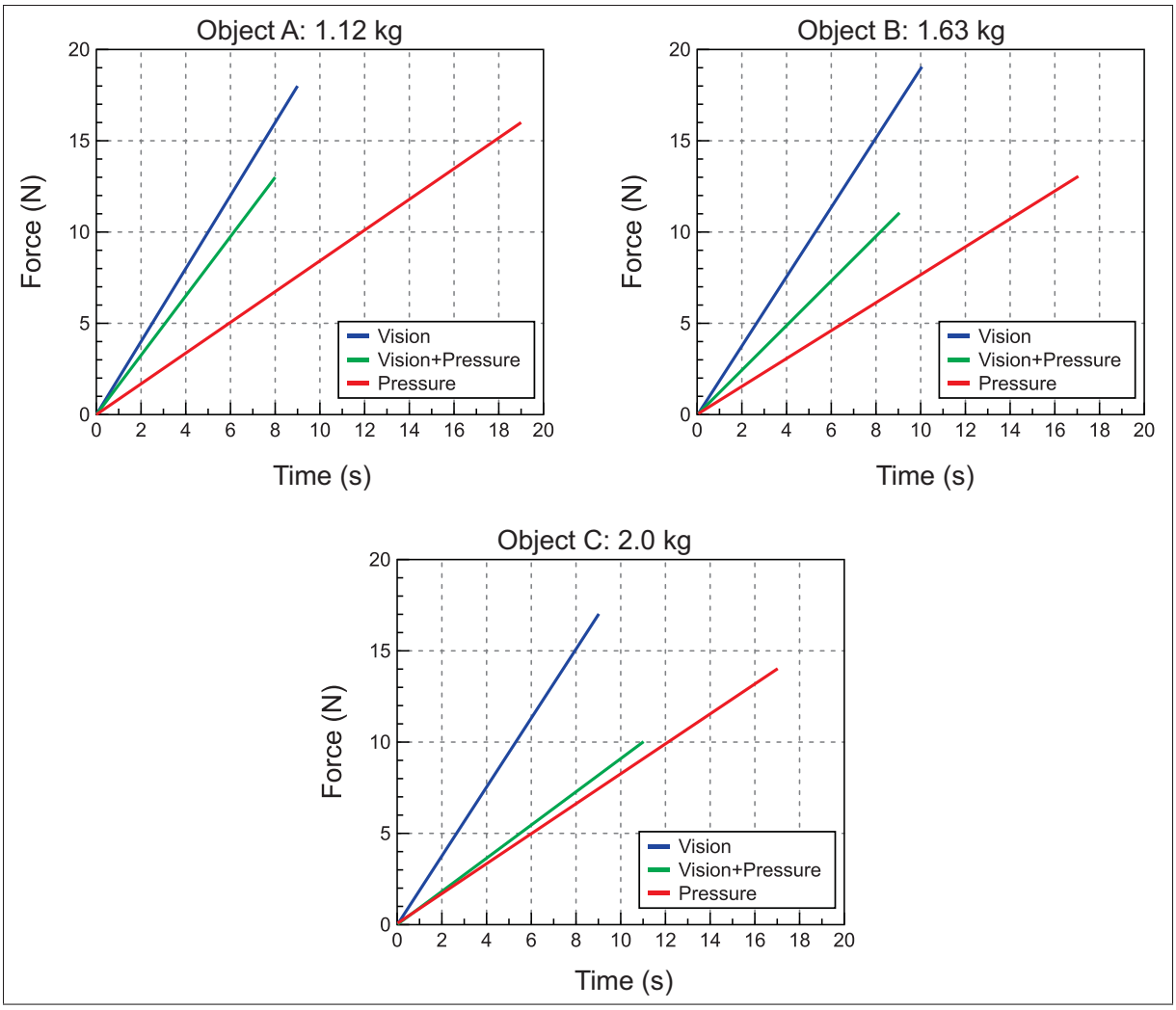

Figure 7.12 Results of the grasp precision tests, based on the average of the twelve subjects' results

the use of pressure alone presented less risk (in terms of potential damage to the object), in that subjects applied the correct amount of pressure, but it took them much longer to transport the object.

The use of visual and pressure feedback together allowed the subjects to manipulate the objects faster than when using pressure alone, and more reliably than when using vision alone, making this combination the best of both worlds.

7.4 Conclusion

Our goal, in this chapter, was to conduct an experiment that was more applicable to everyday life than what we had done previously. We aimed to demonstrate that haptic feedback can be an viable replacement for visual attention during the accomplishment of routine tasks. This was done by comparing the relative effectiveness of subjects using vision alone, vision with haptic feedback, and haptic feedback alone, as they attempted to complete various tasks. As was to be expected, in many cases vision alone was sufficient for the subjects to complete the task. However, our results are promising, as they show that vibration may substituted for vision during slippage and contact detection tasks. Furthermore, even when haptic feedback alone is less effective than vision alone, as in the grasp precision test, haptic feedback can be used to augment vision, resulting in more reliable object manipulation overall.

CONCLUSION

Human touch sensitivity is a complex biological system that deals with a variety of environmental impacts. That is why it is essential to apply the proper stimulus for each type of modality, such as grasping or rubbing, when attempting to provide tactile feedback. Obviously the solution may lie outside what can be found through simply comparing different types of feedback, designing an apparatus, and conducting experiments with human subjects; we hope this study has been a step in the right direction.

Here, we would like to briefly explain what we have done in this thesis, based on the objectives we had outlined, and explore what can be done in future research in order to improve the functionality of haptic feedback for prosthetic applications.

In chapter 2, we investigated the effectiveness of several stimuli, specifically normal stress, tangential force, and vibrotactile stimulation, that were applied to the glabrous skin of the hand. Our goal was to find the best type of haptic feedback for conveying the perception of static pressure to humans. We found that even though all the stimulation methods (normal stress, shear force, and vibrotactile stimulation) provided a sufficient level of feedback, normal stress is more effective than either tangential force, or vibrotactile stimulation, at conveying the sense of pressure.

In chapter 3, we presented a novel wearable haptic device that provides the user with knowledge of a normal force, measured at the fingertips, by applying pressure at three different locations on the user's body. This chapter described the design of our haptic device, the kinematic and dynamic modelling of the actuator, and the results of the experiments that were used to validate the system's functionality. At this stage we decided that further research should focus on improving the proposed device. It contains three pistons, but it requires five pistons to stimulate haptic feedback that will correspond to the five fingers of an advanced prosthetic hand. In addition, the effect of slippage is another piece of information that could be conveyed to the user. Haptic feedback could be carried out for this purpose using the vibrations that are

caused when prosthetic fingers slide across an object's surface. This was the main reason of implementing vibration motor into the haptic device.

We also found that our future work will require us to study the difference between the touch sensitivity of robotic finger pads, and the touch sensitivity of areas of the human body. For instance, when the prosthetic hand touches an object, its sensitive fingertips will detect the amount of pressure that is being applied. However, when this pressure is then transmitted to the user's forearm via the haptic device, the person may not be able to sense the exact same amount of pressure. Even if it is applied accurately, the human forearm may be less sensitive to pressure than the robotic finger pads, and so the haptic device will have to compensate by applying slightly more pressure to the forearm. We might investigate this by asking subjects to estimate the level of pressure that the device applies, and then comparing this estimate to the actual pressure that was applied by both the haptic device and the prosthetic fingertips in the hopes of properly calibrating the sensory feedback. Finally, although we have developed a haptic device for pressure application using an improved twisted wire actuator, we (and the robotics community) have not yet developed a haptic device capable of simultaneously delivering normal pressure, shear, and temperature sensation. As we proceed towards this goal, there is much work to be done in optimizing each of these functions in turn, before they can be brought together in one unified haptic system.

In chapter 4, we investigated how the simultaneous application of two different types of haptic feedback impacts human sensory perception. Our results showed that when vibration was applied at the same time and location as a normal stress, the subjects' perception of the normal stress was less accurate. However, under the same conditions, i.e., vibration applied at the same time and location as the normal stress, the subjects perceived the vibration with greater accuracy. These results gave us new insights on how the simultaneous application of different haptic stimuli to a compact space on the human arm impacts the ability to perceive each stimulus. We believe future work can focus on merging these two endeavours to examine how both types of stimulation methods can be used to help amputees.

In chapter 5, we presented a robotic system that was used to study the restoration of touch sensitivity. In the experiment, a combination of tactile sensors, robotic fingers, and a haptic interface enabled us to undertake different types of experiments on human subjects. To this end, we conducted two separate tests on eight human subjects in order to assess the effectiveness of the static and dynamic modalities in different detectable ranges of skin sensitivity.

Based on the results we obtained in chapter 5, the participants' feedback, and our own experiences, two critical parameters can be taken into account to improve the functionality of the system. First, improving the communicational loop between the system components, such as tactile sensors and the haptic interface, can significantly enhance the effectiveness of the whole system. More specifically, although the vibrations were restituted in real-time under the dynamic condition, we measured an approximate delay of 110 *ms* between pressure sensing and force application on the subject's forearm under the static condition. This is due to the fact that under the static condition, we are not controlling the motor directly from our computer, but through a microcontroller that has some latency. The delay seems to have caused errors when subjects were trying to replicate the pressure they had sensed.

Furthermore, we were not able to create vibrations that correspond perfectly with the characteristics of each texture. This is because the Haptuator has a limited bandwidth that cannot capture the full range of signals produced by the tactile sensor. For instance, when a texture was rubbed very slowly over the sensor, the resulting signal was in a low frequency range. This made it hard to fully transmit the signal to the Haptuator, and the vibrations produced by the Haptuator were too faint for subjects to sense accurately.

Second, providing training to participants allows them to gain familiarity with the procedure and obtain the best possible results from the haptic device. Apart from these considerations, we could likely improve our results by implementing noise-filtering algorithms for dynamic data, and by taking into account the frequency response of the Haptuator by modulating our output signal accordingly.

The main focus of chapter 6 stemmed from an observation we made during the experiment we conducted in chapter 5: we noticed a correlation between how familiar the subjects were with haptic systems, and how well they were able to use the haptic system to accurately identify textures. We began with a group of subjects who were completely unfamiliar with haptic systems, and tracked the improvements in their accuracy over a period of four weeks. This improvement of 16%, after just three additional weeks of training, is even more impressive considering that the subjects themselves only reached a 91% success rate when using their own fingertips to identify the textures. At this step, we realized that the next phase of research should be more task-oriented.

That is why in chapter 7 we conducted three set of tests, using ordinary objects and a robotic system, to assess the functionality of the haptic system during tasks that are more suited to what occur in everyday life. We evaluated the subjects' performances as they used their vision, and static pressure and vibrotactile feedback, during slippage detection, contact detection, and grasp precision tests. The overall results indicate that vibrotactile feedback is a promising replacement for visual attention; and while static pressure may not be able to completely negate the need for visual attention, it can improve people's ability to manipulate objects when the two are used in conjunction.

No research project is without flaws. Although our methods were suitable for theoretical investigations, and industrial applications, to bring our results to the rest of society will require us to work with actual upper-limb amputees, and the prosthetic limbs they will be using. Future work should also be more task-oriented, in that it should examine performance during the completion of actual everyday tasks. We hope that the pursuit of this goal will eventually restore to amputees the complete sense of touch.

REFERENCES

Aggarwal, A., P. Kampmann, J. Lemburg, and F. Kirchner. 2015. "Haptic Object Recognition in Underwater and Deep-sea Environments". *Journal of Field Robotics*, vol. 32, n° 1, p. 167–185.

Antfolk, C., M. D'Alonzo, M. Controzzi, G. Lundborg, B. Rosén, F. Sebelius, and C. Cipriani. 2013. "Artificial redirection of sensation from prosthetic fingers to the phantom hand map on transradial amputees: vibrotactile versus mechanotactile sensory feedback". *Neural Systems and Rehabilitation Engineering, IEEE Transactions on*, vol. 21, n° 1, p. 112–120.

Atkins, D. J., D. C. Heard, and W. H. Donovan. 1996. "Epidemiologic overview of individuals with upper-limb loss and their reported research priorities". *JPO: Journal of Prosthetics and Orthotics*, vol. 8, n° 1, p. 2–11.

Baril, M., L. Thierry, F. Guay, and C. Gosselin. 2010. "Static analysis of single-input/multiple-output tendon-driven underactuated mechanisms for robotic hands". In *ASME 2010 International Design Engineering Technical Conferences and Computers and Information in Engineering Conference*. p. 155–164. American Society of Mechanical Engineers.

Bark, K., J. W. Wheeler, S. Premakumar, and M. R. Cutkosky. 2008. "Comparison of skin stretch and vibrotactile stimulation for feedback of proprioceptive information". In *Haptic interfaces for virtual environment and teleoperator systems, 2008. haptics 2008. symposium on*. p. 71–78. IEEE.

Bark, K., J. Wheeler, G. Lee, J. Savall, and M. Cutkosky. 2009. "A wearable skin stretch device for haptic feedback". In *EuroHaptics conference, 2009 and Symposium on Haptic Interfaces for Virtual Environment and Teleoperator Systems. World Haptics 2009. Third Joint*. p. 464–469. IEEE.

Beebe, D., D. D. Denton, R. Radwin, and J. Webster. Feb 1998. "A silicon-based tactile sensor for finger-mounted applications". *Biomedical Engineering, IEEE Transactions on*, vol. 45, n° 2, p. 151-159.

Ben Porquis, L., D. Maemori, N. Nagaya, M. Konyo, and S. Tadokoro. Nov 2013. "Haptic cue of forces on tools: Investigation of multi-point cutaneous activity on skin using suction pressure stimuli". In *Intelligent Robots and Systems (IROS), 2013 IEEE/RSJ International Conference on*. p. 2023-2029.

Berkelman, P., R. Hollis, and S. Salcudean. 1995. "Interacting with virtual environments using a magnetic levitation haptic interface". In *Intelligent Robots and Systems 95. 'Human Robot Interaction and Cooperative Robots', Proceedings. 1995 IEEE/RSJ International Conference on*. p. 117-122 vol.1.

Bhattacharjee, T., J. Rehg, and C. Kemp. Oct 2012. "Haptic classification and recognition of objects using a tactile sensing forearm". In *Intelligent Robots and Systems (IROS), 2012 IEEE/RSJ International Conference on*. p. 4090-4097.

Biddiss, E. A. and T. T. Chau. 2007. "Upper limb prosthesis use and abandonment: a survey of the last 25 years". *Prosthetics and orthotics international*, vol. 31, n° 3, p. 236–257.

Biggs, J. and M. A. Srinivasan. 2002. "Tangential versus normal displacements of skin: Relative effectiveness for producing tactile sensations". In *Haptic Interfaces for Virtual Environment and Teleoperator Systems, 2002. HAPTICS 2002. Proceedings. 10th Symposium on*. p. 121–128. IEEE.

Blank, A., A. M. Okamura, and K. J. Kuchenbecker. 2010. "Identifying the role of proprioception in upper-limb prosthesis control: Studies on targeted motion". *ACM Transactions on Applied Perception (TAP)*, vol. 7, n° 3, p. 15.

Boundless. 2014. "Somatosensation: Pressure, Temperature, and Pain (Human skin receptors)". <www.boundless.com/psychology/textbooks/boundless-psychology-textbook/sensation-and-perception-5/sensory-processes-38/somatosensation-pressure-temperature-and-pain-165-12700>.

Brown, J., A. Paek, M. Syed, M. O'Malley, P. Shewokis, J. Contreras-Vidal, A. Davis, and R. Gillespie. April 2013. "Understanding the role of haptic feedback in a teleoperated/prosthetic grasp and lift task". In *World Haptics Conference (WHC), 2013*. p. 271-276.

Caldwell, D. G., N. Tsagarakis, and A. Wardle. 1997. "Mechano thermo and proprioceptor feedback for integrated haptic feedback". In *Robotics and Automation, 1997. Proceedings., 1997 IEEE International Conference on*. p. 2491–2496. IEEE.

Caldwell, D., N. Tsagarakis, and C. Giesler. 1999. "An integrated tactile/shear feedback array for stimulation of finger mechanoreceptor". In *Robotics and Automation, 1999. Proceedings. 1999 IEEE International Conference on*. p. 287-292.

Chatterjee, A., P. Chaubey, J. Martin, and N. Thakor. 2008. "Testing a prosthetic haptic feedback simulator with an interactive force matching task". *JPO: Journal of Prosthetics and Orthotics*, vol. 20, n° 2, p. 27–34.

Childress, D. S. 1980. "Closed-loop control in prosthetic systems: Historical perspective". *Annals of biomedical engineering*, vol. 8, n° 4, p. 293–303.

Damian, D., A. Arieta, and A. Okamura. Aug 2011. "Design and evaluation of a multi-modal haptic skin stimulation apparatus". In *Engineering in Medicine and Biology Society, EMBC, 2011 Annual International Conference of the IEEE*. p. 3455-3458.

Dargahi, J. and S. Najarian. 2004. "Human tactile perception as a standard for artificial tactile sensing—a review". *The International Journal of Medical Robotics and Computer Assisted Surgery*, vol. 1, n° 1, p. 23–35.

Davis, B., R. Bull, and J. Roscoe, 2000. *Physical education and the study of sport*.

Deschenes, J.-D., P. Lambert, S. Perreault, N. Martel-Brisson, N. Zoso, A. Zaccarin, P. Hébert, S. Bouchard, and C. M. Gosselin. 2007. "A cable-driven parallel mechanism for capturing object appearance from multiple viewpoints". p. 367–374.

Dexta. 2014. "Dexmo Classic and Dexmo F2". <www.dextarobotics.com/products/dexmo>.

Duchaine, V. and A. Rana. 24 2014. "Dielectric geometry for capacitive-based tactile sensor". <http://www.google.se/patents/WO2014110683A1?cl=sv>. WO Patent App. PCT/CA2014/050,040.

Edin, B. B. 2001. "Cutaneous afferents provide information about knee joint movements in humans". *The Journal of Physiology*, vol. 531, n° 1, p. 289–297.

Edin, B. B. 2004. "Quantitative analyses of dynamic strain sensitivity in human skin mechanoreceptors". *Journal of neurophysiology*, vol. 92, n° 6, p. 3233–3243.

Fan, R., C. Wottawa, A. Mulgaonkar, R. Boryk, T. Sander, M. Wyatt, E. Dutson, W. Grundfest, and M. Culjat. April 2009. "Pilot testing of a haptic feedback rehabilitation system on a lower-limb amputee". In *Complex Medical Engineering, 2009. CME. ICME International Conference on*. p. 1-4.

Ferrington, D., B. Nail, and M. Rowe. 1977. "Human tactile detection thresholds: modification by inputs from specific tactile receptor classes". *The Journal of physiology*, vol. 272, n° 2, p. 415–433.

Fortin, P., M.-D. Otis, V. Duchaine, and J. Cooperstock. Oct 2014. "Event-based haptic vibration synthesis using a recursive filter for lower limb prosthetics". In *Haptic, Audio and Visual Environments and Games (HAVE), 2014 IEEE International Symposium on*. p. 47-52.

Gallery, U. H. 2014. "Pacinian Corpuscle at 40X". <www.bcrc.bio.umass.edu/courses/spring2012/biol/biol523/fall2012gallery?tid%5B%5D=5>.

Gels, E. P. 2004. "Electroactive polymer (EAP) actuators as artificial muscles: reality, potential, and challenges".

Gillespie, R., J. Contreras-Vidal, P. Shewokis, M. O'Malley, J. Brown, H. Agashe, R. Gentili, and A. Davis. Aug 2010. "Toward improved sensorimotor integration and learning using upper-limb prosthetic devices". In *Engineering in Medicine and Biology Society (EMBC), 2010 Annual International Conference of the IEEE*. p. 5077-5080.

Godfrey, S., A. Ajoudani, M. Catalano, G. Grioli, and A. Bicchi. June 2013. "A synergy-driven approach to a myoelectric hand". In *Rehabilitation Robotics (ICORR), 2013 IEEE International Conference on*. p. 1-6.

Godler, I., K. Hashiguchi, and T. Sonoda. 2010. "Robotic finger with coupled joints: a prototype and its inverse kinematics". In *Advanced Motion Control, 2010 11th IEEE International Workshop on*. p. 337–342. IEEE.

Gonzalez-Crussi, F., 1989. *The five senses*.

Goodwin, A. W., V. G. Macefield, and J. W. Bisley. 1997. "Encoding of Object Curvature by Tactile Afferents From Human Fingers". *Journal of Neurophysiology*, vol. 78, n° 6, p. 2881–2888.

Guiatni, M., V. Riboulet, C. Duriez, A. Kheddar, and S. Cotin. June 2013. "A Combined Force and Thermal Feedback Interface for Minimally Invasive Procedures Simulation". *Mechatronics, IEEE/ASME Transactions on*, vol. 18, n° 3, p. 1170-1181.

Hager-Ross, C., K. Cole, and R. Johansson. 1996. "Grip-force responses to unanticipated object loading: load direction reveals body- and gravity-referenced intrinsic task variables". *Experimental Brain Research*, vol. 110, n° 1, p. 142-150.

Iggo, A. and A. R. Muir. 1969. "The structure and function of a slowly adapting touch corpuscle in hairy skin". *The Journal of physiology*, vol. 200, n° 3, p. 763–796.

J-d Otis, M., T.-L. Nguyen-Dang, T. Laliberté, D. Ouellet, and D. Laurendeau. 2009. "Cable tension control and analysis of reel transparency for 6-dof haptic foot platform on a cable-driven locomotion interface".

Jimenez, M. C. and J. A. Fishel. 2014. "Evaluation of force, vibration and thermal tactile feedback in prosthetic limbs". In *Haptics Symposium (HAPTICS), 2014 IEEE*. p. 437–441. IEEE.

Johansson, R. S. and Å. B. Vallbo. 1979. "Tactile sensibility in the human hand: relative and absolute densities of four types of mechanoreceptive units in glabrous skin.". *The Journal of physiology*, vol. 286, n° 1, p. 283–300.

Kaczmarek, K., J. Webster, P. Bach-y Rita, and W. J. Tompkins. Jan 1991. "Electrotactile and vibrotactile displays for sensory substitution systems". *Biomedical Engineering, IEEE Transactions on*, vol. 38, n° 1, p. 1-16.

Kapur, P., S. Premakumar, S. A. Jax, L. J. Buxbaum, A. M. Dawson, and K. J. Kuchenbecker. 2009. "Vibrotactile feedback system for intuitive upper-limb rehabilitation". In *Euro-Haptics conference, 2009 and Symposium on Haptic Interfaces for Virtual Environment and Teleoperator Systems. World Haptics 2009. Third Joint*. p. 621–622. IEEE.

Kargov, A., C. Pylatiuk, R. Oberle, H. Klosek, T. Werner, W. Roessler, and S. Schulz. 2007. "Development of a multifunctional cosmetic prosthetic hand". In *Rehabilitation Robotics, 2007. ICORR 2007. IEEE 10th International Conference on*. p. 550–553. IEEE.

Kawamura, S., W. Choe, S. Tanaka, and S. R. Pandian. 1995. "Development of an ultrahigh speed robot FALCON using wire drive system". In *Robotics and Automation, 1995. Proceedings., 1995 IEEE International Conference on*. p. 215–220. IEEE.

Kim, E., K. Sugg, N. Langhals, S. Lightbody, M. Baltrusaitis, M. Urbanchek, P. Cedema, and G. Gerling. April 2013. "An engineered tactile afferent modulation platform to elicit compound sensory nerve action potentials in response to force magnitude". In *World Haptics Conference (WHC), 2013*. p. 241-246.

Kim, K. and J. Colgate. Nov 2012. "Haptic Feedback Enhances Grip Force Control of sEMG-Controlled Prosthetic Hands in Targeted Reinnervation Amputees". *Neural Systems and Rehabilitation Engineering, IEEE Transactions on*, vol. 20, n° 6, p. 798-805.

Kim, K., J. E. Colgate, J. J. Santos-Munné, A. Makhlin, and M. A. Peshkin. 2010. "On the design of miniature haptic devices for upper extremity prosthetics". *Mechatronics, IEEE/ASME Transactions on*, vol. 15, n° 1, p. 27–39.

Kim, S., M. Spenko, S. Trujillo, B. Heyneman, V. Mattoli, and M. R. Cutkosky. 2007. "Whole body adhesion: hierarchical, directional and distributed control of adhesive forces for a climbing robot". In *Robotics and Automation, 2007 IEEE International Conference on*. p. 1268–1273. IEEE.

Kirk, N., Z. G. Fan Quek, and S. Schorr. 2015. "Skin Stretch Feedback". <www.charm.stanford.edu/Main/TeleoperationAndHapticsForSurgery>.

Klinge, V. 1972. "Effects of exteroceptive feedback and instructions on control of spontaneous galvanic skin responses". *Psychophysiology*, vol. 9, n° 3, p. 305–317.

Kremer, S. R. 4 1989. "Twisted cord actuator". US Patent 4,843,921.

LaMotte, R., R. Friedman, C. Lu, P. Khalsa, and M. Srinivasan. 1998. "Raised object on a planar surface stroked across the fingerpad: responses of cutaneous mechanoreceptors to shape and orientation". *Journal of neurophysiology*, vol. 80, n° 5, p. 2446–2466.

Lederman, S. J. and R. L. Klatzky. 2009. "Haptic perception: A tutorial". *Attention, Perception, & Psychophysics*, vol. 71, n° 7, p. 1439–1459.

Lee, J. C., P. H. Dietz, D. Leigh, W. S. Yerazunis, and S. E. Hudson. 2004. "Haptic Pen: A Tactile Feedback Stylus for Touch Screens". In *Proceedings of the 17th Annual ACM Symposium on User Interface Software and Technology*. (New York, NY, USA 2004), p. 291–294. ACM.

Matulevich, B., G. Loeb, and J. Fishel. Nov 2013. "Utility of contact detection reflexes in prosthetic hand control". In *Intelligent Robots and Systems (IROS), 2013 IEEE/RSJ International Conference on*. p. 4741-4746.

Motamedi, M., J. Roberge, and V. Duchaine. June 2015. "Tactile Sensation Transmission from a Robotic Arm to the Human Body via a Haptic Interface". In *IEEE World Haptics Conference (WHC 2015), Accepted paper*.

Okamura, A. M., J. T. Dennerlein, and R. D. Howe. 1998. "Vibration feedback models for virtual environments". In *Robotics and Automation, 1998. Proceedings. 1998 IEEE International Conference on*. p. 674–679. IEEE.

Paré, M., H. Carnahan, and A. M. Smith. 2002. "Magnitude estimation of tangential force applied to the fingerpad". *Experimental Brain Research*, vol. 142, n° 3, p. 342–348.

Patrick Dougherty, C. T. 2013. "Somatosensory Systems". *Neuroscience Electronic Textbook - Chapter 2, Neuroscience Online - The University of Texas Health Science Center at Houston (UTHealth)*.

Prior, R. E., J. Lyman, P. A. Case, and C. M. Scott. 1976. "Supplemental sensory feedback for the VA/NU myoelectric hand. Background and preliminary designs". *Bull Prosthet Res*, vol. 10, n° 25, p. 170–91.

Provancher, W. R., M. R. Cutkosky, K. J. Kuchenbecker, and G. Niemeyer. 2005. "Contact location display for haptic perception of curvature and object motion". *The International Journal of Robotics Research*, vol. 24, n° 9, p. 691–702.

Pylatiuk, C., A. Kargov, and S. Schulz. 2006. "Design and evaluation of a low-cost force feedback system for myoelectric prosthetic hands". *JPO: Journal of Prosthetics and Orthotics*, vol. 18, n° 2, p. 57–61.

Quanser. 2013. "HD High Definition Haptic Device". <www.quanser.com/products/hd2>.

Rana, A. and V. Duchaine. May 2013. "Improved Soft Dielectric for Highly Sensitive Capacitive Tactile Sensor". In *In 2013 IEEE International Conference on Robotics and Automation: Workshop on Research Frontiers in Electronic Skin Technology (Karlsruhe, Germany*. IEEE.

Robles-De-La-Torre, G. 2006. "The importance of the sense of touch in virtual and real environments". *Ieee Multimedia*, vol. 13, n° 3, p. 24–30.

Robot, U. 2012. "@website: University of Southern Den-mark". <www.universal-robots.com>.

Russell, R. A., 1990. *Robot tactile sensing*.

Schätzle, S., T. Hulin, C. Preusche, and G. Hirzinger. 2006. "Evaluation of vibrotactile feedback to the human arm". In *Proceedings of EuroHaptics*. p. 557–560.

Sensable. 2012. "PHANTOM OMNI - HAPTIC DEVICE". <www.dentsable.com/haptic-phantom-omni.htm>.

Shoham, M. 2005. "Twisting wire actuator". *Journal of Mechanical Design*, vol. 127, n° 3, p. 441–445.

Silverthorn, D. U. 2003. "Restoring physiology to the undergraduate biology curriculum: a call for action". *Advances in physiology education*, vol. 27, n° 3, p. 91–96.

Sonoda, T. and I. Godler. 2010. "Multi-fingered robotic hand employing strings transmission named Twist Drive". In *Intelligent Robots and Systems (IROS), 2010 IEEE/RSJ International Conference on*. p. 2733–2738. IEEE.

Srinivasan, M. A. and C. Basdogan. 1997. "Haptics in virtual environments: Taxonomy, research status, and challenges". *Computers & Graphics*, vol. 21, n° 4, p. 393–404.

Stanley, A. A. and K. J. Kuchenbecker. 2011. "Design of body-grounded tactile actuators for playback of human physical contact". In *World Haptics Conference (WHC), 2011 IEEE*. p. 563–568. IEEE.

Stone, R. J. 2001. Haptic feedback: A brief history from telepresence to virtual reality. *Haptic Human-Computer Interaction*, p. 1–16. Springer.

Suzuki, M. and A. Ichikawa. 2005. "Toward springy robot walk using Strand-muscle actuators". p. 479–486.

Tan, H. Z., R. Gray, J. J. Young, and R. Traylor. 2003. "A haptic back display for attentional and directional cueing". *Haptics-e*, vol. 3, n° 1, p. 1–20.

Tanaka, Y., H. Sato, and H. Fujimoto. Oct 2007. "Development of a finger-mounted tactile sensor for surface irregularity detection". In *Intelligent Robots and Systems, 2007. IROS 2007. IEEE/RSJ International Conference on*. p. 690-696.

Vallbo, Å. B., R. Johansson, et al. 1984. "Properties of cutaneous mechanoreceptors in the human hand related to touch sensation". *Hum Neurobiol*, vol. 3, n° 1, p. 3–14.

Weinstein, S. 1968. "Intensive and extensive aspects of tactile sensitivity as a function of body part, sex and laterality". In *the First Int'l symp. on the Skin Senses, 1968*.

Wheeler, J., K. Bark, J. Savall, and M. Cutkosky. 2010. "Investigation of rotational skin stretch for proprioceptive feedback with application to myoelectric systems". *Neural Systems and Rehabilitation Engineering, IEEE Transactions on*, vol. 18, n° 1, p. 58–66.

Witteveen, H. J., J. S. Rietman, and P. H. Veltink. 2012. "Grasping force and slip feedback through vibrotactile stimulation to be used in myoelectric forearm prostheses". In *Engineering in Medicine and Biology Society (EMBC), 2012 Annual International Conference of the IEEE*. p. 2969–2972. IEEE.

Wurtz, T., C. May, B. Holz, C. Natale, G. Palli, and C. Melchiorri. 2010. "The twisted string actuation system: Modeling and control". p. 1215-1220.

Yao, H.-Y. and V. Hayward. 2010. "Design and analysis of a recoil-type vibrotactile transducer". *The Journal of the Acoustical Society of America*, vol. 128, n° 2, p. 619–627.

Yoshikawa, M., Y. Taguchi, S. Sakamoto, S. Yamanaka, Y. Matsumoto, T. Ogasawara, and N. Kawashima. Nov 2013. "Trans-radial prosthesis with three opposed fingers". In *Intelligent Robots and Systems (IROS), 2013 IEEE/RSJ International Conference on*. p. 1493-1498.